Assessment of Drought in Grasslands: Spatio – Temporal Analyses of Soil Moisture and Extreme Climate Effects in Southwestern Mongolia

Dissertation
for the award of the degree
"Doctor rerum naturalium" (Dr. rer. Nat.) of
the Georg-August-Universität Göttingen

within the doctoral program Geography of the
Georg-August University School of Science (GAUSS)

submitted by
OYUDARI VOVA
born on November 29th, 1986 in Ulaanbaatar (Mongolia)
Göttingen, April 2021

Thesis Committee

Prof. Dr. Martin Kappas
(Department of Cartography, GIS and Remote Sensing / Universität Göttingen)

Prof. Dr. Daniela Sauer
(Department of Physical Geography / Georg-August Universität Göttingen)

Prof. Dr. Heiko Faust
(Department of Human Geography / Georg-August Universität Göttingen)

Prof. Dr. Tsolmon Renchin
(NUM-ITC-UNESCO International Laboratory for Remote Sensing and Space Science / National University of Mongolia)

Dr. Daniel Wyss
(Department of Cartography, GIS and Remote Sensing / Georg-August Universität Göttingen)

Dr. Pavel Groisman
(Cooperative Institute for Climate and Satellites, CISESS, North Carolina State University)

Members of the Examination Board

Reviewer 1:

Prof. Dr. Martin Kappas

(Department of Cartography, GIS and Remote Sensing / Georg-August Universität Göttingen)

Reviewer 2:

Prof. Dr. Daniela Sauer

(Department of Physical Geography / Georg-August Universität Göttingen)

Date of the oral examination: **6th May, 2021**

Assessment of Drought in Grasslands: Spatio - Temporal Analyses of Soil Moisture and Extreme Climate Effects in Southwestern Mongolia

Southwestern Mongolia, source: Oyudari Vova

CONTENT OF DISSERTATION

This doctoral dissertation consists of a general introduction and the following published and submitted articles. The papers will be referred to by their Roman numbers (Papers I-III). The published papers are reprinted by permission from the respective copyright holders.

I. Vova, Oyudari; Kappas, Martin; Rafiei Emam, Ammar. 2019. "Comparison of Satellite Soil Moisture Products in Mongolia and Their Relation to Grassland Condition" Land 8, no. 9: 142. https://doi.org/10.3390/land8090142

II. Vova, Oyudari; Kappas, Martin; Renchin, Tsolmon; Fassnacht, Steven R. 2020. "Extreme Climate Event and Its Impact on Landscape Resilience in Gobi Region of Mongolia" Remote Sensing. 12, no. 18: 2881. https://doi.org/10.3390/rs12182881

III. Oyudari Vova; Martin Kappas; Pavel Groisman; Tsolmon Renchin; Steven Fassnacht. 2021. "Development of a new Drought index using SMOS satellite soil moisture products: Case Study in Southwestern Mongolia" submitted to Journal of Land, MDPI.

A list of relevant book chapters is not included as part of this dissertation

Renchin, T., Kappas, M., Munkhbayar, S., Vova, O., Degener, J. 2015. "Drivers of Land Degradation in Umnugobi province" In: Karthe, D., Chalov, S.R., Kasimov, N.S., Kappas, M., (eds.) Water and Environment in the Selenga-Baikal Basin: international research cooperation for an ecoregion of global relevance Erdsicht: Einblicke in geographische und geoinformationstechnische Arbeitsweisen 23 Ibidem-Verlag, Stuttgart, p. 37-53

TABLE OF CONTENTS

LIST OF ABBREVIATIONS

SM	Soil Moisture
SSM	Surface Soil Moisture
LST	Land Surface Temperature
PET	Potential Evapotranspiration
RS	Remote Sensing
GIS	Geographic Information System
SWIR	Shortwave Infrared Reflectance
NIR	Near-Infrared
GDI	Gobi Drought Index
$_aAI_z$	Seasonal Aridity Index
SPI	Standardized Precipitation Index
SPEI	Standardized Precipitation Evaporation Index
PDSI	Palmer Drought Severity Index
ISDI	Integrated Surface Drought Index
VSDI	Visible and Shortwave Infrared Drought Index
NMDI	Normalized Multi-Band Drought Index
TCI	Temperature Condition Index
VSWI	Vegetation Supply Water Index
VHI	Vegetation Health Index
NDVI	Normalized Difference Vegetation Index
NDWI	Normalized Difference Water Index
DEM	Digital Elevation Model
SRTM	Shuttle Radar Topography Mission
MLRM	Multiple Linear Regression Model
MLR	Multiple Linear Regression
SMOS	Soil Moisture and Ocean Salinity
SMAP	Soil Moisture Active Passive
AMSR-E	Advanced Microwave Scanning Radiometer-Earth
MODIS	Moderate Resolution Imaging Spectroradiometer
SAR	Synthetic Aperture Radars
GCOS	Global Climate Observing System

CRU	Climate Research Unit
ESA	European Space Agency
NASA	National Aeronautics and Space Administration
JAXA	Japanese Aerospace Exploration Agency
UNCCD	United Nations Convention to Combat Desertification
DLDD	Desertification Land Degradation and Drought
CMIP5	Coupled Model Intercomparison Project Phase 5
DAA	Drought-affected Areas
IRIMHE	Information and Research Institute of Meteorology, Hydrology, and Environment
SSMR	Scanning Multi-Channel Microwave Radiometer
SSM-I-DMSP	Special Sensor Microwave Imager, Defense Meteorological Satellite Program
TMI-TRMM	Microwave Imager, Tropical Rainfall Measuring Mission
AMSR-E-EOS	Advanced Microwave Scanning Radiometer – Earth Observing System
MIRAS-SMOS	Microwave Imaging Radiometer using Aperture Synthesis, Soil Moisture, and Ocean Salinity
MARCC	Mongolia Assessment Report on Climate Change
ECV	Essential Climatic Variable
NAMHE	National Agency of Meteorology, Hydrology and Environment Monitoring of Mongolia
LP DAAC	U.S Land Processes Distributed Active Archive Center
CDF	Cumulative Distribution Function
NS	Nash – Sutcliffe
PDF	Probability Density Function
EnMAP	Environmental Mapping and Analysis Program
SIF	Solar Induced Fluorescence
GPP	Gross Primary Production

LIST OF FIGURES:

Chapter 1

Chapter 2

Chapter 3

Chapter 4

Chapter 5

LIST OF TABLES:

Chapter 2

Chapter 3

Chapter 4

Chapter 5

APPENDIX

ABSTRACT

Soil moisture plays an essential key role in the assessment of hydrological and meteorological droughts that may affect a wide area of the natural grassland and the groundwater resource. The surface soil moisture distribution as a function of time and space is highly relevant for hydrological, ecological, and agricultural applications, especially in water-limited or drought-prone regions. However, gauging soil moisture is challenging because of its high variability. While point-scale in-situ measurements are scarce, the remote sensing tools remain the only practical means to obtain regional and global-scale soil moisture estimates.

A Soil Moisture and Ocean Salinity (SMOS) is the first satellite mission ever designed to gauge the Earth's surface soil moisture (SM) at the near-daily time scales. This work aims to evaluate the spatial and temporal patterns of SMOS soil moisture, determine the effect of the climate extremes on the vegetation growth cycle, and demonstrate the feasibility of using our drought model (GDI) the Gobi Drought Index. The GDI is based on the combination of SMOS soil moisture and several products from the MODIS satellite. We used this index for hydro-meteorological drought monitoring in Southwestern Mongolia.

Firstly, we validated bias-corrected SMOS soil moisture for Mongolia by the in-situ soil moisture observations 2000 to 2015. Validation shows satisfactory results for assessing drought and water-stress conditions in the grasslands of Mongolia. The correlation analysis between SMOS and Normalized Difference Vegetation Index (NDVI) index in the various ecosystems shows a high correlation between the bias-corrected, monthly-averaged SMOS and NDVI data ($R^2 > 0.81$). Further analysis of the SMOS and in situ SM data revealed a good match between spatial SM distribution and the rainfall events over Southwestern Mongolia. For example, during dry 2015, SM was decreased by approximately 30% across the forest-steppe and steppe areas. We also notice that both NDVI and rainfall can be used as indicators for grassland monitoring in Mongolia.

The second part of this research, analyzed several *dzud* (specific type of climate winter disaster) events (2000, 2001, 2002, and 2010) related to drought, to comprehend the spatial and temporal variability of vegetation conditions in the Gobi region of Mongolia. We determined how these extreme climatic events affect vegetation cover and local grazing conditions using the seasonal aridity index ($_aAI_Z$), NDVI, and livestock mortality data. The NDVI is used as an indicator of vegetation activity and growth. Its spatial and temporal pattern is expected to reflect the changes in surface vegetation density and status induced by water-deficit conditions. The Gobi steppe areas showed the highest degree of vulnerability to climate, with a drastic decline of grassland in arid areas. We found that under certain *dzud* conditions, rapid regeneration of vegetation can occur. A thick snow layer acting as a water reservoir combined with high livestock losses can lead to an increase of the maximum August NDVI. The snowy winters can cause a 10 to 20-day early peak in NDVI and the following increase in vegetation growth. However, during a year with dry winter conditions, the vegetation growth phase begins later due to water deficiency and the entire year has a weaker vegetation growth. Generally, livestock loss and the reduction of grazing pressure was played a crucial role in vegetation recovery after extreme climatic events in Mongolia.

At the last stage of our study, we develop an integrated Gobi drought index (GDI), derived from SMOS and LST, PET, and NDVI MODIS products. GDI can incorporate both, the meteorological and soil moisture drought patterns and sufficiently well represent overall drought conditions in the arid lands. Specifically, the monthly GDI and 1-month standardized precipitation index SPI showed significant

correlations. Both of them are useful for drought monitoring in semi-arid lands. But, the SPI requires in situ data that are sparse, while the GDI is free from the meteorological network restriction. Consequently, we compared the GDI with other drought indices (VSWI, NDDI, NDWI, and in-situ SM). Comparison of these drought indices with the GDI allowed assessing the droughts' behavior from different angles and quantified better their intensity.

The GDI maps at fine-scale (< 1km) permit extending the applicability of our drought model to regional and local studies. These maps were generated from 2000 to 2018 across Southwestern Mongolia. Fine-scale GDI drought maps are currently limited to the whole territory for Mongolia but the algorithm is dynamic and can be transported to any region. The GDI drought index can be served as a useful tool for prevention services to detect extremely dry soil and vegetation conditions posing a risk of drought and groundwater resource depletion. It was able to detect the drought events that were underestimated by the National Drought Watch System in Mongolia.

In summary, with the help of satellite, climatological, and geophysical data, the integrated GDI can be beneficial for vegetation drought stress characterization and can be a useful tool to monitor the effectiveness of pasture land restoration management practices for Mongolian livelihoods. The future application of the GDI can be extended to monitor potential impacts on water resources and agriculture in Mongolia, which have been impacted by long periods of drought.

Chapter 1 General Introduction

1.1 Introduction

Mongolia is located in north-east Asia and is bounded between 41°35’ - 52°06’N latitudes and 87°47 - 119°57’E longitudes. The total area of the country is 1,562,950 km^2, with an average altitude of 1,580 meters above sea level. This is the world's second-largest landlocked country with high mountains (up to 4,380 m) covering its northern and western regions and the Gobi Desert in the south. The country is located in a transition zone at the crossroads of the northern Asia and Boreal Arctic regions where the Siberian Taiga meets the Asian deserts and steppe. The mean annual temperature is -8 °C (in the northern areas) and 6 °C (in the southern areas) and the average annual precipitation lies between 50 mm (in the Gobi Desert) and 400 mm (in the northern mountainous area) (Batima P et al., 2005). Mongolia has six natural zones based on the next vegetation types: such as high mountains, taiga, forest-steppe, steppe, semi-desert, and the Gobi Desert zones (Figure 1.1). The dry and cold climate and geographical features of Mongolia are associated with the fragility of natural ecosystems (Ministry of Environment, 2009). Forests cover is limited to the Khangai, Khuvsgul, and Khentii mountainous regions in the north and on the hillsides of the Mongolian Altai and Gobi Altai mountains.

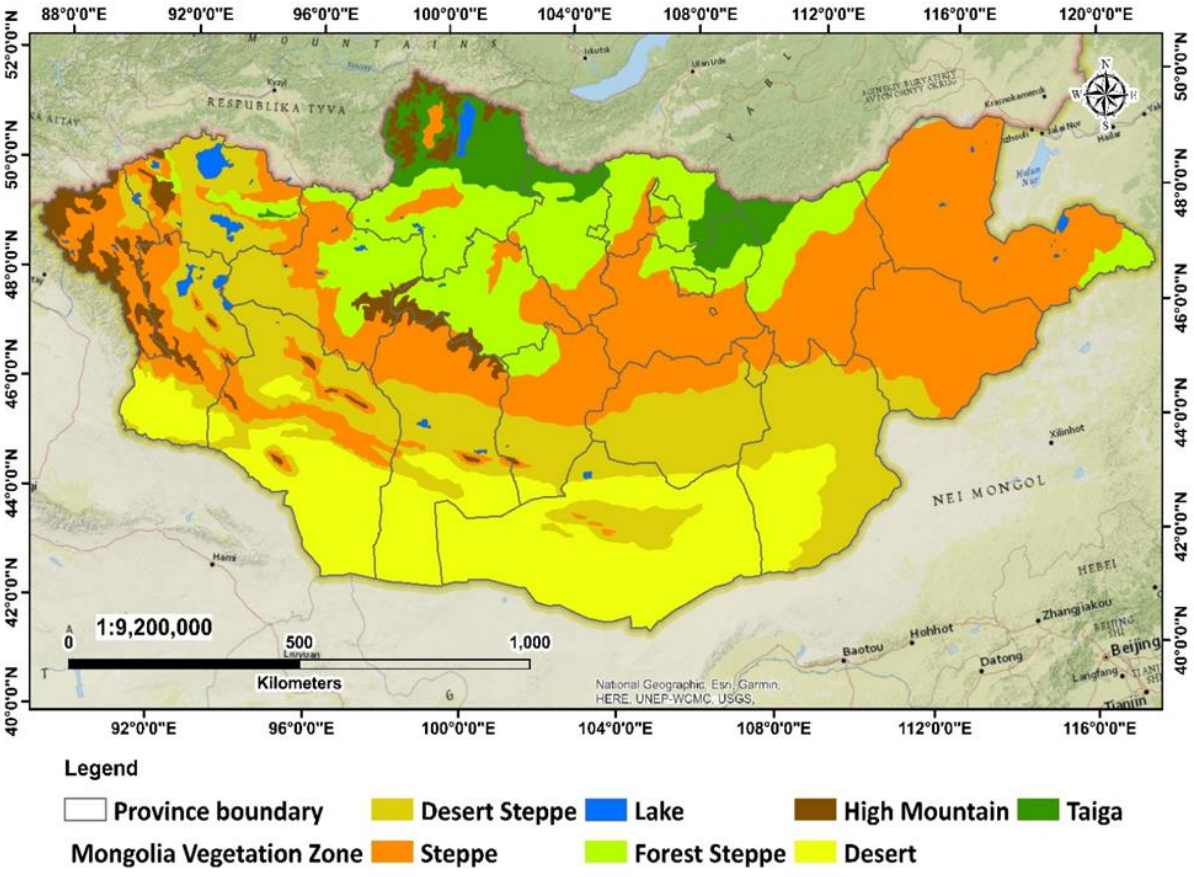

Figure 1.1 Natural ecozones of Mongolia. Data source: (Information And Research Institute Of Meteorology, Hydrology And Environment of Mongolia, 2019)

Mongolia is a country of pastoralists. Here over 71 million head of livestock are herded, providing a livelihood for one-third of Mongolia's population and support for the national economy *National Statistical Office of Mongolia : Annual reports* (2019). The livestock is herded in open pastures by nomadic pastoralists who migrate seasonally due to climatic variability, natural conditions, and water availability (Fernandez-Gimenez, 2000). The pastoralist depends directly upon natural resources for their livelihoods and is vulnerable to the impacts of climate change (Fernández-Gimenez et al., 2012). Increases in extreme weather events are the principal phenomenon that can increase the vulnerability of peoples dependent on weather conditions (Downing, 1991).

The climate change issue has become one of the most important global environmental challenges facing humanity, social-economic structures, and ecosystems (Miao et al., 2020a; Sathaye et al., 2006). The effects of global warming in Mongolia have been already occurring with an annual average air temperature rose by 2.4° C between the years 1940 and 2018, which was higher than the global average temperature rise of 0.85° C (Sustainable Adapted Use the Crop, 2020). Warming combined with variable precipitation can lead to land surface drying and will potentially increase the incidence and severity of droughts. One of the most significant impacts of climate change is an increase in the intensity and frequency of extreme climate events (Beniston et al., 2007). The occurrence of such events has been rapidly increased (Batima P et al., 2005; Oyudari Vova et al., 2020). Subsequently, drought is to become a major natural disaster in Mongolia (Nandintsetseg & Shinoda, 2013b). Approximately 88 % of the territory of Mongolia is considered agricultural land, of which 98 % is pasture as the main source of livestock grazing. Less than 1 % of the country's territory is arable land (Rasmussen & Annor-Frempong, 2015). A drought directly influences livestock production, economic losses, and accelerates the processes of desertification by destructive human activities (i.e., overgrazing) (Chang et al., 2021), and natural ecosystem demise (Punsalmaa Batima et al., 2013).

Soil moisture (SM) is an important variable influencing hydrological and meteorological exchange processes at the land surface (Awe et al., 2015; Robinson et al., 2008; D. Zhang et al., 2015; D. Zhang & Zhou, 2016). It is used to indicate drought in grassland because the water content is an essential factor for vegetation growth (W. Palmer, 1965a; Takagi & Lin, 2011). Drought and excessive heat conditions cause significant losses of crop yield and negatively impact vegetation biomass. Natural processes like erosion, drought, flooding, and evaporation are directly or indirectly driven by soil moisture. Reliable soil moisture information contributes to improving the accuracy of weather and climate hazards forecasting. It is difficult to continuously monitor SM on a large scale, due to scarce SM stations. In particular, the spatial distribution of soil moisture with high-resolution images in Mongolia has been one of the basic problems in remote sensing, agricultural, meteorological, and environmental communities. On the other hand, the lack of SM measurements makes it challenging to validate remote sensing SM estimates over the large territory of Mongolia. The soil moisture product is a potential input variable for numerous geophysical applications including the drought indices that have been widely used for drought monitoring. In drought-prone areas (e.g., Mongolian grassland), the appropriate methods for regional SM assessment are still needed for the improvement of drought monitoring.

1.2 Research objectives

This work aims to develop an integrated method, which is based on the set of indices that can be used to characterize meteorological and hydrological drought conditions in the Southwestern Mongolian grassland.

Overall objectives:

i. To evaluate spatial and temporal changes of soil moisture related to drought in the Mongolian grassland

ii. To examine how the climate extremes such as drought and *dzuds* impact the vegetation growth cycle

iii. To establish a new model as a tool for the assessment of spatial and temporal patterns of meteorological and hydrological drought severity in Southwestern Mongolia.

The objectives (i) and (ii) were addressed in Chapters 3 and 4, and the objective (iii) was addressed in Chapter 5.

1.3 Overview of the thesis

This section provides an overview of the content of each chapter of the dissertation. This thesis is a cumulative version of my work. It is divided into 6 chapters, of which chapters 3, 4, and 5 have been written in the form of scientific manuscripts.

This thesis analyzes spatial and temporal changes of grassland drought by the integration of different remote sensing products and approaches on the regional scale. Finally, it presents a model that assesses meteorological and hydrological droughts by characterization of the vegetation and soil moisture conditions. The thesis is structured into six main parts (chapters).

Chapter 1 presents a basic background of the research proposal development. A brief introduction of the research problem and objectives are put forward. The main concept, literature review, and methodologies are also introduced in this chapter.

Chapter 2 provides information about the research area, including location, geographical characteristics, soil type, and other social and economic conditions of our study area in the southwestern part of Mongolia.

Chapter 3 focuses on the evaluation of spatial and temporal patterns of SMOS SM related to hydrological drought on the regional scale. The spatial and temporal SMOS SM moisture analysis is conducted in the Uvurkhangai, Arkhangai, Bayankhongor, and Gobi-Altai provinces of Southwestern Mongolia. The validation of SMOS SM has been conducted through in-situ SM observations measured at the National Meteorological stations of Mongolia. Specifically, we compared Soil Moisture and Ocean Salinity (SMOS) first passive L-band satellite data with in situ measurements and investigate whether in situ and remotely sensed data in the unaccounted areas of Southwestern Mongolia are consistent with each other. We corrected biases of SMOS soil moisture (SM) data using the in situ measured soil moisture with both the simple ratio and gamma methods and verified the bias-corrected SMOS data with Nash–

Sutcliffe method. Our analyses showed that bias correction enhanced the reliability of the SMOS data, resulting in a higher correlation coefficient between in situ data and remote sensing products. Both, the SMOS and in situ measured soil moisture data show that for the period 2010 to 2015, spatial soil moisture distribution matches the rainfall events pattern in Southwestern Mongolia. The results of this Chapter confirmed that the bias-corrected, monthly-averaged SMOS data has a high correlation with the monthly-averaged normalized difference vegetation index NDVI (R^2 > 0.81). For the first time in the grassland of Mongolia, the SMOS SM product was quantified in the areas with heterogeneous vegetation zones and applied for investigation of the soil moisture droughts.

Chapter 4 analyses the effects of *dzud*-related factors (e.g., summer drought and winter heavy snowfall) on the vegetation growth cycle in the subsequent year. This chapter comprehends the mechanical concept of dzud after droughts. Using Moderate Resolution Imaging Spectroradiometer MODIS-NDVI data (2000 – 2013), we show how vegetation responds to various *dzud* situations. Subsequently, we assess the impact of drought (using such climatic variables as Seasonal Aridity Index ($_aAI_z$) (Munkhtsetseg et al., 2007), precipitation, and temperature) on vegetation throughout the *dzud* period. We assessed the vegetation NDVI from MODIS products, spatiotemporal NDVI variations after *dzud* events, and quantified the length of the growing season during the *dzud* period. The extreme climate event (drought - *dzud*) was investigated in this Chapter.

Chapter 5 focuses on the development of the meteorological and hydrological regional drought index (we named it the Gobi Drought Index, GDI). The GDI is based on multiple remote sensing products with a high contribution of the satellite SMOS SM and the Moderate Resolution Imaging Spectroradiometer (MODIS) data. It was found that the GDI is an effective tool for a new drought model for monitoring hydrological and meteorological drought conditions in semi-arid regions. The Multiple Linear Regression (MLR) method was used for the estimation of the GDI parameters. The approach is based on the combination of the satellite SMOS SM data, the MODIS-based land surface temperature (LST), normalized difference vegetation index (NDVI), and potential evapotranspiration (PET) products. The established GDI demonstrates considerable relationships with other remote sensing-derived drought indices. We also analyzed the efficiency of these indices, using the in-situ SM observations as a reference for validation. The validation is based on the relationship between standardized precipitation index SPI and in-situ soil moisture (SM) observations, and their comparison to remote sensing (RS) – derived indices. Moreover, in a selected region, we compared the GDI monitoring results with the past and actual drought intensity reported by the other hydro-meteorological drought indices and data recorded at the national meteorological sites. Our findings indicated that the GDI drought mapping confers advantages in the accuracy and spatial resolution for drought monitoring. Furthermore, it has significant potential for grassland drought detection in the semi-arid grassland of Mongolia that is not covered by in situ observations.

Chapter 6 summarizes the main conclusions of this work, states its limitations, and gives a brief outlook on possible further research.

Results of this research demonstrate that:

- SMOS SM data can be used alone or in conjunction with other parameters in estimating meteorological and hydrological droughts.
- SMOS SM data reflects well the in-situ SM observations.
- The drought (GDI) index was established on the combination of SMOS SM and NDVI, LST, PET data. The drought model resulting in hydrological processes and the spatial-temporal pattern of the regional drought was assessed. The spatial pattern of GDI follows the general precipitation trend across the region.
- The variables that we integrated to generate the GDI (SMOS SM, NDVI, LST, and PET) can examine the state of soil moisture and vegetation and the role of temperature and evaporation for specific Gobi regions. The GDI combines essential factors for the determination of drought triggers, thus it is an efficient index for monitoring meteorological and hydrological drought in different ecological zones.
- Compared with a standardized precipitation index SPI index and other remote sensing derived indices, the integrated GDI could characterize the soil moisture depletion and vegetation stress due to evaporation and spatial heterogeneity of regional drought.
- The proposed drought monitoring approach can provide technical support for a comprehensive understanding of drought, it may be related to climate change and, therefore, be used to relieve future drought disasters.

Separately, in our study, we advanced in the clarification of the role of *dzud* climate drivers. We assessed the relationship between the seasonal aridity index and summer NDVI (as a proxy for vegetation conditions) and found a significant relationship. The summer conditions represented by seasonal aridity index and drought risk have an impact on livestock mortality, which is heightened by *dzud.*

1.4 Concept, literature review, and methodologies

Drought is considered a natural hazard that devastates impacts on regional agriculture, economic losses, water resources, and the environment, with extending impacts in an increasingly globalized world (Sternberg, 2011). According to the United Nations Convention to Combat Desertification (UNCCD, 2018) as a result of global warming and climate change, about 40 % percent of the world population was affected by water scarcity and 85.5 % of livestock losses are related to drought conditions (*The ripple effect: A Fresh Approach to Reducing Drought Impacts and Building Resilience | UNCCD*). The lack of precipitation and high evapotranspiration have caused increasing aridity and resulted in widespread land degradation, soil erosion, and severe water scarcity (Miao et al., 2020b; Musolino et al., 2017). Droughts are among the most damaging natural hazards in terms of economic cost (Wilhite, 2000b) and social problems, such as hunger and loss of life.

Drought can lead to widespread plant death and restrict the geographical distribution of plant species (Gang et al., 2016; Sala et al., 1988; Tilman & El Haddi, 1992; M. Zhao & Running, 2010). Thus, droughts can be regarded as one of the disturbances of ecosystem structure and function. Drought-related vegetation stress can have many serious ecological consequences. The impact of drought on vegetation can have substantial serious water resource implications as the use of limited surface and groundwater supplies to support agricultural crop production competes against other sectoral water interests (Wardlow et al., 2012). The ecological and economic systems can be disrupted by drought.

From the 1970s to the early 2000s, the total percentage of Earth's land area affected by serious drought has more than doubled (J. Huang et al., 2017a). The drylands of the globe continue to be the most vulnerable, threatened by desertification, land degradation, and drought (DLDD). A study on changes in vegetation and climate over dryland areas of China during the late Holocene showed a drying trend, although the responses were regionally diverse during the early Holocene (Y. Zhao et al., 2009).

Land degradation is a global phenomenon with 78 % of total degraded land located in terrestrial ecosystems[1] (United Nations General Assembly, 2011). As global temperature rises, potential evapotranspiration (PET) and soil moisture demand become an increasingly important factor in the severity of drought and represent serious threats to ecosystems and societies (Hessl et al., 2018). The European Commission reported that the frequency of droughts has already increased and will further increase (Georgi et al. 2012). Anthropogenic factors of climate change will also speed up the droughts. Different disciplines, e.g., water resource management and agriculture, focus on different variables of the hydrological cycle, soil moisture, and vegetation growth respectively. This was also led to the classification of droughts into four types: meteorological, agricultural, hydrological, and socio-economic droughts (Wilhite & Glantz, 1985a). The translation of a drought signal from deviating meteorological conditions into soil moisture and/or hydrological drought has been identified as drought propagation (W. Wen et al., 2016). Because drought propagation strongly depends on climate and catchments' characteristics, hydrological drought shows a pronounced variation globally (Van Lanen et al., 2013). Investigations on drought have resulted that the catchment-scale studies confirm that climate seasonality can lead to severe drought events. However, there is a limited number of such studies because their geographical reference is limited to individual catchments or regions (Van Loon et al., 2014)

A term associated with dryland is aridity. This signifies a permanent water deficiency closely related to strong insolation, high temperature, and the deficit of water. Evapotranspiration (ET) is a key variable of the terrestrial water balance. It describes the exchange of water between the land surface including plants and the atmosphere (Crocetti et al., 2020). Dryland is defined by the PET ratio, as referred to by the Aridity Index (AI) (J. Huang et al., 2017a). The studies on PET show that aridity has increased globally and this drying will continue because of global warming, especially over drylands (Dai & Zhao, 2017; Jianping Huang et al., 2016; Scheff & Frierson, 2014; Trenberth et al., 2014). Several studies emphasized that warming across all semiarid regions may be also related to other parts of the Earth (Guan et al., 2015; J Huang et al., 2017b). Interannual variations and probability distributions of temperature were closely related to the high frequency of extreme climate events and indicating the increasing probability of dry winters and summer droughts (Y.C. Zhang & Zhang, 2005).

Studies of soil moisture changes based on the global climate models indicate severe drying trends and increased frequency of droughts (Sheffield & Wood, 2008; G. Wang, 2005; T. Zhao & Dai, 2015). A land surface temperature (LST) is defined as a fundamental parameter in the physics of surface energy and water balance ("Taking the Temperature of the Earth," 2019). It serves as a proxy for assessing evapotranspiration, vegetation water stress, soil moisture, and thermal inertia (Karnieli et al., 2010). The surface drying trend induced by increased evaporative demand (i.e., PET) would reduce the surface soil moisture more rapidly than in the deeper layers of the soil. Furthermore, the deep soil layer could

[1] UN General Assembly, 2012. High-level meeting on addressing desertification, land degradation and drought in the context of sustainable development and poverty eradication. A/65/861

become increasingly dry particularly in the growing season related to the temperature increase (Schlaepfer et al., 2017). The soil moisture and temperature response contribute substantially to the amplified warming during the hottest days (Kala et al., 2016; Vogel et al., 2017). Thus, clear SM drying signs were observed over transitional areas between dry and wet regions (Cheng & Huang, 2016). The variation of SM and its response to vegetation biomass are important for water resources and hydro-meteorological drought monitoring in semi-arid lands (Rodriguez-Iturbe, 2000).

Understanding and monitoring the drought stress of vegetation is a critical component of proactive drought planning designed to mitigate the impact of this natural hazard. Comprehensive approaches that characterize the spatial extent, intensity and duration of drought-related vegetation stress provide essential information for a wide range of management and planning decisions. For instance, such information could be used by agricultural producers and water resource managers to adjust crop irrigation schedules and by ranchers to determine stocking rates and grazing rotations for livestock.

This knowledge also helps natural resource managers to carry out best management practices under drought conditions and to other decision-makers to improve target assistance and response activities (e.g., the release of Conservation Reserve Program grasslands for emergency grazing or early detection of hot spots for wildfires) in a real-time manner. The satellite-based remote sensing data provide a fast and economic source of information to monitor and estimate the extent of drought, land cover classification, biophysical estimates, and vegetation phenology (L. Wang & Qu, 2007). Besides, the ground condition manifests the overall effect of rainfall and soil moisture, thus, satellite-based monitoring plays a significant role in drought monitoring and early warning system (Fekade Mekuria, 2012; Vicente-Serrano et al., 2010). Up to now in Mongolia, there are no spatial-temporal continuous soil moisture products that satisfy the needs of meteorology, hydrology, and drought monitoring due to the limiting of information about its spatiotemporal variations.

1.4.1 Soil Moisture and Satellite Observations and their use in Drought Applications

Soil moisture is defined as the amount of water stored in the unsaturated soil zone (Hillel, 1998). Extend research has shown that the spatial and temporal distribution of soil moisture is key to identifying Earth's hydrological and energy cycles (Seneviratne et al., 2010). Soil moisture (SM) has been identified as an essential climate variable for the Global Climate Observing System (GCOS) ((WMO) et al., 2006).

SM controls the partition between infiltration and runoff and impacts the potential rate of soil water uptake by vegetation. It controls plant water availability, the vegetation distribution, and is a critical factor controlling the net primary productivity of the planet. The state of soil moisture mainly depends on the balance of precipitation and evapotranspiration, as well as on the winter soil freezing and snow melting (Nandintsetseg & Shinoda, 2011a). There are various techniques to estimate soil moisture, including direct and indirect methods. It can be measured or estimated in various ways such as through in situ measurements (using climate stations and ground measurements), and by costly direct measurement in the field (by gravimetric method) (Rahimzadeh-Bajgiran & Berg, 2016). There are also indirect SM observations through satellite images. The uncertainty introduced by global climate change brings into question the temporal stability of model parameters (Peel & Blöschl, 2011), which can be better calibrated by the incorporation of soil moisture data (Koren et al., 2008). The benefits of soil moisture data have already been proven for many geophysical applications using in situ measurements with poor spatial representativeness (Koren et al., 2008) or at coarse spatial resolution (Bolten & Crow, 2012; Walker & Houser, 2001). The observations show that in the warm season, total

soil moisture is significantly decreasing from the north to the south of Mongolia (Oyudari Vova, Kappas, & Emam, 2019).

1.4.2 Satellite Soil Moisture observations and Soil Moisture Retrievals

A microwave part of the electromagnetic spectrum is well suited for remote sensing of the Earth surface conditions because the longer wavelengths are known to penetrate clouds and rain (Janssen, 1994). The most common frequencies for the remote sensing of soil moisture are 3.9-5.75 GHz (C band) and the longer wavelength 0.39-1.55 GHz (L band). Microwave energy at the L band is particularly well suited for the SM remote sensing because it easily penetrates short and moderate vegetation cover and thus, theoretically, is assumed to be free of interference (Yann H. Kerr et al., 2010). The land surface interacts with microwave energy, both active and passive ways.

The microwave energy directly interacts with a solid vegetation structure. The microwave signal is determined by the physical structure of vegetation and by the vegetation water content (Wigneron et al., 2007). The microwave signal passes through greater amounts of vegetation causing greater attenuation of the soil moisture signal and larger influence of the vegetation signal, respectively (Yann H. Kerr et al., 2012). Active microwave remote sensing consists of the use of synthetic aperture radars (SAR), which illuminate the surface with radar pulse and which thereafter backscatters to the satellite for analyses. This remote sensing approach provides high resolution, but signal interference, having multiple radar reflections, results in a noisy signal. The SAR use is also limited by long revisit periods and high energy requirements that limit the operational cycle for each orbit (Albergel et al., 2009). Passive radiometers observe the microwave energy that is naturally emitted or reflected by the Earth's surface. This allows for higher radiometric accuracy and less interference with microwave signals, which poses a physical limitation for satellites (Yann H. Kerr et al., 2010). The results have a coarse spatial resolution (~ 40 km), although the satellite revisits time can be as little as three days at the equator. Despite the low resolution, the short revisit times of radiometers and scatterometers are better suited for operational hydrological and geophysical applications.

Subsequently, remote sensing techniques have been used for estimating soil moisture at a global and regional scale. Contemporary, available soil moisture products are retrieved from various remote sensed sensors, such as the Soil Moisture Ocean Salinity (SMOS) from the European Space Agency (ESA), the Soil Moisture Active Passive (SMAP) from the National Aeronautics and Space Administration (NASA), and the Advanced Microwave Scanning Radiometer-Earth observing system (AMSR-E) from the Japanese Aerospace exploration agency (JAXA). The active and passive approaches offer various advantages because of their instrumental characteristics (Kolassa et al., 2017). In this research, we focused on satellite observations from the European Space Agency (ESA) Soil Moisture Ocean Salinity (SMOS) mission, which was launched in November of 2009. SMOS L-band microwave mission is the first directly designed for the remote sensing of soil moisture. The SMOS L-band frequency (1.4 GHz) offers global coverage with a spatial resolution of approximately 40 km with a revisit time of 3 days. SMOS provides brightness temperature measurements of the soil with different incidence angles, with an accuracy target of 0.04 m^3 m^{-3} (Kerr et al., 2010).

Most SMOS calibration and validation efforts have been focused on the validation of L2 soil moisture products. SMOS retrievals have been validated in the United States (Collow et al., 2012; Jackson et al., 2011), Canada, Europe, Australia, and East Asia (H. Kim & Choi, 2015; Kornelsen & Coulibaly, 2014; Schlenz et al., 2012). Furthermore, it was demonstrated that assimilation of soil moisture information from satellite retrievals improves the accuracy of land surface models (Draper et

al., 2012), weather prediction (De Rosnay et al., 2013), drought monitoring (Ahmadalipour et al., 2017; Chakrabarti et al., 2014), and flood forecasting (Niko Wanders et al., 2014). Most satellite observations of soil moisture have a spatial resolution of 25 – 40 km. To overcome this impediment, much attention was directed to the downscaling of satellite observations (González-Zamora et al., 2015; Sanchez et al., 2012). The satellite source may have biases affecting land surface or hydrological drought monitoring models. Thus, the bias correction technique is an important and necessary step of the remote sensing analysis (Abbaspour et al., 2009; B. K. Mishra et al., 2018) (Chapter 3).

1.4.3 Impact of drought in Mongolia

A number of studies were carried out on drought monitoring in Mongolia (N. K. Davi et al., 2006; Dorjsuren et al., 2016a; Sternberg, 2018). Impacts of intensifying drought and desertification processes and their feedback mechanisms on a regional climate in Mongolia have been significantly increased during the last thirty years (*THIRD NATIONAL COMMUNICATION OF MONGOLIA Under the United Nations Framework Convention on Climate Change*). In this context, regional temperatures of Southern Mongolia have also increased by 0.1° C – 3.7 °C and spring precipitation has decreased by 17 % (Chang et al., 2017a). A recent study demonstrated that in the Gobi region, intensive drought in the spring and summer seasons can occur four times every five years (Karrouk, 2007). Nanzad et al. (Nanzad et al., 2019b) showed that about 41 - 57 % of the country was affected by mild to severe droughts for the last seventeen years. Consecutive severe drought events in 2002, 2005, 2007, 2010, 2013, and 2015 severely affected the spring wheat production (Fao, 2017). Numerous investigations in Mongolia have shown the effect of drought not only on agriculture productivity and hydrological resources but also on natural vegetation conditions (Dorjsuren et al., 2016b). Dry summers and droughts decrease pasture productivity by 12 to 48 % in the high mountains and by 28 to 60 % in the Gobi desert-steppe regions (Punsalmaa Batima, 2006). Also, herders keep complaining that climate extremes increasingly influenced their pasture quality and livelihoods (Fernández-Giménez et al., 2015, 2017, Tumenjargal et al. 2020).

Shifts and precipitation decline in arid lands, signify an increase in the occurrence of dust events, which in turn, decreases the relative humidity via the semi-direct effect on dry land. Indeed, rainfall has become shorter and lasted only for few hours with high intensity and low infiltration into the soil. This adversely affects the recharge of water resources in shallow wells and springs (Tumenjargal et al., 2020). Moreover, in case of a high level of pasture stress due to a drought scenario, all parameters of the pasture including carbon and nitrogen, and below-ground biomass will be substantially reduced. This proves that excessive intensity drought pressure has drastic negative impacts on soil and plant productivity. A recent study revealed that the vegetation heat supply at the Mongolian Plateau has increased, whereas, the crop yield limitation became more acute being associated with decreasing moisture supply (Liu et al., 2019). In this context, there is an urgent need to consider soil moisture as one of the substantial indicators of drought in order to better investigate the impacts of climate extremes. The current investigations suggested that variability in precipitation patterns and rising temperatures are the key factors of increasing climate severity in drylands, with extreme events more inclemently affecting Mongolian herders (N. Davi et al., 2010). It is important to have more detailed weather forecasts for the days with a sharp increase in dryness (Natsagdorj & Renchin, 2010), in all-natural zones including high mountains, taiga, forest-steppe, steppe, semi-desert, and desert.

1.4.4 A potential impact of severe winter conditions "*Dzud*" and their relation to drought events

"*Dzud*" in Mongolian, characterizes the cumulative consequences of natural hazards that result in mass destruction of livestock due to poor forage available to livestock and extremely cold winter that undermine the livelihood security of herders (Farkas & Kempf, 2002). Several studies substantiate that in arid and semi-arid climatic zones which have vulnerable ecosystems from droughts, the harsh winter "*Dzud*", and dust storms occur frequently (Nandintsetseg & Shinoda, 2011c; NYAMTSEREN et al., 2015; Sternberg et al., 2011). The local people stated that their environment has become more challenging due to frequent extreme winter events and drought.

Specifically, "*Dzud*" is attributed to changing weather patterns, shifts in pastoralism, lack of preparedness, socio-economic forces, and most frequent droughts (UNDP/NEMA, 2010), respectively. According to the national "*Dzud*" report, from 2009-2010 *dzud*, about 8.5 million livestock had perished. This was approximately 20 % of the country's livestock and affected 769,000 people or 28 % of Mongolia's population (Fernández-Gimenez et al., 2012). The *dzud* 2009-2010 was the most severe *dzud* that has occurred since the consecutive *dzud* winters of 1999-2002, as highlighted in red below (Figure 1.4.1).

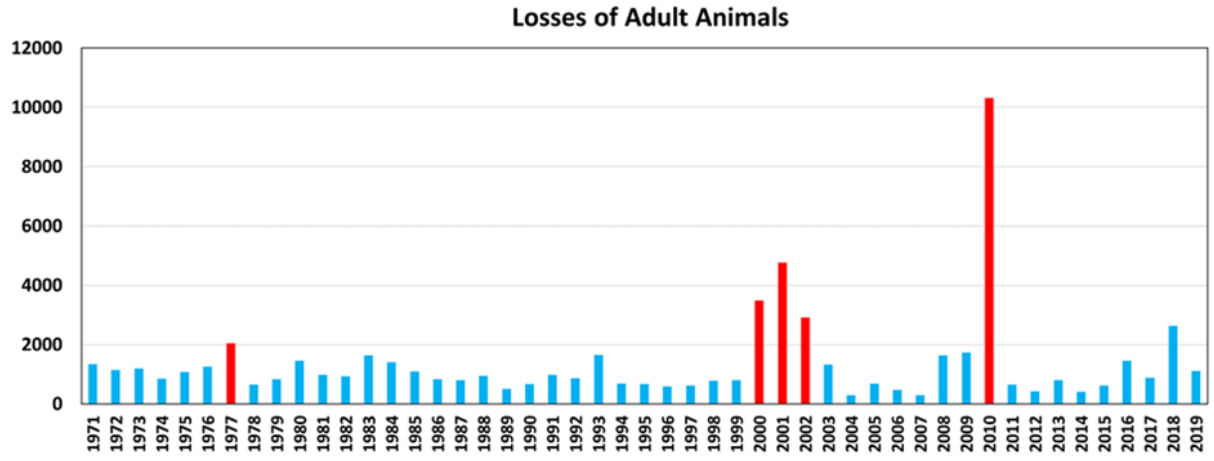

Figure 1.4.1 Losses of adult animals in Mongolia according to the National Statistical Office (National Statistics Office of Mongolia, 2019)

Several studies show that the *dzud* events have a severe impact on the present vegetation cover (Tumenjargal et al., 2020). For instance, these *dzud* events are visible in the Spot-VEGETATION-NDVI series, for the Mongolian annual average (Gutman et al., 2020). Projections for drought and *dzud* showed an increasing trend in summer and winter conditions defined by monthly air temperature and precipitation data for future climate change in Mongolia (Ministry of Environment, 2009) derived by Global Climate Models. Consequently, a considerable amount of works was done that assessed impacts of climate extremes (drought - *dzud*) on pastoral livestock (Nandintsetseg & Shinoda, 2013a; Tachiiri et al., 2008). The investigation of (Begzsuren et al., 2004) highlighted that the livestock does not and will not get enough strength to overcome subsequent *dzuds* during the drought years. Many herder households traveled long distances (up to 1 000 km) to collect hay in less affected areas (Fao, 2017). Besides, the unpredictability of pasture quality and resources, the danger of drought exacerbating extreme winter (*dzud*) conditions, and climatic limitations on potential agricultural production in the steppe zones aggravate the ongoing threat to livelihoods dependent on the natural

environment for sustenance and survival (Fassnacht et al., 2018; Fernández-Giménez et al., 2012). The study results of (Van Loon et al., 2014) demonstrated that the drought duration is related to seasonal precipitation. This implies that the effect of seasonality on drought propagation is stronger in cold-season climates. Seasonality would led to heavy severe drought conditions and modifies drought duration and water deficit.

Thus, keeping in mind that investigating the effect of climate extremes and seasonality, water cycle, and their relation to global warming is crucial for understanding and predicting drought durations and the future dryland climate changes (M. Shinoda et al., 2010a; Masato Shinoda & Morinaga, 2005) (Chapter 4).

1.4.5 In-situ based drought indices and their use in drought monitoring

Traditional meteorological drought indices include the Standardized Precipitation Index (SPI) (Mckee et al., 1993), and Palmer Moisture Anomaly Index (z-index) (W. Palmer, 1965b), and the classical Palmer Drought Severity Index (PDSI) (W. Palmer, 1965a). For instance, most studies applied climate parameters as indicators for drought, for example, Standardized Precipitation Index (SPI) (Ivits et al., 2014; Sternberg et al., 2009a), Standardized Precipitation Evaporation Index (SPEI) (Vicente-Serrano et al., 2013), or soil moisture (Nandintsetseg & Shinoda, 2011b; Masato Shinoda & Nandintsetseg, 2011). Usage of these characteristics assumes the following vegetation response during the previously detected climate extremes. (T. Zhao & Dai, 2015) analyzed the PDSI, the top-10 cm soil moisture content, and runoff directly from 14 CMIP5[2] models, of which at least nine models included the effect of stomatal closure under increasing CO_2 levels. Under a low-moderate emissions scenario, they found that aridity and the frequency of drought in the 21st century will increase with the soil moisture-based estimates being the largest. These aridity changes happened because the actual evapotranspiration is often limited by moisture availability in the soil. The ground station SM observations include single-point-based specific location measurements. These measurements are provided by the direct and most accurate method called the gravimetric method (Engman, 1991). However, the point scale SM measurement stations are scarce and their use is limited due to a large spatial scale that should be covered. The study of (Bayarjargal et al., 2006) suggested that the combination of satellite-derived drought indices effectively identifies wider drought-occurred areas better than the PDSI and traditional ground observed drought-affected areas (DAA) maps. Generally, the present soil moisture detection methods are based on fixed ground field observations, model simulations, and remote monitoring. The ground fixed-point observations can observe the soil moisture changes over time, but it is time-consuming, restricted by the conditions in the study area, and it is difficult to use them to describe the SM spatial variation. Drought monitoring model can demonstrate the temporal and spatial changes of soil moisture content, but the results are highly dependent also on the input parameters. The model drought indices ingest gridded terrestrial meteorological datasets and are widely used to observe meteorological droughts. However, they do not resolve local surface peculiarities or provide information regarding drought effects on vegetation because the actual soil moisture available for plant growth is represented only indirectly (Crocetti et al., 2020).

[2] Coupled Model Intercomparison Project Phase 5 (CMIP5) which provide a multi-model context 1) assessing the mechanisms responsible for model differences in poorly understood feedbacks associated with the carbon cycle and with clouds, 2) examining climate "predictability" and exploring the ability of models to predict climate on decadal time scales, and, more generally, 3) determining why similarly forced models produce a range of responses.

Except for the present study (Oyudari Vova, Kappas, & Rafiei Emam, 2019), as far as we know, there is no current research that inter-compares remote sensing retrievals of the L-band SMOS SM products with bias correction technique against in-situ SM observations across Southwestern Mongolia. We believe that this comparison will be a good option for remote sensing data validation in Mongolia (Chapter 3). Therefore, in this study, we choose the less-studied, most drought vulnerable region where satellite-based monitoring should play a crucial role in drought monitoring and early warning system (Gu et al., 2008a; Scaini et al., 2015a; Vicente-Serrano et al., 2012) (Chapter 5).

1.4.6 Satellite-based drought indices and their use in drought monitoring

Consequently, advances in remote sensing technologies revolutionized the field of drought monitoring by enabling continuous observations of key drought-related variables available over large spatial and temporal scales (West et al., 2019). The remote sensing data has improved the ability to track drought conditions, particularly in data-poor regions, provides surface soil moisture, evapotranspiration, and vegetation data (Anderson et al., 2007; Du et al., 2013; Enenkel et al., 2016). Available drought monitoring systems diagnose drought in a given area in various ways. For instance, the German Drought Monitor (Zink et al., 2016) uses a hydrological model driven by meteorological observations, estimates daily soil moisture, and then transforms it into a soil moisture index.

Concerning meteorological and hydrological drought assessment, the examination of satellite-based drought indices has become an important method when no field measurements, interpolation, or large-scale modeling are available or required. Numerous satellite-based indices have been widely used to detect and identify drought conditions globally. For investigating soil moisture and vegetation status under different climate conditions, several medium-resolution satellite data sets (e.g., SMOS, NOAA-AVHRR, Spot-VEGETATION, MODIS) were used in previous drought studies (Bento et al., 2018; Champagne et al., 2015; F. Kogan et al., 2004; Martínez-Fernández et al., 2015; Nilda Sánchez et al., 2016a; Tuvdendorj et al., 2019).

Regarding the drought-caused stress to vegetation, the extent of drought can be reflected by changes in vegetation indices. In most cases, agricultural drought affects vegetation, increases plant mortality, promotes poor vegetation health, and lowers yields. The most well-known such index is the normalized difference vegetation index (NDVI). It is the normalized difference between near-infrared (NIR) and red reflectance which is effectively used for drought monitoring (Ji & Peters, 2003; Karnieli et al., 2010; Tucker, 1979b). NDVI is a valuable index for identifying plant stress due to drought and can be used in pasture land, crop management, and monitoring of drought conditions (Bao et al., 2014; Dorigo et al., 2007) (Chapter 4).

Several indices based on NDVI have been applied for the identification of drought conditions at large and regional scales. For example, an integrated surface drought index (ISDI), composed of the NDVI and land surface temperature (LST) was developed by (Wu et al., 2013) and serves for agricultural drought monitoring in China. To assess the impacts of climate on vegetation, a vegetation condition index (VCI) was developed by (F. N. Kogan, 1995a). Visible and shortwave infrared drought index (VSDI) based on a combination of the blue, red, and shortwave infrared reflectance SWIR optical bands and the water-sensitive indices were purposed by (N. Zhang et al., 2013). Combining information from multiple near-infrared and short-wave channels into normalized multi-band drought index (NMDI), the authors of (L. Wang & Qu, 2007) concluded that their method is suited to estimate both soil and vegetation moisture. Solar Induced Fluorescence (SIF) is a relatively new emerging satellite product,

which provides information on photosynthetic activity versus NDVI, which is a greenness index. It serves as a strong proxy to gross primary production (GPP), capturing dynamic responses of vegetation to stressors such as drought and temperature.

Land surface temperature (LST) derived from thermal radiance bands is a good indicator of the energy balance of the land surface. Since temperature can rise quickly under water stress, a temperature condition index (TCI) developed by (F. N. Kogan, 1995b) can also be a good indicator of water stress and drought. The combination of different indices indicating vegetation stress, water deficit, and soil moisture status can describe changes in drought better than each index in isolation. Recently, a study showed that vegetation supply water index (VSWI), is a cost-effective method that can detect soil moisture changes in agricultural land (Toby N. Carlson et al., 1990). In several countries, the vegetation health index (VHI) was often used for agricultural monitoring assessments (Shen et al., 2019; Unganai & Kogan, 1998). The study by (Chang et al., 2017d) demonstrated that the normalized difference water index (NDWI) effectively detects drought conditions but only in forest-steppe areas in Mongolia.

Noteworthy, that all these indices were focused on drought research in different countries or regions. Due to the influence of factors such as atmospheric circulation, soil type, vegetation type, different growth periods in a forest, steppe, and semi-desert zones, the spatial and temporal characteristics of drought events are also different. Also, a reference to meteorological observations could moderate the spatial representativeness of these indices. This implies that satellite bands in different regions have different responses to drought conditions, and the degree of drought varies in different regions respectively (Vicente-Serrano et al., 2012) (Chapter 5). Generally speaking, drought monitoring that will reliably deliver timely information, extent, and intensity of drought, could help to reduce drought-related fatalities and economic losses (Wilhite & Rhodes, 1993). To serve (propose, improve) such monitoring is an overall objective of our study.

1.4.7 Methodologies in an overview

Surface soil moisture (SSM), vegetation indicator (NDVI), and Evapotranspiration (PET) play an important role in hydrological and meteorological drought assessment. The approach of this study was to validate the satellite data using in-situ observations, to produce a regional spatial pattern of soil moisture maps, and to quantify the regional hydro-meteorological drought conditions using these data.

We used a bias-correction technique (ratio and gamma distribution) to compare in situ SM measurements and remotely sensed SMOS SM data. Specifically, we determine whether in situ and remotely sensed data in Southwestern Mongolia are consistent with each other, by comparing SMOS passive L-band satellite data with in situ measurements. Verification of bias-corrected SMOS data was conducted by Nash–Sutcliffe method. In addition, the comparison results suggest that bias correction enhances the reliability of the SMOS data, resulting in a higher correlation coefficient with the in-situ observations. The bias-corrected SMOS soil moisture values of the topsoil layer were used for studying the spatial pattern of the SM change mapping (Chapter 3).

The assessed changes in drought characteristics were focused on the seasonal aridity index ($_{\alpha}AI_{z}$). Due to local arid climatic conditions, the modified seasonal aridity index was applied to detect the respective drought years. In our study, we tried to link spatially variable climatic circumstances with specific summer characteristics before *dzud* events. This approach is based on daily temperature and precipitation in the summer season. The $_{\alpha}AI_{z}$ was used to quantify the drought risk and periodic

NDVI temporal pattern. The analysis of the NDVI-based vegetation conditions after drought – *dzud* (i.e., the map of NDVI spatial pattern after drought -*dzud*) was used for projections of the future vegetation state (Chapter 4).

The multiple regression analysis was applied to develop the Gobi drought index (GDI). This model (as an indicator of drought) was used for the analysis of the drought occurrence and intensity in the Gobi region. The model shows how SMOS SM depends on NDVI, LST, and PET in the Gobi region. The model results were correlated with the standardized precipitation index SPI at the climate stations, other drought indices derived from satellite images, and in-situ SM data. Pearson's correlation coefficients were used. We have chosen six drought indices (SPI, TCI, NMDI, VSWI, NDDI, and NDWI) which are commonly used for the arid regions. The detailed information on this analysis is included in Chapter 5.

- **Statistical analysis**

During the validation of the SMOS soil moisture product, a bias correction technique was used to evaluate the differences between the SMOS and in situ SM data. The gamma and ratio method were used to assess the differences of bias-corrected SMOS and observed SM data between within two soil layers (Chapter 3). To characterize the meteorological and hydrological drought conditions in Chapters 3, 4, and 5, we used Pearson correlation analysis, student-T test, Nash Sutcliffe model efficiency coefficients and applied them to meteorological and several RS-based drought indices.

- **Geographical information systems and remote sensing**

Geographical Information System (GIS) and Remote Sensing (RS) play an essential role in this study. Various input data were extracted from RS resources such as spatiotemporal soil moisture (SMOS SM), MODIS products, vegetation (NDVI), precipitation and temperature (CRU), elevation (DEM), GDI drought index maps. The research also used map data from different formats and coordinate systems. All maps were created, analyzed, and stored in the ArcGIS software format. Two types of GIS data were used in this study (i.e. spatial databases and attribute data). The details of both the GIS and RS methods are described in each chapter of this thesis.

- **Multiple Linear Regression Model (MLRM)**

Regression analysis is a statistical method used to estimate the quantitative relationship between two or more variables. Multiple linear regressions are the commonly used strategies in many applications. In this method, the researcher uses several explanatory variables to predict the outcome of a response variable. The goal of MLR is to model the linear relationship between the explanatory (independent) variables and response (dependent) variables (Tranmer & Elliot, 2008). The coefficient of determination (R^2) is a statistical metric that is used to measure how much of variation in the response variable output can be explained within the linear approximation by the variations of independent variables. R^2 always increases as more predictors are added to the MLR model, even though the predictors may not be related to the output variable (Islam & Tiku, 2005). R^2 can only be between 0 and 1, where 0 means that the response variable cannot be predicted by any of the independent variables, and 1 indicates that the MLRM output reproduces the response variable without error by the linear combination of the independent variables (Uyanık & Güler, 2013). In this dissertation, the dependent (response) variable in MLRM was SMOS SM and independent variables were NDVI, LST, and PET from MODIS products. The model was used to develop a drought model in the Gobi region of Mongolia.

The impact of drought on grassland and monitoring of drought is a process that comprises a great number of attributes and requirements across multiple levels. Therefore, the estimation of regional drought conditions can be adjusted based on a multiple linear regression model (MLRM). This model developed by linear regression analysis is frequently used in meteorological and hydrological drought modeling (Anshuka et al., 2019; Bayissa, 2018; S. W. Kim et al., 2020; Ribeiro et al., 2019) and ecological studies. It is intended to use with different goals and aspects in mind. In Chapter 5, we describe in detail how the drought model was developed by using the MLR analysis that incorporated different remote sensing products. Multiple regression model allows an analyst to define (predict) a drought based on SMOS SM and the MODIS-provided multiple explanatory variables.

Chapter 2 Overview of the research area

The study region comprises the central-southwestern part of Mongolia, with a particular focus on the Arkhangai, Uvurkhangai, Bayankhongor, and Gobi-Altai aimags (administrative province of Government of Mongolia), with a total size of 376.408 km^2 (Figure 2.1). The climate of Mongolia is characterized by high continental semi-arid to arid conditions. From north to south, the climatic zones, the ecological zones, and relief characteristics vary considerably. However, the study regions are the most vulnerable to climate change and climate extremes such as drought - *dzud* (Johnston, 1992; Wen & Fu, 2000). About 79 % of the area is characterized as agricultural land, including pasture and meadowlands (National Statistical Office of Mongolia, 2019). The west to east trending "Valley of Gobi" with Buun Tsagaan Nuur (269 km^2) and Orog Nuur (106 km^2) lies between the Khangai Mountains and the Gobi – Altai in the south. The altitude of the study area ranges from sea level to 4000 m.a.s.l. (Khangai Mountain).

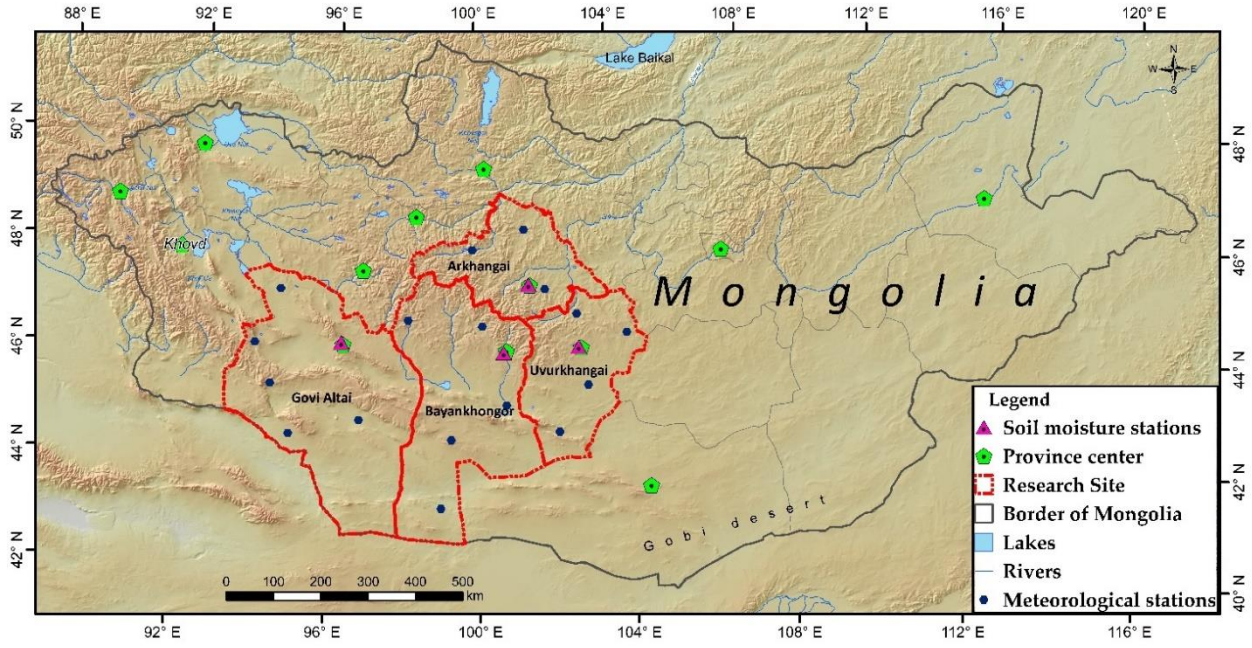

Figure 2.1 Geographical location of meteorological stations with SM measurements in Bayankhongor, Uvurkhangai, Arkhangai, and Gobi-Altai Provinces. Map includes province boundaries, meteorological stations (blue color), and in situ SM measurement stations (pink color). Data source: Information and Research Institute of Meteorology, Hydrology, and Environment (IRIMHE) of Mongolia (Information And Research Institute Of Meteorology, Hydrology And

Environment). Digital Elevation Model (DEM) from SRTM (Shuttle Radar Topography Mission) data (Shuttle Radar Topography Mission).

An annual average temperature range between -2 °C to 3.3 °C from 2000 to 2014 (Figure 2.2) (O. Vova, Kappas, & Emmam, 2019). The average annual temperature of the last 15 years (2000 – 2014) is higher than the temperature from 1985 to 1999. The mean annual precipitation range resides between 108 mm in the southern desert regions and up to 400 mm in the northern steppes from 2000 to 2014 (Figure 2.2). During the winter season, the Siberian high-pressure cell produces cold and dry weather. Most rainfall occurs between June and September. The seasonal precipitation distribution is characterized by 70 – 80 % of the annual precipitation falling during the summer months (Lehmkuhl et al., 2018). Steppe lies in the northwest of the study area, whereas the southern part encompasses the Gobi Desert and has a very dry climate. Nationwide, the vegetation cover of the forest-steppe, steppe, and Gobi desert is 53 %, 25 %, and 15 %, respectively (Gunin et al., 1999). The soil type of the steppe areas is mainly Kastanozems and Chernozems. The desert area soil types are Calcisols, Solonetz, and Solonchak, while the northern part of the mountain areas has Phaeozems and Cambisols. The soils are frozen from late November to the middle of March.

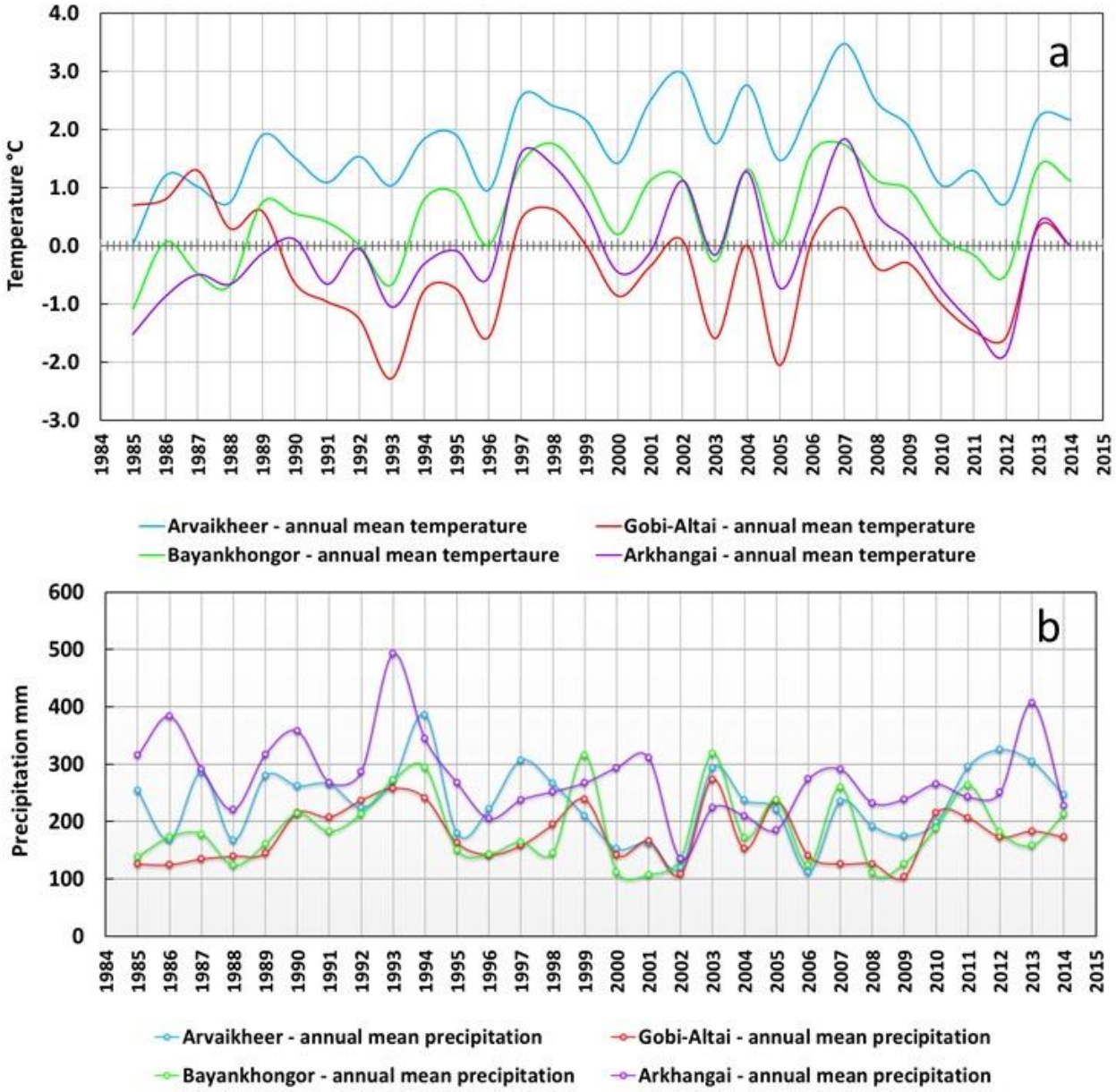

Figure 2.2 Mean annual temperature (a) and mean annual precipitation (b) of Southwestern Mongolia (1985 - 2014). Data source: (Information And Research Institute Of Meteorology, Hydrology And Environment of Mongolia).

The locations of the SM sampling stations have been categorized into four natural zones: forest-steppe, steppe, High Mountain, and desert (Table 2.1). The SM measurements were made at vertical layers of soil from 10 to 15 cm depth. For this research, in situ SM measurements, climate data, and soil maps were provided by the Institute of Meteorology and Hydrology of Mongolia.

Table 2.1 Meteorological and in situ measured SM data stations with information on location, elevation, natural zone, and soil types.

Station number	Station Name	Province Name	Lat (°N)	Long (°E)	Soil Type	Elevation (m)	Natural Zone
287	Bayankhongor	Bayankhongor	46.192	100.718	Kastanozems haplic	1860	Steppe
277	Altai	Gobi-Altai	46.373	96.257	Chernozems calcic, Calcisols haplic	2147	High mountain and desert
288	Arvaikheer	Uvurkhangai	46.266	102.778	Kastanozems haplic	1831	Steppe
281	Tuvshruulekh	Arkhangai	47.388	101.906	Kastanozems haplic	1900	Forest-steppe

Figure 2.3 displays the soil type map of the research area. In situ SM measurements data has been taken from four different stations in different aimags at the uncultivated land (natural rangeland). The southern region of the study area is the semi-desert area, characterized by very sparse vegetation cover (shrubs) where agriculture and pasture fodder for livestock herds is scarce. The northern-central region is more humid than the southern areas and has forest-steppe and steppe.

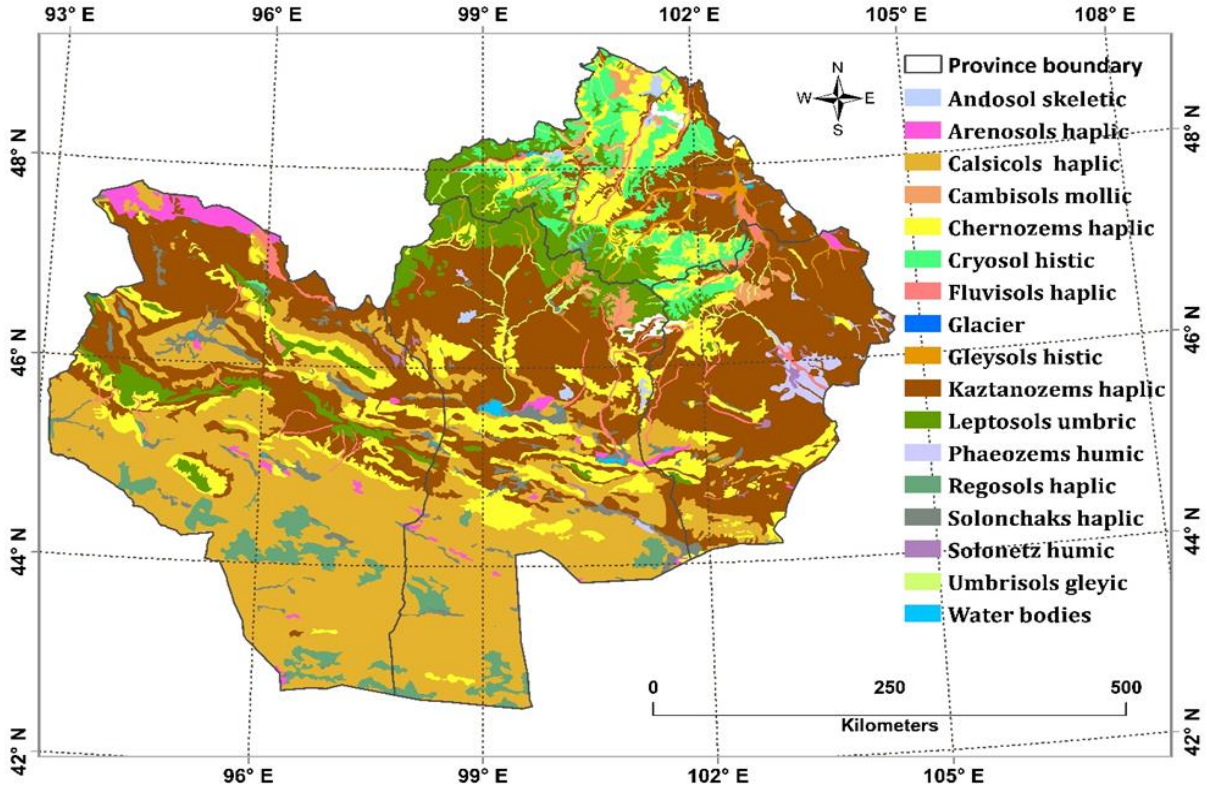

Figure 2.3 Soil type map of Southwestern Mongolia. Data source: (Information And Research Institute Of Meteorology, Hydrology And Environment of Mongolia, 2019).

The following three chapters (3 through 5) comprise three papers published (Chapters 3 and 4) or submitted (Chapter 5) by the thesis author. Because these papers were submitted separately, the defendant apologizes for redundancy in introductions, the study area, and methods descriptions in these three Chapters. This redundancy and the respective overlaps with the content of Chapters 1 and 2 of this Thesis are inevitable.

Chapter 3 Comparison of Satellite Soil Moisture Products in Mongolia and Their Relation to Grassland Condition

Oyudari Vova [1,] *, Martin Kappas [1], Ammar Rafiei Emmam[1]

[1] Cartography, GIS and Remote Sensing Department, Institute of Geography, University of Göttingen, 37007 Göttingen, Germany

* Correspondence Author

This chapter was published as a research article: Journal of Land 2019, 8(9), 142; DOI: https://doi.org/10.3390/land8090142

3.1 Abstract

Monitoring soil moisture dynamics provides valuable information about grassland degradation since soil moisture directly affects vegetation cover. While the Mongolian soil moisture monitoring network is limited to the urban and protected natural areas, remote sensing data can be used to determine the soil moisture status elsewhere. In this paper, we determine whether in situ and remotely sensed data in the unaccounted areas of Southwestern Mongolia are consistent with each other, by comparing Soil Moisture and Ocean Salinity (SMOS) first passive L-band satellite data with in situ measurements. To evaluate the soil moisture products, we calculated the temporal, seasonal, and monthly average soil moisture content. We corrected the bias of SMOS soil moisture (SM) data using the in situ measured soil moisture with both the simple ratio and gamma methods. We verified the bias-corrected SMOS data with Nash–Sutcliffe method. The comparison results suggest that bias correction (of the simple ratio and gamma methods) enhances the reliability of the SMOS data, resulting in a higher correlation coefficient. We then examined the correlation between SMOS and Normalized Difference Vegetation Index (NDVI) index in the various ecosystems. Analysis of the SMOS and in situ measured soil moisture data revealed that spatial soil moisture distribution matches the rainfall events in Southwestern Mongolia for the period 2010 to 2015. The results illustrate that the bias-corrected, monthly-averaged SMOS data has a high correlation with the monthly-averaged NDVI ($R^2 > 0.81$). Both NDVI and rainfall can be used as indicators for grassland monitoring in Mongolia. During 2015, we detected decreasing soil moisture in approximately 30% of the forest-steppe and steppe areas. We assume that the current ecosystem of land is changing rapidly from forest to steppe and also from steppe to desert. The rainfall rate is the most critical factor influencing the soil moisture storage capacity in this region. The collected SMOS data reflect in situ conditions, making it an option for grassland studies.

Keywords: *SMOS; soil moisture; statistics methods; Nash–Sutcliffe; NDVI; precipitation*

3.2 Introduction

Soil moisture (SM) is an essential indicator of the hydrologic cycle that can affect vegetation growth, impacting both global agriculture and grassland condition (D'Odorico et al., 2007; N. Wanders et al., 2014). These impacts significantly concern herders in Mongolia, who depend on the pastureland for their livelihood. Mongolia is located in the Silk Road Economic Belt and has a high amount of grassland, most of which is used for pastoral purposes, which makes up a significant amount of the economic activity there (Yang et al., 2016). Soil moisture can be used to evaluate drought risk and grassland conditions in these arid lands. Accurate soil moisture data is necessary for short and long-term monitoring of grassland development. One previous study determined that 90% of pastureland in Mongolia is vulnerable to land degradation and desertification and that 72% of that total territory is degraded to some degree; slight, moderate, severe, and severely degraded grassland occupies 23%, 26%, 18%, and 5% of the vulnerable pastureland, respectively (Batkhishig, 2013). Climate change and overgrazing have caused significant grassland degradation in semi-arid regions (Emam et al., 2015; Kawamura et al., 2005; Sekiyama et al., 2014).

Multiple analyses have compared satellite SM data to in situ SM measurements (Champagne et al., 2016; A. Souza et al., 2018; Zeng et al., 2015). As point measurements, in situ measurements cannot necessarily be applied to a large area, and are difficult to obtain in high-altitude areas where few ground stations are available. Remote sensing data is beneficial for retrieving spatial and temporal soil moisture measurements over large and mountainous areas. SM derived from remote sensing only applies to up to the first five centimeters of soil depth, depending on the soil characteristics (Jonard et al., 2018). de Beurs et al. and Wessels et al. have found that vegetation changes, increasing temperatures, decreasing rainfall, and larger livestock populations have led to droughts and grassland degradation (de Beurs et al., 2015; Wessels et al., 2007). Several remote sensing vegetation indices, e.g., Normalized Difference Vegetation Index (NDVI), Enhanced Vegetation Index (EVI), and Soil-Adjusted Vegetation Index (SAVI) are widely used to assess changes in vegetation (Sternberg et al., 2015; Tucker et al., 1991; W. Zhou et al., 2015).

The Soil Moisture and Ocean Salinity (SMOS) satellite, the first and most successful space mission dedicated to monitoring global soil moisture, was launched in November 2009 (Y.H. Kerr et al., 2016; Yann H Kerr et al., 2010). The passive L-band (1.4 GHz) radiometer installed on this satellite acquires data for the entire globe every three days, with a spatial resolution of approximately 44 km. The overpass ascending time is 6:00 am local time and descending overpass time is 12 hours later (Yann H Kerr et al., 2012). Several studies have found that the quality and reliability of the SMOS products is sufficient (Bircher et al., 2012; Rüdiger et al., 2011; Schlenz et al., 2012), validation of SMOS SM data have been successful, and comparative analysis between SMOS data and in situ SM measurements have demonstrated a strong correlation (Marczewski & Łukowski et al., 2014). One study even suggested that there is no difference between using a SMOS-derived time series and the daily average of in situ SM measurements (Sanchez et al., 2012). Recent studies suggest that SMOS provides successful results for North America, Australia, and central Asia (Al-Yaari et al., 2014). The Soil Water Index (SWI), determined from SMOS products, has also been found to be an appropriate tool for drought monitoring (González-Zamora Ángel - Sánchez, Martínez-Fernández, José - Wagner, Wolfgang, 2016). A development overview of soil moisture studies from satellite sensors and their characteristics is summarized in Appendix A.

Accurate SM data collection depends heavily on atmospheric circulation and the weather. Previous research indicates that precipitation changes affect SM variability (Lindroth et al., 1998). The annual temperature in Mongolia has warmed by 2.1 °C from 1940 to 2007, which, according to climate

forecasts, will continue to rise to 3.1 °C above 1940 levels by 2050, as defined by the Mongolia Assessment Report on Climate Change (Ministry of Environment Mongolia, 2009). Many studies have attributed grassland degradation to climate and precipitation patterns like drought and winter precipitation (Ravi et al., 2010; H. Zhou et al., 2005). Few studies, however, have compared satellite SM products with in situ measurements in Mongolia. The SMOS SM data is an affordable indication of soil moisture and vegetation conditions, as well as drought monitoring (Usowicz et al., 2019). Further analysis is necessary to identify the importance of SM for the future status of grassland conditions and the preservation of ecological functions. The objectives of this study are: (1) To examine the spatial distribution of SMOS, SM, and Moderate Resolution Imaging Spectroradiometer (MODIS) NDVI and their relationship, and (2) compare satellite SMOS SM data with in situ measured SM data to evaluate grassland condition between 2000 and 2015 in Southwestern Mongolia.

3.3 Material and Methods

3.3.1 Study Area

The study area is located in central-southwestern Mongolia, consisting of four provinces Arkhangai, Uvurkhangai, Bayankhongor, and Gobi-Altai (Figure 3.1). From north to south, the climatic zones, the ecological zones, and relief characteristics vary considerably. The winter monthly average temperature is between −20 °C and −21 °C. The summer monthly average temperature is between 16 °C and 17 °C. Most rainfall occurs between June and September, showing an uneven distribution throughout the year. The altitude of the study area ranges from sea level to 4000 m.a.s.l. (Khangai Mountain). Steppe lies in the northwest of the study area, whereas the southern part encompasses the Gobi Desert and drier climate. The vegetation growing season is from April–September. The soil type of these regions is mainly Kastanozems and Chernozems. The soils are frozen from late November to the middle of March. The desert area soil types are Calcisols, Solonetz, and Solonchak, while the northern part of the mountain areas has Phaeozems and Cambisols. The southern region is almost exclusively a desert landscape, where agriculture and pasture fodder for livestock herds is scarce. These regions are more vulnerable to the impacts of climate change and droughts.

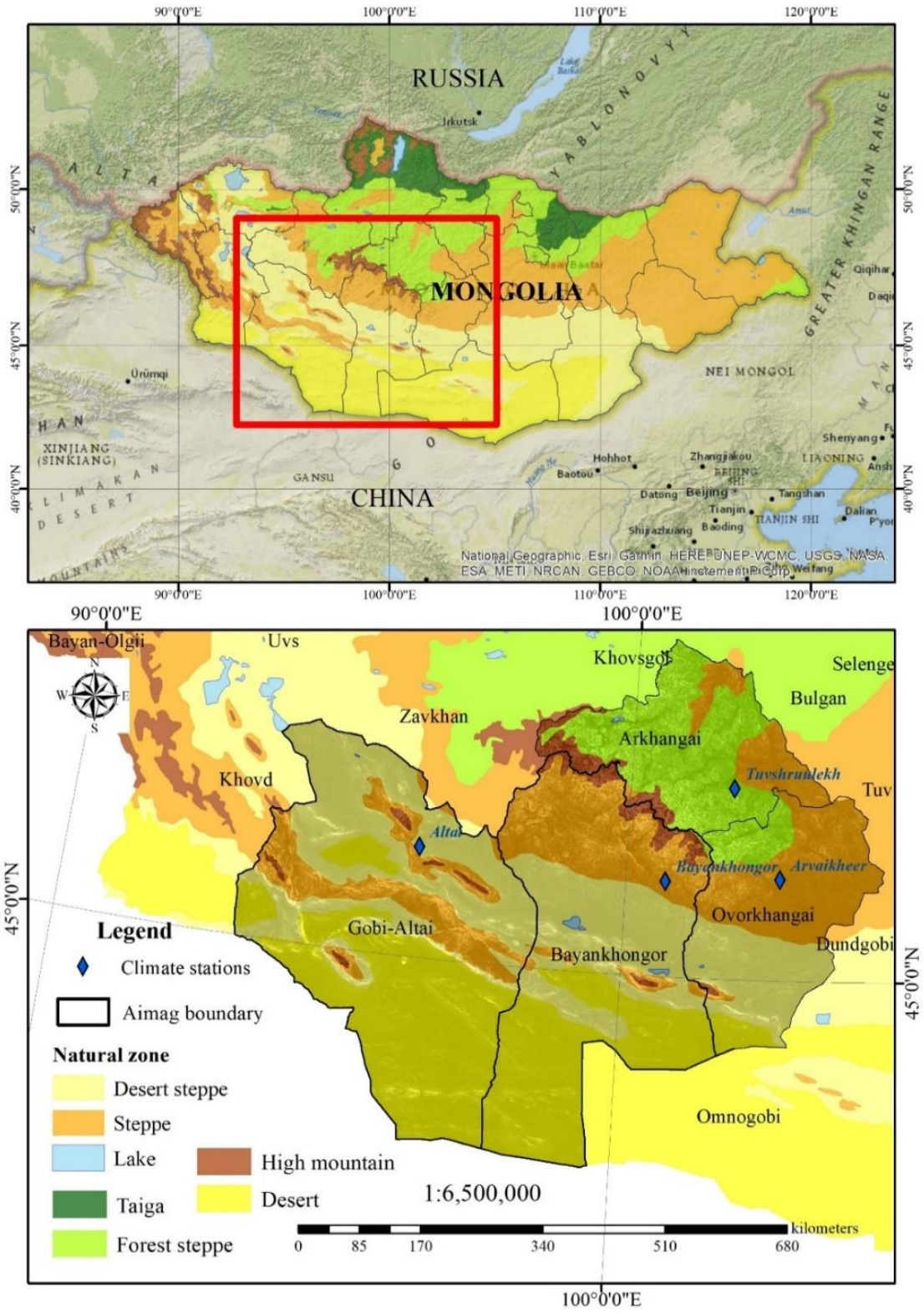

Figure 3.1 Meteorological stations of soil moisture (SM) measurements in Bayankhongor, Uvurkhangai, Arkhangai, and Gobi-Altai provinces, represent each of the zone elevations. The figure shows the province boundaries and in situ SM measurement stations (blue color).

In this study, in situ SM measurements, precipitation data, and soil maps were obtained from the Institute of Meteorology and Hydrology of Mongolia.

Table 3.1 In situ measured SM data stations with information on location, elevation, natural zone, and soil types.

Station code	Station name	Province name	Lat (˚N)	Long (˚E)	Soil type	Elevation (m)	Natural zone
287	Bayankhongor	Bayankhongor	46.192	100.718	Kastanozems haplic	1860	Steppe
277	Altai	Gobi-Altai	46.373	96.257	Chernozems calcic, Calcisols haplic	2147	High mountain and desert
288	Arvaikheer	Uvurkhangai	46.266	102.778	Kastanozems haplic	1831	Steppe
281	Tuvshruulekh	Arkhangai	47.388	101.906	Kastanozems haplic	1900	Forest-steppe

The locations of the SM sampling stations have been categorized into four natural zones: forest-steppe, steppe, High Mountain, and desert (Table 3.1). Nation-wide, the vegetation cover of the forest-steppe, steppe, and Gobi desert is 53%, 25%, and 15%, respectively ("Vegetation Dynamics of Mongolia," 1999). The SM measurements were measured at vertical layers of soil from 10 to 15 cm depth.

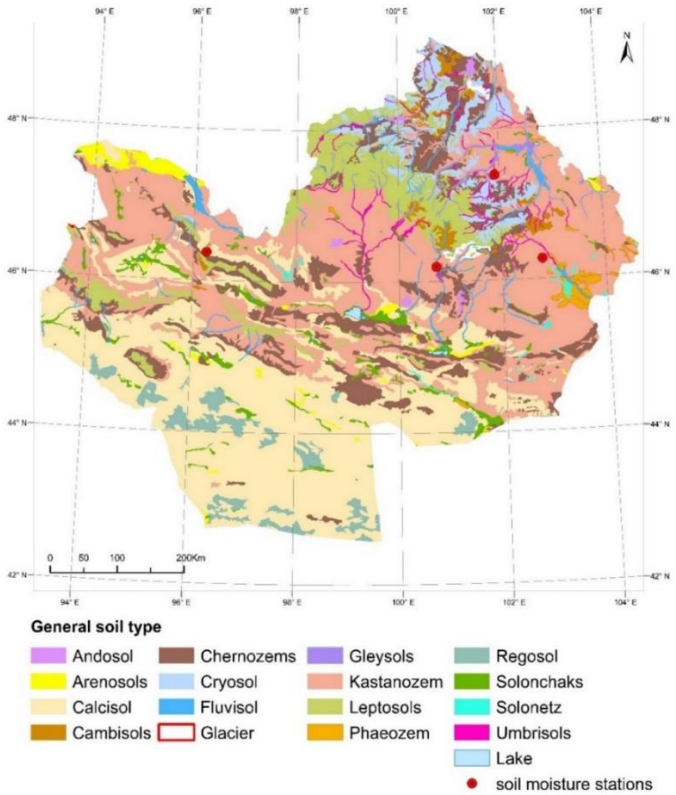

Figure 3.2 Overview of soil moisture stations and soil types in Southwestern Mongolia. Data is sourced from the Institute of Meteorology and Hydrology of Mongolia.

Figure 3.2 presents the soil type map of the study area. In situ SM measurements data has been taken from four different stations (provinces) and the uncultivated land (natural rangeland). The southern region of the study area is the desert steppe area, characterized by very sparse vegetation cover (shrubs), and the northern central region is more humid than the southern area and has forest-steppe and steppe.

3.3.2 Methods

In this study, the SMOS L2 SM products were compared with in situ SM measurements. An area of 1822 × 684 km was examined, comprised of 918 SMOS L2 datasets. The statistical calculation of SM distributions of this region was studied from June to October to determine monthly averaged SMOS SM data for 2010–2015. These periods correspond to spring, summer, and autumn. We validated the SMOS SM data to assess the grassland conditions. We also examined the bias-corrected SMOS SM and NDVI data temporally and spatially from 2000 to 2015. Figure 3.3 presents a framework of the study that comprises pre-processing and GIS data processing, image processing, bias correction, and the relationship between SMOS SM, rainfall, and NDVI.

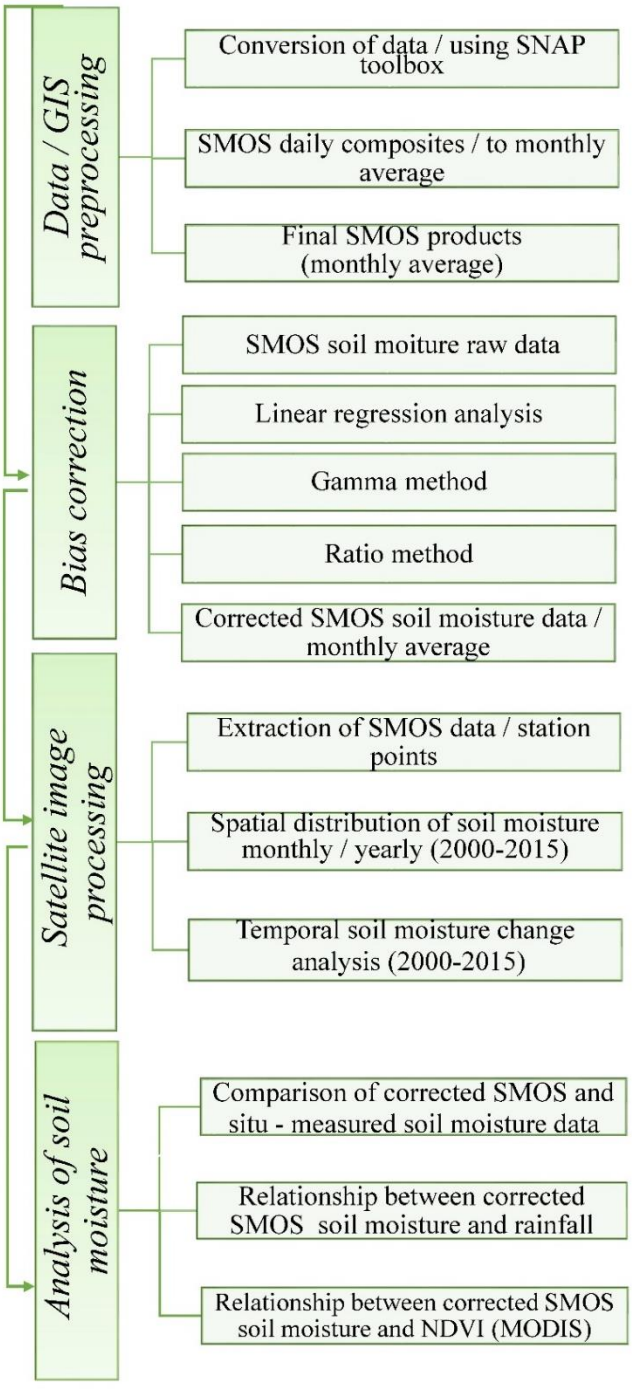

Figure 3.3 Flowchart of soil moisture evaluation steps.

3.3.2.1 Remote Sensing Data and Pre-processing

- **SMOS (SM Data)**

The SMOS L2 data from January 2010 to December 2015 were selected for the comparative analysis and to determine the SM distribution. The SMOS data was extracted using the ArcGIS tool "Extract multi values to point." The data available are daily values, the monthly averages, and three parts per month. To accomplish further analysis, SMOS SM measurements were provided three times per month (normally between the 29th and 8th, 9th and 18th, and 19th and 28th of every month) during the warm period of the

year, which runs from April until the end of October. The radiometric SMOS SM data with an average spatial resolution of 43 km. Since the SMOS satellite data cover a large spatial area, it appears more reasonable to use the monthly average values. The datasets are provided in the netCDF format, ranging from regional to global scales and at a temporal resolution of three days. For checking the accuracy of the data, the bias-correction technique was used for different evaluation aspects. The bias-correction technique emphasizes the statistical characteristics of data and successfully reduces the error in data outputs, and has become very popular for correcting biases in multiple datasets and analyses (Abbaspour et al., 2009; B. K. Mishra et al., 2018).

- **In Situ Measured SM Data (Observation Dataset)**

The National Agency of Meteorology, Hydrology, and Environment Monitoring of Mongolia (NAMHEM) provided SM datasets from four different stations. In situ SM measurements used in this research were collected from 2010 to 2015. At each SM station, they collected one sample with the gravimetric method and converted the values to volumetric water content (Saxton & Rawls, 2006). In situ measured SM data were obtained at a 10–15 cm depth at a monthly interval. For the majority of the stations, no data is available from April 8th and October 28th. For that reason, both these dates were excluded from the analysis.

- **MODIS NDVI Data (Vegetation Dataset)**

The Moderate Resolution Imaging Spectroradiometer (MODIS) NDVI data used in this study are version 5 MODIS/Terra and MODIS/Aqua 1 km resolution daily daytime products (MOD13A2). These products are freely distributed by the U.S. Land Processes Distributed Active Archive Center (Kamel Didan et al., 2015, *LP DAAC : NASA Land Data Products and Services*; Zhengming Wan, 2006). The Normalized Difference Vegetation Index (NDVI) computed from space-borne observations at visible infrared wavelengths has been widely used since the 1980s to study the vegetation changes, soil, and drought (Tucker, 1979a). The MODIS NDVI vegetation dataset used in this study is monthly averaged from 2010 to 2015. The NDVI was calculated using the following equation:

$$NDVI = (NIR - Red) / (NIR + Red),$$

where Red is the visible light of the red wavelength (from 400 - 700 nm) and NIR is the intensity of the near-infrared wavelength (from 700–1100 nm). The spectral reflectance ratios indicate the reflected radiation over the incoming radiation in each spectral band, therefore these values range from 0.0 to 1.0. Individual NDVI pixel values were extracted from the images at each station location. For further statistical analysis, we resampled the MODIS NDVI data resolution to SMOS pixel size. At the regional scale, grassland degradation has been monitored in semi-arid regions using vegetation indices derived from remote sensing.

3.3.2.2 Processing of the Soil Moisture

Both the SMOS datasets and the in-situ datasets were available in volumetric water content. Recently, the bias correction method is often used for validation and comparison analysis. The bias correction technique significantly reduces the error in data output and emphasizes the statistical characteristics of observation data. Because of the coarse spatial resolution of the SMOS data, we applied two statistical approaches, the simple ratio method and the gamma method (Abbaspour et al., 2009; B. K. Mishra et al., 2018; Rafiei Emam et al., 2017). The simple ratio method dictates that the

average SMOS SM for each month is divided by the corresponding in situ SM measurement. This factor is then multiplied by the daily SMOS SM data in order to receive a bias-free daily SM value. The gamma method is a bias-correction technique to decrease the biases in the SMOS SM data. The gamma distribution is a function of the probability density function (PDF) and the cumulative distribution function (CDF). More details about the bias technique can be found in (B. K. Mishra et al., 2018). Mishra et al. (2018) applied the bias correction technique to minimize the biases in the GCM precipitation data (B. K. Mishra et al., 2018). In substance, the two-parameter gamma distribution was employed for bias correction. Applying α and ß as shape and scale parameters, the gamma distribution can be expressed by probability density function (PDF) and the (CDF) as mentioned earlier (Equations (3.1) and (3.2)):

$$f(\mathcal{X}) = \frac{1}{\beta^{a}\Gamma(a)}\chi^{a-1}\exp\left(-\frac{\chi}{a}\right) \tag{3.1}$$

$$f(\mathcal{X}) = \int_{0}^{\chi} f(t)dt \tag{3.2}$$

where χ represents the monthly average SM for the range $0 < \chi < \infty$ and t is a dummy variable. Later, the bias-corrected SMOS SM data was evaluated by the Nash–Sutcliffe efficiency (NSE) and root mean square (R^2). We used the Web-based-Hydrograph Analysis Tool for our calculations (https://engineering.purdue.edu/mapserve/WHAT/cgi-bin/compute_r2_nash_sutcliffe.cgi). The tool is used in many cases of modeling to compute R^2 (Nash–Sutcliffe) coefficients to validate the model. This Web-based statistics module provides a tool for the computation of these coefficients. The NSE value ranges from $-\infty$ to 1, and the R^2 value ranges from 0 to 1.

3.4 Results

3.4.1 Temporal SMOS Soil Moisture (SM) Analysis

We compared SMOS SM data to the in-situ SM measurements and examined their relation to climate (e.g. rainfall). Figure 3.4 shows the density scatter plots, which provide a quantitative comparison between the SMOS SM after bias correction and in situ SM measurements for the entire five-year monthly SM mean value in Southwestern Mongolia (encompassing four different stations). The bias-corrected SM values are more consistent with in situ SM data than the original satellite SMOS SM products. The ratio method resulted in an R^2 = 0.81 in Bayankhongor, R^2 = 0.77 in Uvurkhangai, R^2 = 0.74 in Gobi-Altai, and R^2 = 0.60 in Arkhangai. The results suggest that SMOS SM data and precipitation time series show moderate compatibility. The monthly averaged SMOS SM data were strongly correlated with the average in situ SM measurements in the steppe and forest-steppe areas. These findings demonstrate that SM in these areas is relatively higher than SM in dry regions. In particular, 2012 was a relatively wet year in the provinces of Uvurkhangai and Arkhangai, when (on 19 July) SM reached a peak value of 16.8% and 15.9%, respectively. During the spring and summer, SMOS SM increased in May, reached a peak value in mid-July, and then began decreasing through the end of August. The consistency of this SM cycle between SMOS SM and in situ measured SM data implies that the absolute maximum reached at the end of July may be correlated with the vegetation development. However, the soil water that accumulated during the winter and spring precipitation events was sufficient for vegetation growth. Subsequently, the spatial distribution of SM depends on the soil parameters that were not distributed homogeneously in the study areas (soil texture, vegetation, and topography).

Figure 3.5 shows the density scatter plots that compare the SMOS SM data after the gamma distribution with in situ measurements. The gamma distribution algorithm successfully replicated in situ measurements. The bias-corrected SMOS SM data correlated well with the in-situ SM data for all stations: Bayankhongor (R^2 = 0.69), Uvurkhangai (R^2 = 0.83), Gobi-Altai (R^2 = 0.74), and Arkhangai (R^2 = 0.84). Most of the in-situ SM distribution was similar to the bias-corrected SMOS SM distribution, and thus met the primary conditions of the bias correction technique. According to Moriasi et al. (2007), the performance of the model is acceptable when the NSE and R^2 values are both greater than 0.5. Mostly, the greatest variations of SM were observed during October and April in both datasets. Assessment of gamma results indicates that, generally, strong correlations were noted for moist soils (Figure 3.5b, d), while lower correlations were noted for dry soils (Figure 3.5a, c). The results presented in Table 3.2 (as an example) show the summary of the gamma distribution algorithm applied in this study.

Table 3.2 Summary of statistical parameters (gamma distribution algorithm) applied for bias correction of SMOS SM data in this study.

Bias-correction (gamma distribution algorithm) Station 288/Arvaikheer	**In situ measurements (observation data)**	**SMOS data (raw)**	**SMOS data (corrected)**
Average moisture %	6.68	11.05	6.69
Standard Deviation	2.49	5.85	2.46
shape, alpha	7.19	3.57	7.39
scale, beta	0.93	3.09	0.91

a)

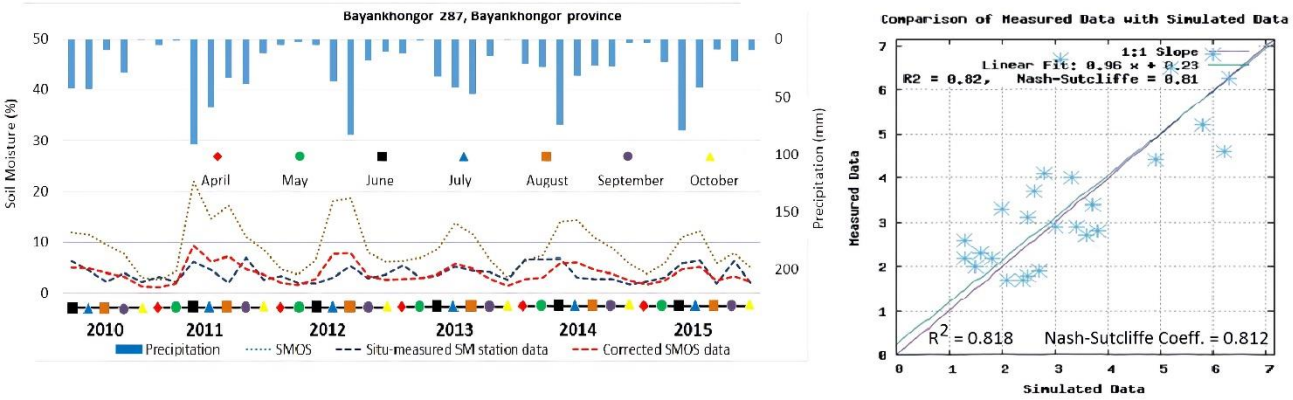

b)

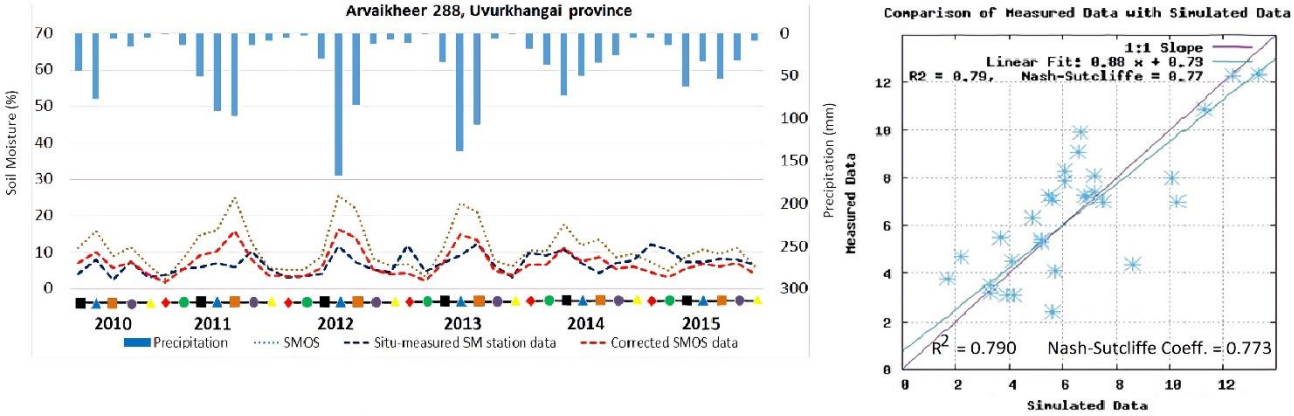

c)

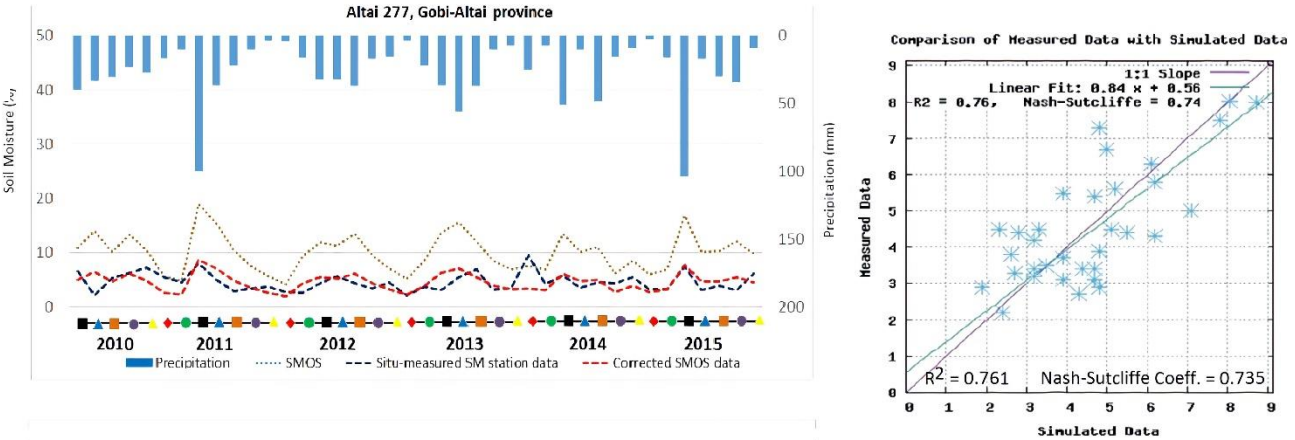

d)

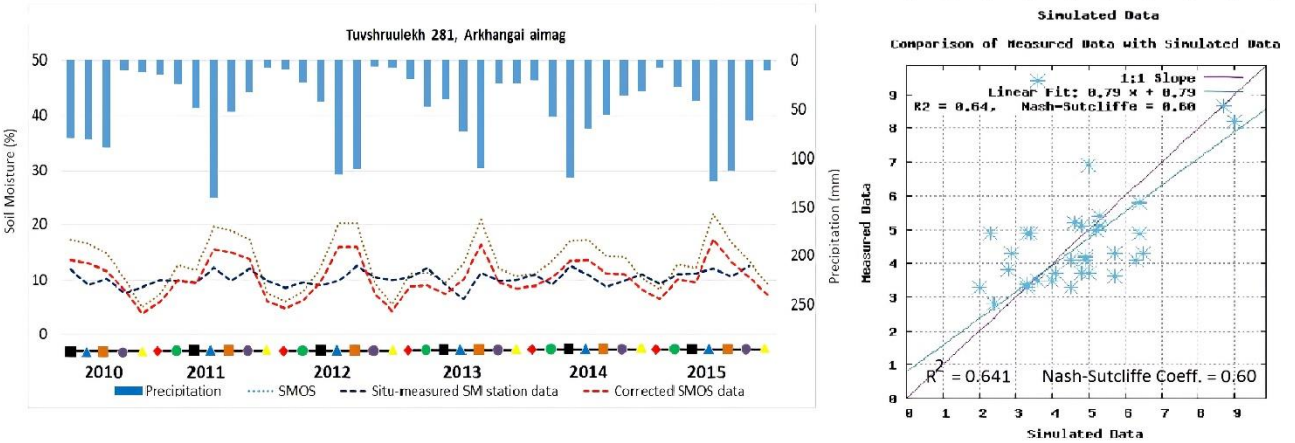

Figure 3.4 Result of ratio method and comparison of the in-situ measurements SM data, and Soil Moisture and Ocean Salinity (SMOS) bias-corrected SM, and antecedent precipitation for (a) Bayankhongor, (b) Uvurkhangai, (c) Gobi-Altai, and (d) Arkhangai provinces.

a)

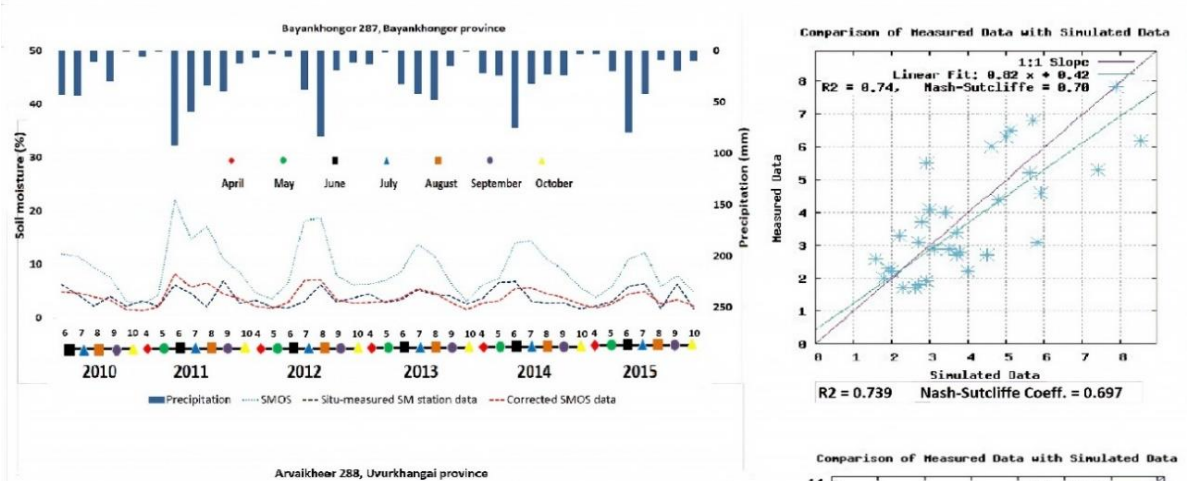

b)

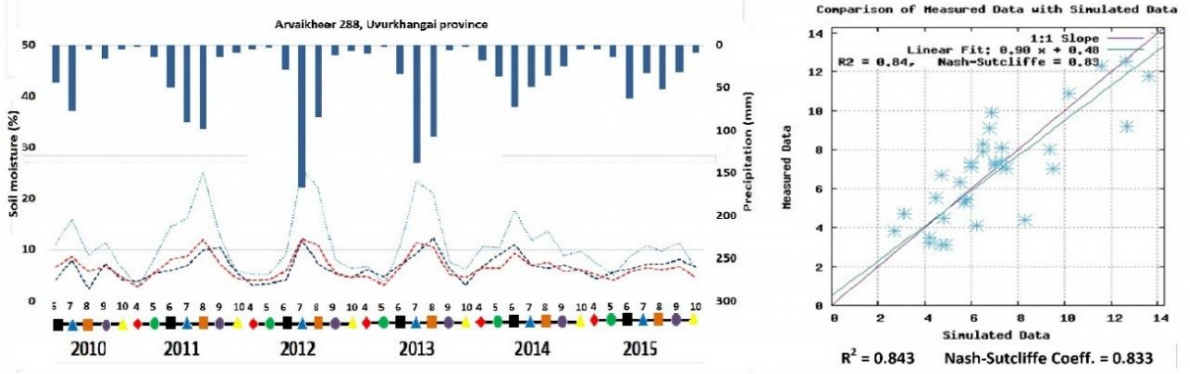

c)

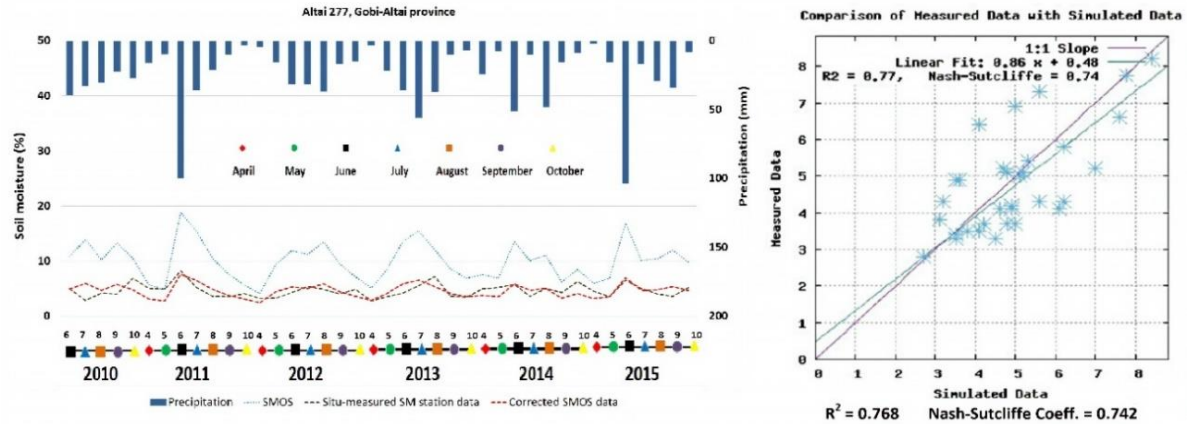

d)

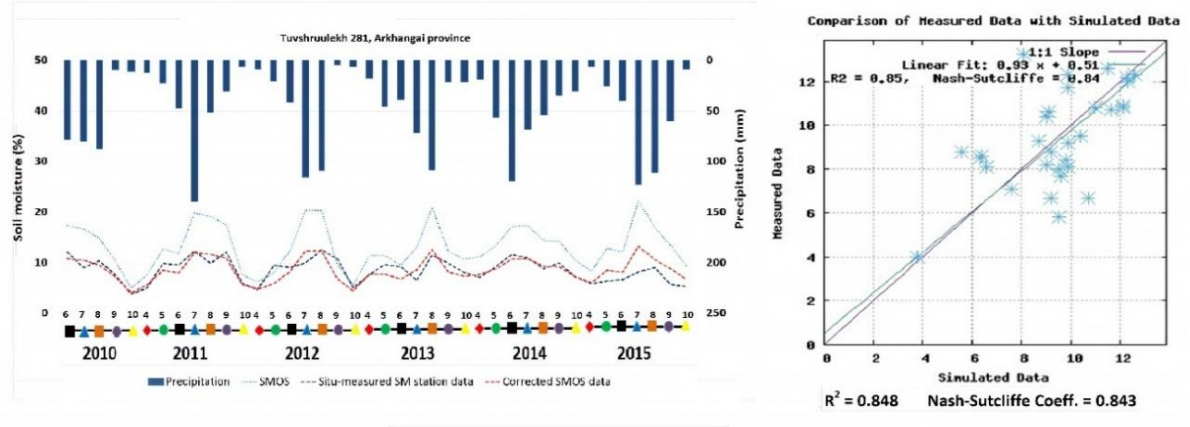

Figure 3.5 Result of gamma distribution method and comparison of the in-situ measurements SM data, and SMOS bias-corrected SM and antecedent precipitation for (a) Bayankhongor, (b) Uvurkhangai, (c) Gobi-Atai, and (d) Arkhangai provinces.

The bias-corrected SMOS SM data was applied to assess the grassland development status. Overall, the SMOS SM data show moderately good compatibility with expected relationships, in particular, increasing SM after rainfall. During the winter period, SMOS had no SM data signal because of snow, which produced outlier values at the beginning (April) and end of the periods (October).

3.4.2 Spatial Distribution of SMOS SM

We examined the spatial variability of SM data with bias-corrected SMOS SM data. Figure 3.6 shows the result of a corrected SMOS SM spatial distribution map (absolute differences from 2010 to 2015). The maps indicate that the SM increased approximately 20% to 30% in 2011 in the northern part of Bayankhongor and northern central part of Uvurkhangai provinces, respectively. For 2012, we observed that SM increased by 2.5% to 10% for most of the investigated areas. Hence, significant changes in SM can be seen in bias-corrected SMOS SM map Figure 3.6b, c. However, a subsequent SM distribution showed a significant SM decrease (30%) in the steppe and forest-steppe regions that contain Kastanozems haplic soils (Figure 3.6f). Further, bias-corrected SM distribution maps allowed the delineation of wet areas in the northwestern and southeastern dry areas of Mongolia. Hence, the bias-corrected SMOS SM products imply that they could be effective for soil moisture monitoring.

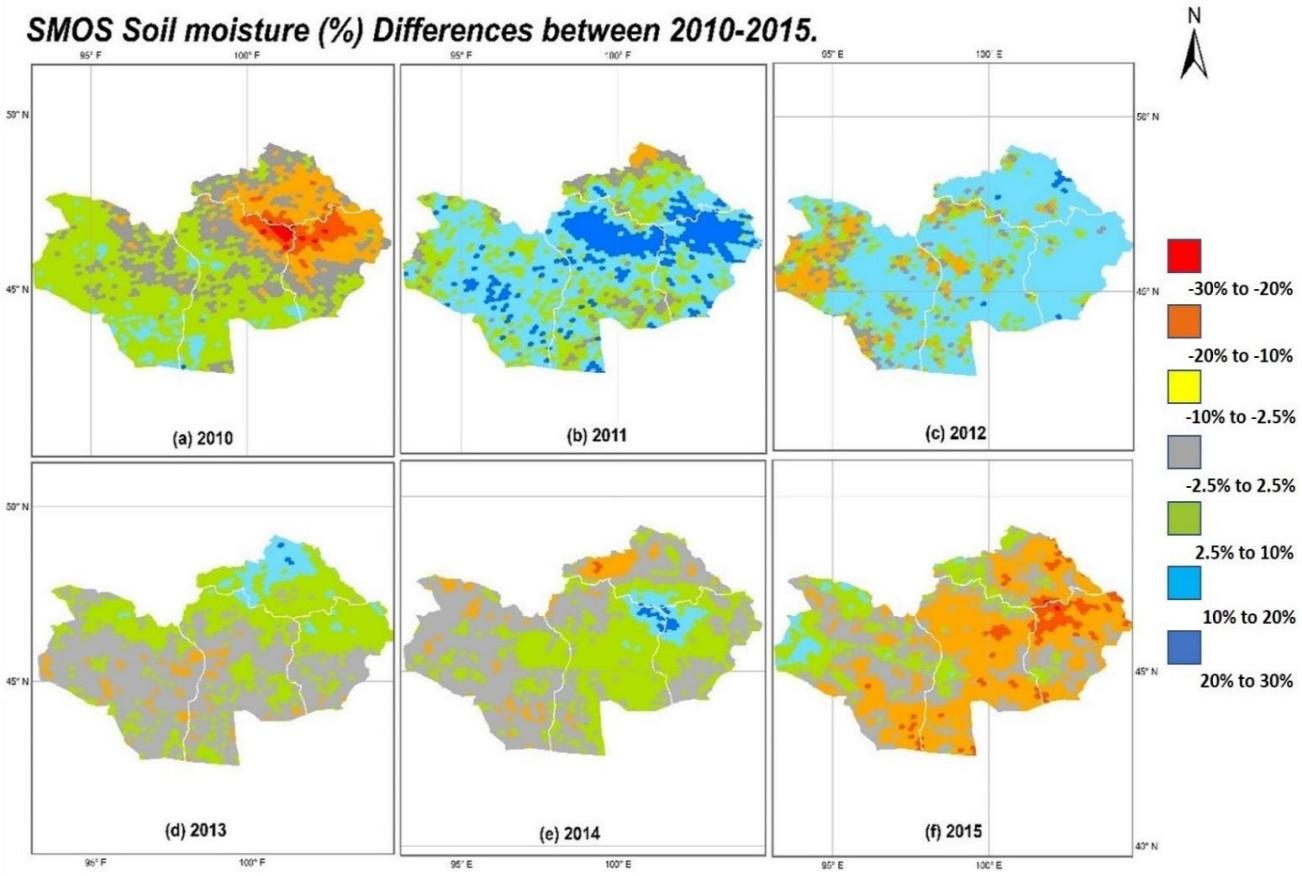

Figure 3.6 Spatial distribution of bias-corrected SMOS SM maps from 2010 to 2015 in Southwestern Mongolia.

3.4.3 The Relationship between SMOS SM and MODIS NDVI Vegetation

In order to check how NDVI represents the spatial differences in vegetation, we examined the relationship between SMOS SM and NDVI. Consistently, the NDVI is a proven indicator of vegetation,

drought, and the thermal state of the land surface (Yengoh et al., 2016). Figure 3.7 displays the relationship between SMOS SM (annual average) and MODIS NDVI (annual average) from 2010 to 2015. The results show that there is a positive tendency relating to the spatial patterns of NDVI. The bias-corrected SMOS SM favorably correlated with NDVI in the area around different soil types such as (Kastanozems haplic) with R^2 = 0.94 and R^2 = 0.72 (Figure 3.7b, d). Furthermore, lower correlations were found in semi-arid and desert regions (Chernozems calcic and Calcisols haplic) soils with R^2= 0.65 and R^2= 0.62, respectively (Figure 3.7a, c). The cause of these varying correlations is the different vegetation types. For instance, the southern region corresponds to open shrub-land, which is drier and has a smaller degree of vegetation content.

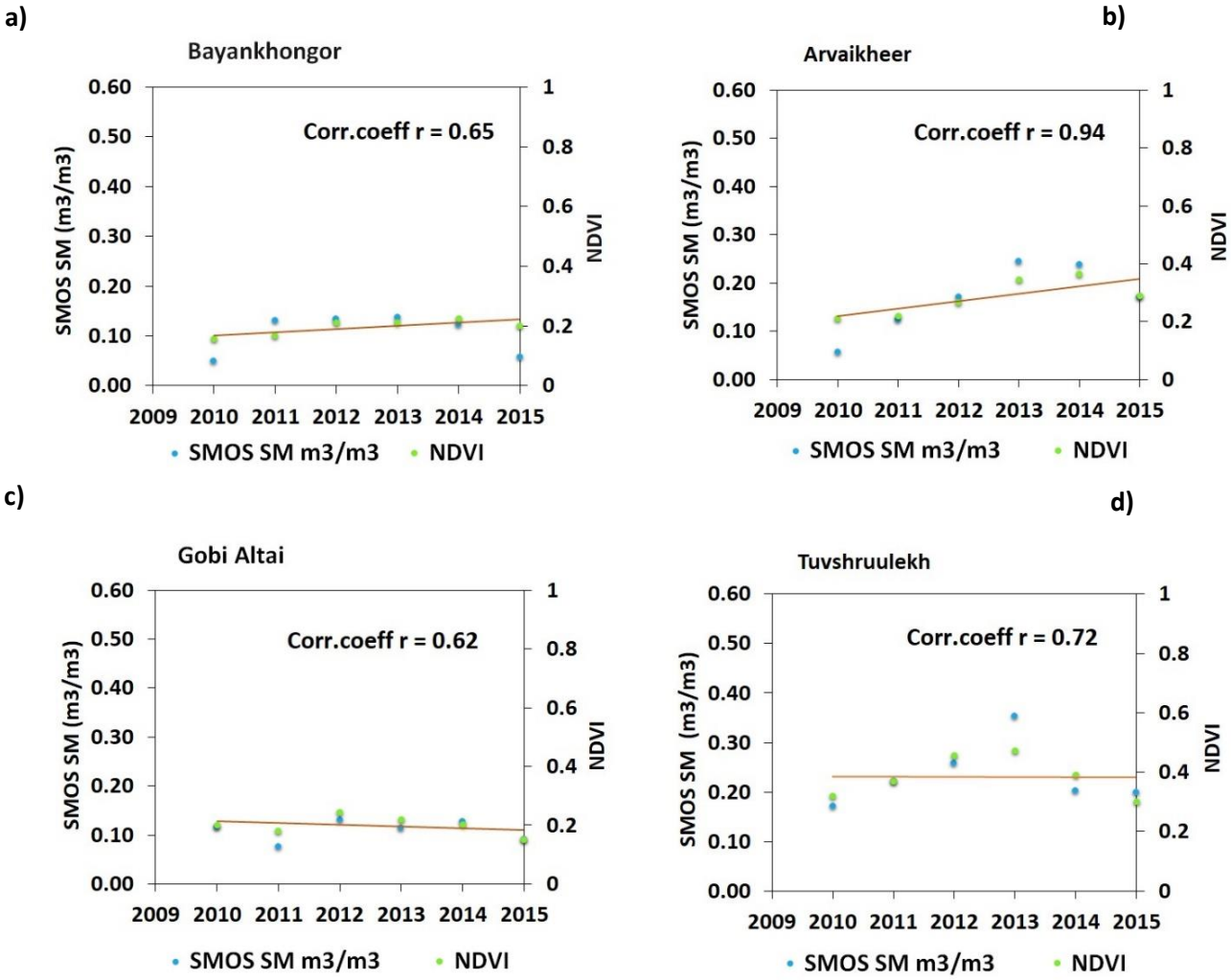

Figure 3.7 Scatter plot showing the annually-averaged correlation values obtained between SMOS SM and Moderate Resolution Imaging Spectroradiometer (MODIS) Normalized Difference Vegetation Index (NDVI) in the provinces: (a) Bayankhongor, (b) Arvaikheer, (c) Gobi-Altai, and (d) Tuvshruulekh.

Figure 3.8 presents the seasonal correlations between SMOS SM and NDVI. The relationship between SM and NDVI was examined using the seasonal SM values from April to July and July to October. From the regression plots, it can be seen that the seasonal values of NDVI and SMOS SM have the highest correlation during the growing season (Figure 3.8a, c, e, g). We detected a far

weaker correlation for estimates during the non-growing season (Figure 3.8b, d, f, h). The seasonal NDVI values over the growing season correlate better in the humid and dense vegetation areas.

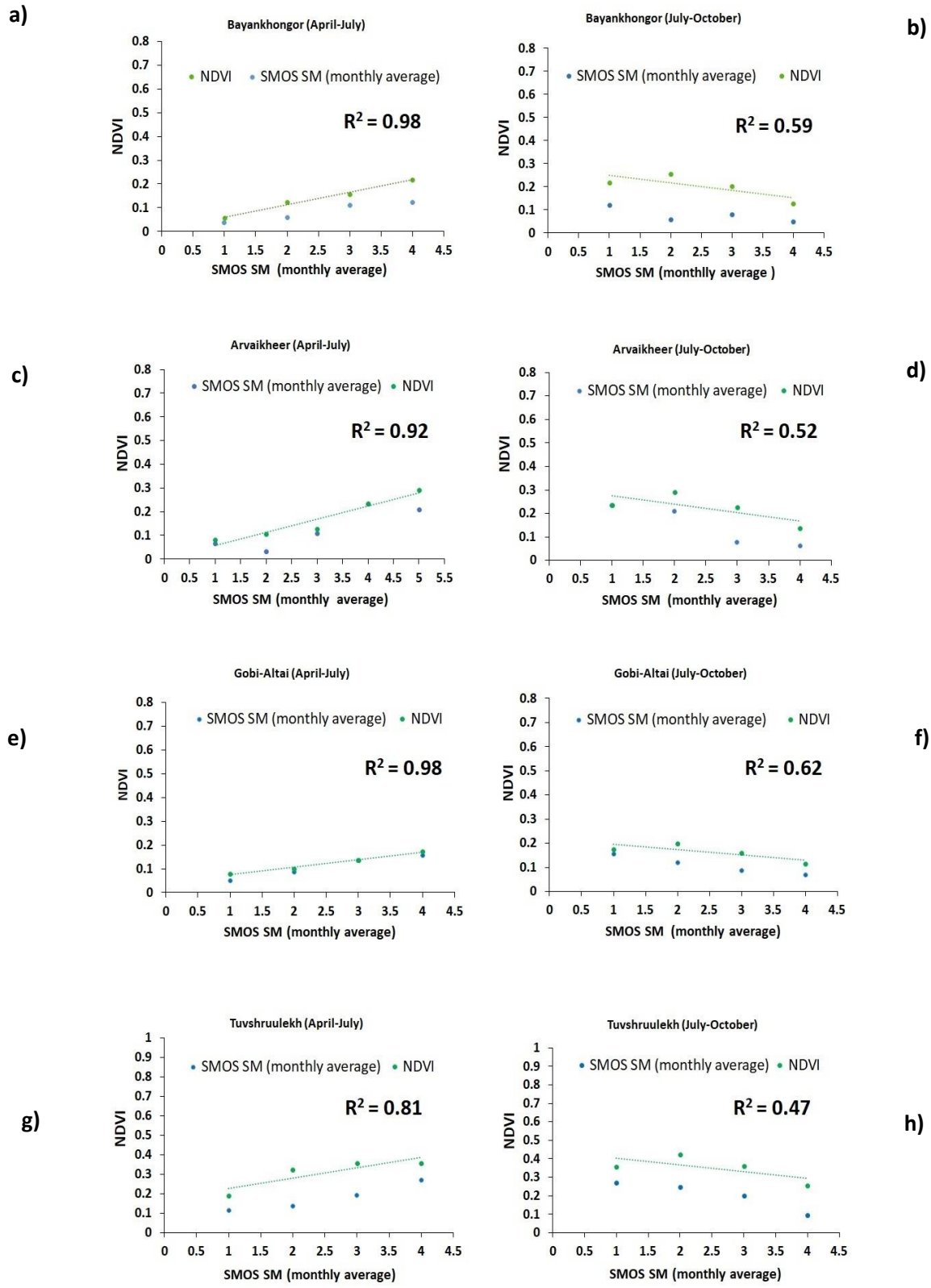

Figure 3.8 Scatter plot showing the monthly-averaged correlation values obtained from SMOS SM and MODIS NDVI during two seasons, April through June and July through October, in the provinces: (a, b) Bayankhongor, (c, d) Arvaikheer, (e, f) Gobi-Altai, and (g, h) Tuvshruulekh.

3.5 Discussion

3.5.1 Seasonal Precipitation and SM

The results reveal that the temporal variation and spatial distribution of the bias-corrected SMOS SM were generally related to precipitation, in agreement with other findings (Usowicz et al., 2019). For the entire study area, peak SM was observed in late July and decreased in mid-August. The lowest SM was observed at the beginning of spring (i.e., April/May), which was due to the snow cover melting from the winter. Significant rainfall in July 2011 caused an increase in SM, which was recorded in both the bias-corrected SMOS SM data and the precipitation records at stations like Arkhangai (336 mm/year). In 2011 and 2012, the maximum SM (in July) depended strongly on the precipitation. In Gobi-Altai province (desert/high mountain region) the wettest year was 2011, however, the highest SM value was detected in June and decreased in July. The lower than average rainfall during this rainy season was the main cause of the SM reduction in late July. Subsequently, in dry years, we found a shift of the SM depression from August to mid-July. These findings could indicate that SM conditions during the early plant growth stage critically impact the vegetation condition, which is consistent with other studies (M. Shinoda et al., 2010b). When there is a lack of rainfall in drylands (Bayankhongor, Gobi-Altai), higher temperatures reduce SM, which is precipitation driven in these areas (Jung et al., 2010). Moreover, low precipitation leads to SM deficits, increasing aridity, and leading to drought. It is worth noting that many lakes in Mongolia have shrunk or dried up over the past decades (Tao et al., 2015). In relatively dry areas covered by sparse vegetation, dry summer months also transport dust storm events causing additional damage related to, e.g., health, the environment, and the economy.

3.5.2 NDVI Vegetation Index and SM

Most of the bias-corrected SMOS SM distributions in this study were similar to NDVI and have similar dynamics. This is particularly the case in open shrub-lands, where NDVI values are low. Because of the widespread droughts, the dry regions are becoming drier and the growing season is getting shorter (Hessl et al., 2018). A previous study highlighted that data from satellite remote sensing data SMOS are strongly correlated with vegetation dynamics (Prigent et al., 2005). Bias-corrected SMOS SM and in situ SM were most correlated in humid areas (Figure 3.7). Considerably, the spatial distribution of SM depends on soil parameters that are not distributed homogeneously in the area. This indicates, in general, that SM in dry steppe areas could change very rapidly in the topsoil layer. The dynamics of NDVI show good compatibility and a strong correlation with the bias-corrected SMOS SM when measured in the seasonal cycles (Figure 3.8).

3.5.3 Relation of SMOS SM to Measured SM

The SMOS SM data strongly correlates with in situ SM measurements; the SMOS SM datasets successfully captured the spatiotemporal dynamics of the in-situ SM measurements in the transition zones between dry and humid climates (as seen in the comparison analysis). Furthermore, for comparison analysis, it is important to capture the correct temporal pattern of the in-situ SM measurements. The SMOS data exhibited weaker correlations in some of the desert areas (e.g., Gobi desert), possibly caused by the relatively small range of SM values in these regions (which corresponds to remote sensing accuracy (Yann H Kerr et al., 2001)). The desert and desert steppe regions are too dry to transmit an adequate signal to the sensor. With rising SM, the quality of the signal may increase and allow a stronger statistical context in the northern regions. Some differences between SMOS SM and in situ SM measurements were observed, which may be explained by the respective depths of the

measurement; SMOS data is for depths from 0 cm to 5 cm, while the in situ measurements are between 10 cm and 15 cm (Szlazak et al., 2017). Particularly, in the early spring and late autumn, the greatest variations of soil moisture were observed in both datasets. The SMOS data exhibited a certain underestimation in April and October compared to the ground observations, although the SMOS data reacted to rainfall events more quickly (Figures 3.4 and Figure 3.5), which was also detected in previous validation experiments (González-Zamora et al., 2015).

3.6 Conclusions

This study compared satellite SMOS SM with the in situ measured SM at depths between 10 cm and 15 cm from 2010 to 2015 in the southwest part of Mongolia. The spatial distribution of SMOS SM, MODIS NDVI, and their relationship were used to assess the grassland condition. SMOS SM was also compared with in situ SM measurements to examine the reliability of SMOS SM. Two techniques (i.e., ratio and gamma) were applied to correct the bias between the in-situ SM and SMOS SM data. The in situ measured SM distribution was close to the bias-corrected SMOS SM distribution, and thus met the primary condition of the bias-correction technique. The two algorithms utilized for comparison analysis successfully recreated the in-situ measurements. For all investigated stations, the coefficient of determination (R^2) ranged from 0.6 to 0.8 for the validation results. The distribution patterns of bias-corrected SMOS SM correctly reproduced the precipitation season from June to July as well as the drying out period starting in October. In both datasets, the highest variability of SM occurred in the northern part of the study area in 2011, with an increase in SM of up to 30% above 2010 levels. The lowest SM values were observed in 2015, with a significant decrease (30% compared to 2010) in the steppe and forest-steppe regions with Kastanozems haplic soils. Overall, the small seasonal changes in the bias-corrected SMOS SM and situ measurements were generally similar throughout the study area during the three phases of observed vegetation growth (i.e., warm spring, summer recharging, and autumn drying season). The study site lies in a zone that transitions between steppe, forest-steppe, and desert. The lowest correction between SMOS SM and in situ SM was observed in the dry, lowland regions. While the spatial resolution of SMOS is coarse, the high temporal resolution of the SMOS SM data will be useful to determine large-scale temporal SM changes.

This study confirms a simple bias-correction technique (ratio and gamma distribution) is a valid method to compare in situ SM measurements and remotely sensed SMOS SM data in the southwestern part of Mongolia. The use of SMOS SM data allows easier monitoring of spatial and temporal changes. The geostatistical results and spatial distribution SM maps will be useful in grassland development studies to address drought in Mongolia. In the future, the bias-corrected SMOS SM products can be used as an extra tool for monitoring the grasslands of Mongolia.

Chapter 4 Extreme Climate Event and Its Impact on Landscape Resilience in Gobi Region of Mongolia

Chapter 4 Extreme Climate Events and their Impact on Landscape Resilience in Gobi Region of Mongolia

Oyudari Vova [1,] *, Martin Kappas [1], Tsolmon Renchin [2] and Steven R. Fassnacht [1,3,4,5]

[1] Cartography, GIS and Remote Sensing Department, Institute of Geography, University of Göttingen, 37007 Göttingen, Germany
[2] Physics department, National University of Mongolia, Ulaanbaatar 14200, Mongolia
[3] Department of Ecosystem Science and Sustainability—Watershed Science, Colorado State University, Fort Collins, CO 80523-1476, USA
[4] Cooperative Institute for Research in the Atmosphere, CSU, Fort Collins, CO 80523-1375, USA
[5] Natural Resources Ecology Lab, Colorado State University, Fort Collins, CO 80523-1499, USA
* Correspondence Author

This chapter was published as a research article: Journal of Remote Sensing 12(18):02881; Special Issue "Earth Observations for Ecosystem Resilience" DOI: **https://doi.org/10.3390/rs12182881**

4.1 Abstract

The dzud, a specific type of climate disaster in Mongolia, is responsible for serious environmental and economic damage. It is characterized by heavy snowfall and severe winter conditions, causing mass livestock deaths that occur through the following spring. These events substantially limit socioeconomic development in Mongolia. In this research, we analyzed several dzud events (2000, 2001, 2002, and 2010) to understand the spatial and temporal variability of vegetation conditions in the Gobi region of Mongolia. The present paper also establishes how these extreme climatic events affect vegetation cover and local grazing conditions using the seasonal aridity index ($_{o}AI_{Z}$), time-series Moderate Resolution Imaging Spectroradiometer (MODIS) Normalized Difference Vegetation Index (NDVI), and livestock data. We also correlated $_{o}AI_{Z}$, NDVI, and seasonal precipitation in the varied ecosystems of the study area. The results illustrate that under certain dzud conditions, rapid regeneration of vegetation can occur. A thick snow layer acting as a water reservoir combined with high livestock losses can lead to an increase of the maximum August NDVI. The Gobi steppe areas showed the highest degree of vulnerability to climate, with a drastic decline of grassland in humid areas. Another result is that snowy winters can cause a 10 to 20-day early peak in NDVI and the following increase in vegetation growth. During a drought year with dry winter conditions, the vegetation growth phase begins later due to water deficiency, which leads to weaker vegetation growth. Livestock loss and the reduction of grazing pressure play a crucial role in vegetation recovery after extreme climatic events in Mongolia.

Keywords**:** *dzud types; vegetation; aridity index; drought; livestock mortality*

4.2 Introduction

Featuring a mix of monsoon, and harsh Siberian climates, the south Gobi of Mongolia is a unique desert steppe and nomadic living area, and one that is sensitive to global climate changes. Over the past 20 years, meteorological disasters in the Mongolian plateau have become increasingly severe, and its dynamic succession has become increasingly investigated partly through large-scale monitoring. The interaction between drought-*dzud* and vegetation has been an essential concern for pastureland use in Mongolia. Originally, *dzud* was the Mongolian term for a natural, winter-related climate disaster. *Dzuds* are now defined, biophysically, as anomalous climatic or land surface conditions (i.e., snow and ice cover) that lead to reduced accessibility or availability of pastures (Nandintsetseg, Shinoda, Du, et al., 2018). It often causes very high livestock mortality during the winter. Changes in the frequency and intensity of extreme climate events (e.g., heavy winter, snowfall, drought, and freezing rain) substantially affect societal well-being (Groisman et al., 2016). Hence, (Bulygina et al., 2011) and Groisman and Soja 2009.) have pointed out that extreme climate conditions impact the regional water deficit for the growing season. Some studies concluded that several factors influence *dzud* disasters, depending not only on climate hazards but also on the vulnerability of herders and livestock (e.g., (Nandintsetseg, Shinoda, Du, et al., 2018; NATSAGDORJ & L., 2001). *Dzud* causes years with growing-season drought and severe winter weather (i.e., deep snow and extreme cold), which can lead to high livestock mortality. Related studies have identified five different types of *dzud* (Table 4.1): white, black, iron/ice, cold, and hoof, but a combination of these is also possible (Punsalmaa Batima et al., 2013; Begzsuren et al., 2004). For example, a white *dzud* occurs when a severe winter follows heavy snow; A black *dzud* occurs when there is no snowfall. (Dagvadorj et al., 2009; Morinaga et al., 2003). Climate changes and other extreme events, such as overgrazing by goats, have led to the degradation and desertification of 76% of grasslands (8% of the land in Mongolia as of 2015). This has become one of the most problematic issues for the country, especially economically. (Masao Shinoda, 2015) and (Templer et al., 1993) reported that *dzud* events tend to follow droughts. Therefore, drought could serve as a strong predictor of a *dzud* event (Mukund Palat et al., 2015a).

Table 4.1 Types of dzuds in Mongolia and their local nomenclature (Punsalmaa Batima et al., 2013; Begzsuren et al., 2004).

Type of *Dzud*	Weather Condition	Effects
Tsagaan (white)	The average thickness of the snow layer on pasture land exceeds 21 cm in high mountains and forest regions, 16 cm in steppes, and 10 cm in the Gobi region. Snow density reaches 200 kg/m^3 or greater in any region.	Prevents access to grass. The most common form of *dzud* and the most disastrous when it affects large areas.
Khar (black)	No snow during winter and the monthly or ten-day average temperature is 5.0^{o}C lower.	Causes water supply shortages, often exacerbated by lack of winter grass.
Tumur (iron or ice)	Snow cover melts and freezes due to rapid changes in temperature creating an ice cover that prevents livestock from grazing. Snow density reaches 0.30 g/cm^3 or greater.	Prevents access to grass.
Khuiten (cold)	Air temperature is 5 to 10 °C lower than the monthly mean temperature for several consecutive days.	Extreme cold and strong freezing winds prevent animals from grazing. Animals spend most of their energy maintaining their body heat.

Turen (hoof)	Extremely dry weather.	Causes complete depletion of grass due to drought and/or trampling and heavy grazing.
Khavsarsan (combined)	Two or more of the above occurring simultaneously.	

The United Nations Convention to Combat Desertification (UNCCD) defines desertification as "land degradation in arid, semi-arid and dry sub-humid areas resulting from various factors, including climatic variations and human activities" (Ma et al., 2018). Desertification, therefore, denotes a form of land degradation specific to drylands. The UNCCD defines drought as "the naturally occurring phenomenon that exists when precipitation has been significantly below normally recorded levels, causing serious hydrological imbalances that adversely affect land production systems" (Ma et al., 2018). Droughts increase the frequency and severity of *dzud* (Nandintsetseg, Shinoda, Du, et al., 2018; Nandintsetseg & Shinoda, 2013b). A drought mechanisms analysis revealed that severe water scarcity results from a combination of insufficient precipitation, high evaporation, and over-exploitation of water resources (Bhuiyan et al., 2006). It is important to note that reduced winter precipitation promotes drier summer conditions by reducing the soil water available for evapotranspiration in summer (Nandintsetseg & Shinoda, 2011c).

The livestock sector of Mongolia has struggled with the harsh climate, overgrazing, and an imbalance in livestock species. These factors have led to significant damage to regional vegetation (Kakinuma et al., 2019). The winter of 2010 was the "most severe winter in nearly five decades" (FAO, 2010), in which more than 10 million livestock died across the country. This represented a national disaster for a country where animal husbandry is the traditionally dominant form of livelihood, providing 16% of the Gross Domestic Product (GDP) for the country and employment to 366,000 herders, as well as indirect economic support to about one million people or about a third of the 3.1 million inhabitants (UNDP/NEMA, 2010). The impact on many herders was particularly severe during the three consecutive *dzud* winters of 1999 to 2002 when 30% of the livestock in the nation perished (Fernández-Giménez et al., 2012; Sternberg, 2010). More recently, the *dzuds* of 2009 to 2010 were even harsher. (Fernández-Giménez et al., 2012) analyzed the changing climate over the past 70 years (Appendix A), stating that the frequency and range of *dzuds* and summer droughts are expected to increase, particularly in central and northern Eurasia (Groisman et al., 2009; Hansen et al., 2010). The effects can vary according to the type of *dzud* (Table 4. 1).

Analysis of extreme climate events has become an urgent task to understand *dzud* mechanisms in Mongolia. By studying the mechanisms of *dzuds*, we will be able to prepare herders and their livestock for *dzud* effects. Limited research has examined the response of vegetation conditions to *dzuds* and summer droughts for different ecosystems on the Mongolian plateau using long-term satellite observations (Tachiiri et al., 2008; Xu et al., 2012). One of the most cost-effective remote sensings approaches to detect vegetation changes across large scales is the Normalized Difference Vegetation Index (NDVI) (Zucca et al., 2015). NDVI features a nonlinear combination of the red and near-infrared (NIR) spectral irradiance, exhibiting a relationship with vegetation and green biomass. The NDVI index has been widely used to monitor global vegetation phenology from space across large scales (Karlsen et al., 2008; Y. Y. Liu et al., 2013). This study focuses on the impacts of *dzud*-related factors (e.g., drought and snowfall), as well as provides a more in-depth analysis of its spatial and temporal distribution and losses. The goal of this paper is to describe the effects of *dzud* on the vegetation growth cycle in the subsequent year. To comprehend the mechanical concept of *dzud* after droughts, and how vegetation responds to various *dzud* situations, we used MODIS-NDVI data (2000–

2013) to estimate the spatiotemporal changes in NDVI. In this paper, we (1) determine the spatiotemporal variations in NDVI after *dzud* events and the length of the growing season, and (2) assess the impact of drought (using the climatic variables Aridity Index ($_aAI_z$), precipitation, and temperature) on vegetation throughout the *dzud* period.

4.3 Materials and Methods

4.3.1 Study Area

The study area comprises the Bayankhongor and Gobi-Altai provinces (*aimags*) in southwestern Mongolia (Figure 4.1), with a total size of 258,200 km^2 (National Statistical office of Mongolia 2015, n.d.). This is part of the central Asian desert belt (Klinge & Sauer, 2019) and has an arid ecosystem (John et al., 2008; Yu et al., 2003). It has an elevation that ranges from the sea level to 4000 m.a.s.l. and the average temperature is 17 °C in July and −24 °C in January. The area has become drier and hotter in recent years, due to the impact of climate change (Herzschuh, 2006). The Siberian high-pressure cell in this area causes cold and dry conditions in winter (P Batima et al., 2005). The annual average rainfall varies from 200 to 300 mm, with an annual average wind speed of 3.1 m/s. The climate datasets and maps of vegetation zones were provided by the Institute of Meteorology and Hydrology of Mongolia. Six meteorological stations were examined for each province (Table 4.2). The dominant plant species are *Stipa grandis*, *Leymus Chinensis,* and multiple species of *Artemisia* spp. and *Festuca* spp. (Kang et al., 2007). Annual germination occurs between April and July, depending on the antecedent soil moisture and rainfall (BOHNER, 2008; Hilker et al., 2014; John et al., 2008).

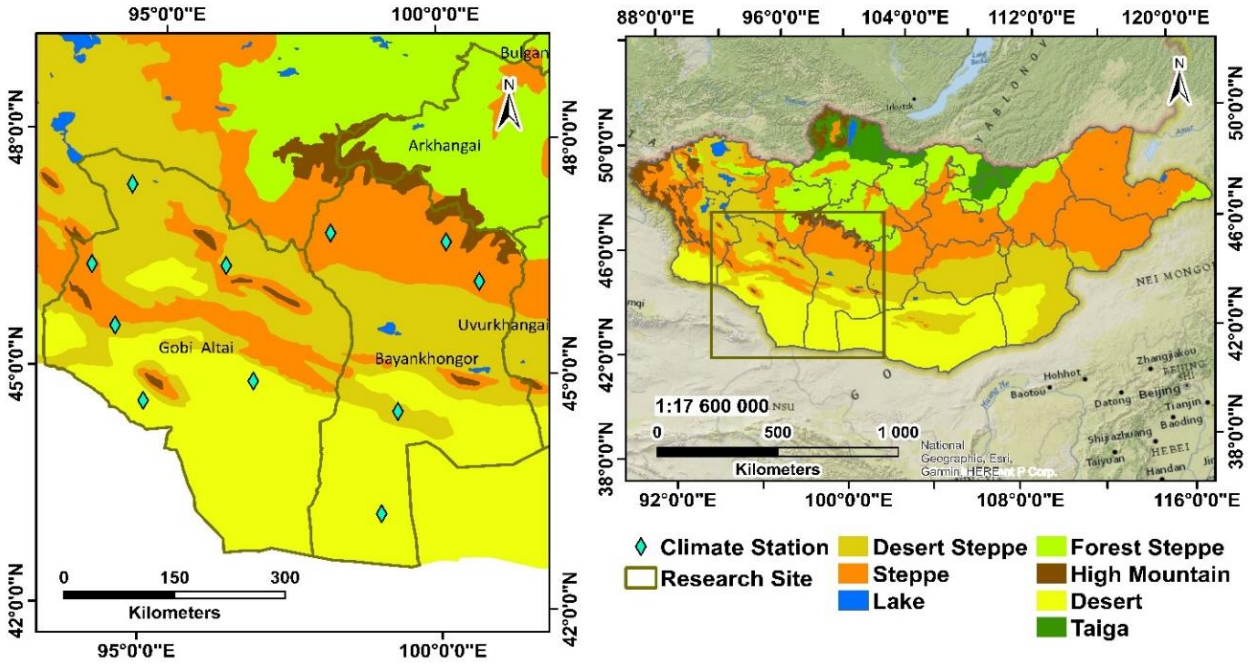

Figure 4.1 Location of meteorological stations for NDVI measurements in Gobi-Altai and Bayankhongor Provinces. Data are sourced from the Institute of Meteorology and Hydrology of Mongolia.

Table 4.2 Meteorological stations with location information, and vegetation zones.

Meteorological Station	Province Name	Vegetation Zones	Latitude	Longitude
Bayankhongor	Bayankhongor	steppe	46° 11’40’’ N	100° 42’2’’ E
Galuut	Bayankhongor	steppe	46° 43’30’’ N	100° 8’35’’ E
Bogd	Bayankhongor	desert steppe	45° 40’10’’ N	100° 7’75’’ E
Ekhiingol	Bayankhongor	desert	43° 14’48’’ N	99° 21’14’’ E
Shinejinst	Bayankhongor	desert steppe	44° 32’13’’ N	99° 17’34’’ E
Bayanbulag	Bayankhongor	steppe	46° 49’32’’ N	98° 40’10’’ E
Bugat	Gobi-Altai	desert steppe	45° 34’55’’ N	94° 22’91’’ E
Khukhmorit	Gobi-Altai	desert steppe	47° 35’23’’ N	94° 28’51’’ E
Aj Bogd	Gobi-Altai	desert	44° 37’52’’ N	94° 54’48’’ E
Tooroi	Gobi-Altai	desert	44° 54’39’’ N	96° 47’42’’ E
Altai	Gobi-Altai	desert steppe	46° 23’12’’ N	96° 15’14’’ E
Tonkhil	Gobi-Altai	steppe	46°18’23’’ N	93° 54’51’’ E

4.3.2 Methods

In this study, we combined Moderate Resolution Imaging Spectroradiometer (MODIS) NDVI satellite data products, climate data from the Mongolian meteorological stations, spatial snow-cover data from global climate data sets, and livestock data from the National Statistics Office of Mongolia (National Statistical Office of Mongolia, 2010). We examined extreme climate events NDVI trends, and the relationship between NDVI and aridity index ($_aAI_z$) to characterize vegetation growth cycles after *dzud* events. Figure 4.2 presents a framework of the study that comprises pre-processing and meteorological data processing to compute $_aAI_z$, remote sensing data processing of NDVI, precipitation, temperature, snowfall, and livestock mortality.

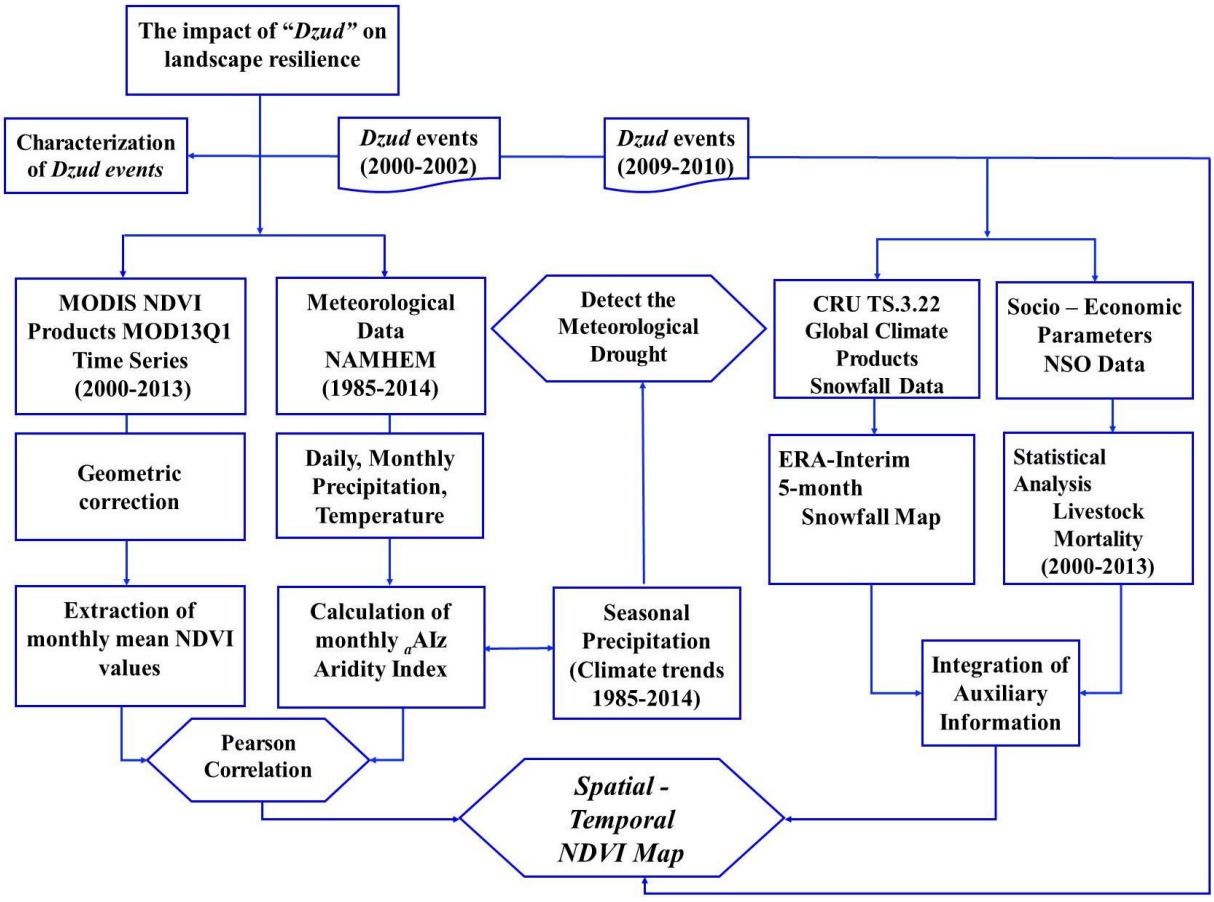

Figure 4.2 Schematic flow chart of Geographic Information System (GIS)–based dzud evaluation methodology.

4.3.2.1 Remote Sensing Data and Pre-Processing.

- **MODIS NDVI Data (Vegetation Dataset)**

We examined vegetation variation in the Gobi region by using MODIS NDVI (MOD13Q1) data (K. Didan, 2015), which provides global data records with a spatial resolution of 250 m and a time resolution of 16 days from the year 2000 to the present. We used data from 2013 to extend over the most severe *dzud* years. The MOD13Q1 products are derived from atmospherically corrected bi-directional surface reflectance function (BDRF) that have been masked for clouds, shadows, water, and aerosols (K. Didan, 2015). Comprehensive information and characteristics of MODIS NDVI can be obtained from (Kamel Didan et al.,) in TIFF format (*LP DAAC - MOD13Q1*,). In this study, we only processed NDVI data during *dzud*-related years, specifically during and after *dzud* events to estimate the mean monthly August NDVI value. Besides, we ensured that the areas were at least 500 x 500 m to fit the spatial resolution of the MODIS sensor (250 x 250 m). NDVI is defined by the following equation:

$$NDVI = (NIR - red) / (NIR + red) \quad (4.3)$$

where *red* is the visible light of the red wavelength (from 400 to 700 nm) and NIR is the intensity of the near-infrared wavelength (from 700 to 1100 nm). The formula uses the specific reflective behavior of plant surfaces. NDVI values are normalized to a range from −1 to 1, where gross values over 0.1 represent vegetation. A higher value indicates more vegetation, while negative values indicate water,

ice, or snow surfaces (Bannari et al., 1995). The MODIS NDVI data were then transformed into the same geographic coordinate system (UTM 48N) to ensure coverage equality. We used the "buffer" tool in ArcGIS (with a radius of 10 km) around the climate stations, afterward, computed the average MODIS NDVI for each area.

4.3.2.2 Meteorological Data (Climate Dataset)

The National Agency of Meteorology and Environment Monitoring of Mongolia (NAMHEM) provided climate datasets (i.e., precipitation and temperature) from twelve different stations (Figure 1). The station data were measured and documented for all study regions as average monthly temperature and total monthly rainfall. There were some limitations in data availability at (Khukhmorit, Bugat, and Tooroi) stations. The data from 1990 to 2013 were selected for aridity index analysis, while the data from 1985 to 2014 were selected for climate trend analysis in Bayankhongor and from 1990 to 2014 for the climate trend analysis in Gobi-Altai. The maximum and minimum temperatures were arithmetically derived from this data set. Rainfall and temperature records were averaged by season: summer (June, July, August), autumn (September, October, November), winter (December, January, February), and spring (March, April, May). We divided the time range (30 years) into three groups; 1985–2014, 1985–1999, 2000–2014, and trends were detected. The snowfall map was derived from the Climatic Research Unit (CRU) TS 3.22 global climate records for the period 1999 to 2010. The dataset was provided as an accumulation of the precipitation (i.e., snowfall) amount from November to March. The gridded CRU TS 3.22 data are monthly variations in weather from 1901 to 2013 with high resolution (0.5 × 0.5 degrees) grids, created by the Climatic Research Unit (CRU) at the University of East Anglia (Climatic Research Unit). The gridded data, along with the monthly station observations, are freely available at the British Atmospheric data center (Centre for Environmental Data Analysis, 2015).

4.3.2.3 Socio-Economic Data (Statistical Dataset)

The livestock data used is from 2000 to 2013 and was provided by the National Administrative Department of Statistics (National Statistical Office of Mongolia). The Ministry of Livestock Husbandry composed the mortality data of the livestock each December, and the National Statistical Office (NSO) of Mongolia (1990–2015) collected the total livestock numbers for all provinces. We combined the statistical results to check the spatial and temporal variability of *dzud* events and the relationship between climate variability and livestock loss. To examine livestock mortality, livestock data were first converted to equivalent 'sheep forage units' (SFU) to standardize feed requirements, as each type of livestock requires different amounts of feed (Bedunah & Schmidt, 2000). The conversion rates to SFU were: 1 camel = 5 SFU, 1 horse = 7 SFU, 1 cow = 6 SFU, 1 sheep = 1 SFU and 1 goat = 0.9 SFU. The percent relative mortality for each province was calculated as the ratio of livestock deaths during winter and spring to the number of livestock at the beginning of the year. Consequently, the examined stock loss can be either a factor of the *dzud* of the prior year (in the case of drought temperatures) or of the current year (in the case of winter temperatures).

4.3.2.4 The Implementation of the Aridity Index

Drought indices often integrate precipitation, temperature, and other variables, but may emphasize different aspects of drought and must be carefully selected concerning the drought

characteristics. For this purpose, we assessed changes in drought characteristics by focusing on the aridity index (AI_z). Due to the local arid climatic conditions, we applied an adapted approach of the aridity index based on the respective drought years (Munkhtsetseg et al., 2007). This method was originally developed for the southern regions of Mongolia, to define the drought intensity during the summer months to estimate the relevant connection to pasture yields. In our study, it is intended to link spatially variable climatic circumstances and evaluate specific summer characteristics before *dzud* events. Hence, the aridity index was applied to each province (National Agency Meteorology and the Enviromental Monitoring, n.d.) to develop a zonal adapted seasonal aridity index ($_aAI_z$). Subsequently, the $_aAI_z$ was used to show the drought risk and periodic temporal patterns in NDVI. We then arranged the standardized $_aAI_Z$ values into three groups, represented by values less than zero (dry years), values between zero and five (normal years), and values greater than five to show the wet years.

This method is based on daily temperature and precipitation values to assess the summer weather. The aridity index itself is based on a supply and demand concept of the water balance equation. The annual mean evapotranspiration and runoff rates are regulated by the amount of available energy (demand) and precipitation (supply). Equation (4.2) defines *AI* as a function of precipitation (*P*), the supply, and temperature (H_i), the demand.

$$AI = \frac{P7}{H_i6 + H_i7} \tag{4.4}$$

where *P7* is the cumulative precipitation in July, while H_i6 and H_i7 are the average maximum daily temperatures during June and July, respectively. The basic theory behind this approach lies in the disproportionate significance of the July precipitation on biomass growth and its maximum in mid to late August. Within the southern parts of the study area, rainfall is usually limited to the summer months of July and August, with rainfall in August having a lower impact on the maximum growth stated, due to a response period of 10 to 20 days (Purevsuren et al., 2012). Evapotranspiration is highest in June due to the long days, high levels of incoming solar radiation, and high temperatures. Evapotranspiration can also be high in July due to the hot conditions (Munkhtsetseg et al., 2007). This aridity index approach demonstrates a stronger correlation to pasture yield in the southern part of the study area (i.e., arid climates) than in the central and northern parts. An expanded AI calculation as a zonal component (AI_Z) is beneficial for regional assessment in the north, where precipitation increases in July and August, and a growth period spans from May to September ($P_{May\text{-}Sept}$). The denominator was extended by an empirically derived number (10) to compensate for different locations (Ni, 2003; J. E. Oliver & Fairbridge, 1987). Equation (4.3) represents the zonal aridity index.

$$AI_z = \frac{P_r}{10 + H_i} \tag{4.5}$$

where H_i (**T**$max_{June\text{-}July}$) signifies the sum of the maximum daily temperatures from June and July, and P_r is the total precipitation during the respective season (in this case, summer). The seasonal precipitation (P_r) was applied to the zonal aridity index formula because seasonal and annual precipitation is the main factor that controls the spatial distribution of plant activity (Ni & Zhang, 2000). Greater negative values indicate increased aridity (i.e., drought). With this approach, we have developed our own regionally adapted index. In our study, the daily temperature data from June and July were accessible to find the maximum monthly temperature. The adjusted aridity index ($_aAI_Z$) is:

$$_aAI_z = \frac{P_r}{10 + 6m\ + 7m} \tag{4.6}$$

where 6*m* and 7*m* stand for the average daily temperature in June and July, respectively. This value allows us to estimate the drought intensity at individual study area stations. Lower values of the ${}_{a}AI_{Z}$ generally represent drier conditions in summer and a lower than maximum NDVI in August. Nevertheless, the prospect of direct comparability of the study area stations is problematic, since they are subject to different mean values and standard deviations. The steppe vegetation area shows a particularly strong correlation in terms of the ${}_{a}AI_{z}$, whereas the more arid desert regions show a lower correlation. This suggests that the vegetation that is present is very sparse or only present in small areas so that no significant vegetation signal can be detected. Thus, the calculated ${}_{a}AI_{Z}$ values confirm the spatial variability of climatic conditions. Pearson's correlation coefficients were applied to determine the sensitivity of ${}_{a}AI_{Z}$ to different seasonal conditions as well as the relationship between mid-August NDVI and seasonal precipitation.

4.4 Results

4.4.1 Spatio Temporal MODIS NDVI Analysis

We examined the spatial variability of MODIS NDVI data for *dzud* events in 2009/2010. Figure 4.3 shows the NDVI spatial patterns in southwestern Mongolia (encompassing twelve different stations). The NDVI vegetation value of dry, shrub, desert regions were typically under 0.1. While NDVI values, associated with different vegetation types, varying environmental conditions, and station locations followed a similar trend. The maps designate that NDVI increased approximately (62.2%) in 2010, mostly in high mountain (steppe) regions in the northern part of Bayankhongor and the north-central part of Gobi-Altai. These results suggest that MODIS NDVI data showed a strong recovery after the 2010 *dzud* events (Figure 4.3b). The NDVI data from 2010 exhibited maximal vegetation growth (mid-August). This early growth phase depends on the weather conditions and the quantity of the snow cover. Through the exceptionally wet year of 2010 (${}_{a}AI_{z}$ = 0.91), vegetation reached its maximum interim growth. A *dzud* may be a determinant for a more substantial vegetation growth phase (outside of extremely arid desert zones). NDVI spatial distribution maps after *dzud* events also allowed the delineation of wet areas in the northwestern and southwestern dry regions of Mongolia.

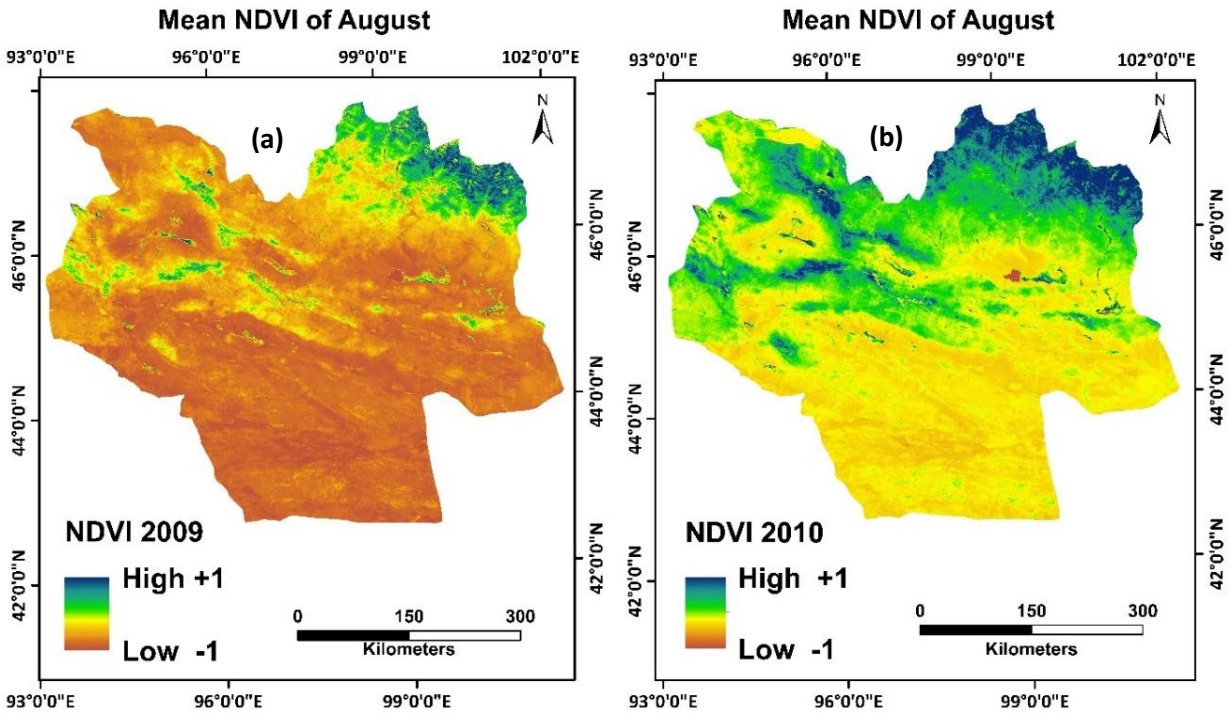

Figure 4.3 Spatial distribution of MODIS NDVI maps from 2009 to 2010 for the study area. The NDVI map after dzud events: (a) Mean NDVI of August 2009; (b) Mean NDVI of August 2010.

Figure 4.4 shows the spatiotemporal variations of mean MODIS NDVI from 2000 to 2013 among six different stations (Shinejinst, Bogd, Bayanbulag, Ekhiingol, Galuut, and Bayankhongor). The NDVI trend showed a remarkable increase in August 2003, August 2010, and August 2011. Only four of the 12 climate stations exhibited a weak trend in NDVI. Two of them were within the extremely arid desert zone, where changes in NDVI values are severely restricted due to sparse vegetation.

Positive NDVI trends can only be expected in the presence of relatively high precipitation. In 2002, a lack of precipitation led to substantial NDVI losses compared to the previous years. This pattern was widespread between the different station locations. The northern region vegetation had a stronger negative reaction to extreme droughts, while the southern region vegetation was well adapted to short-term and long-term droughts. The examination of vegetation response indicates that, generally, drought and water supply due to snow accumulation are essential in terms of the impact of *dzud* on vegetation development.

Figure 4.5 shows the mean NDVI during 2001/2002 and 2009/2010. The most significant variations in NDVI were observed during both drought and *dzud* years at most stations. The combined drought-*dzud* of 2002 had a strong negative impact on vegetation.

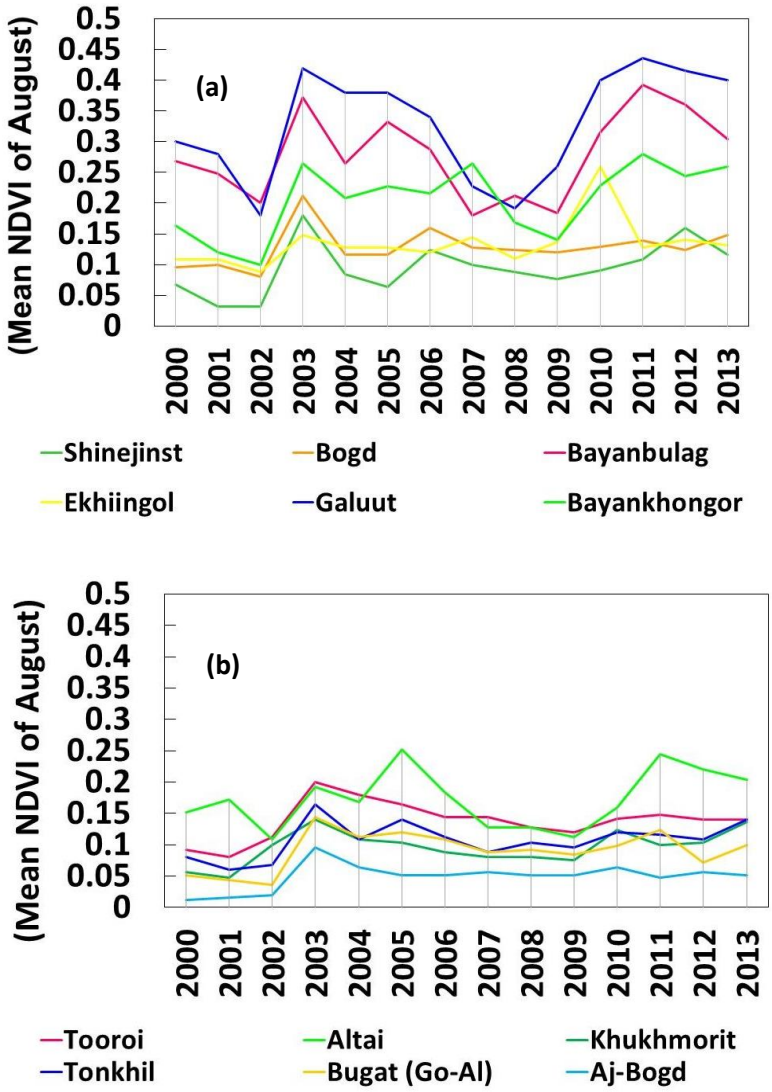

Figure 4.4 Trends of mean NDVI of August for the period from 2000 to 2013 at meteorological stations in (a) Bayankhongor province; (b) Gobi-Altai province.

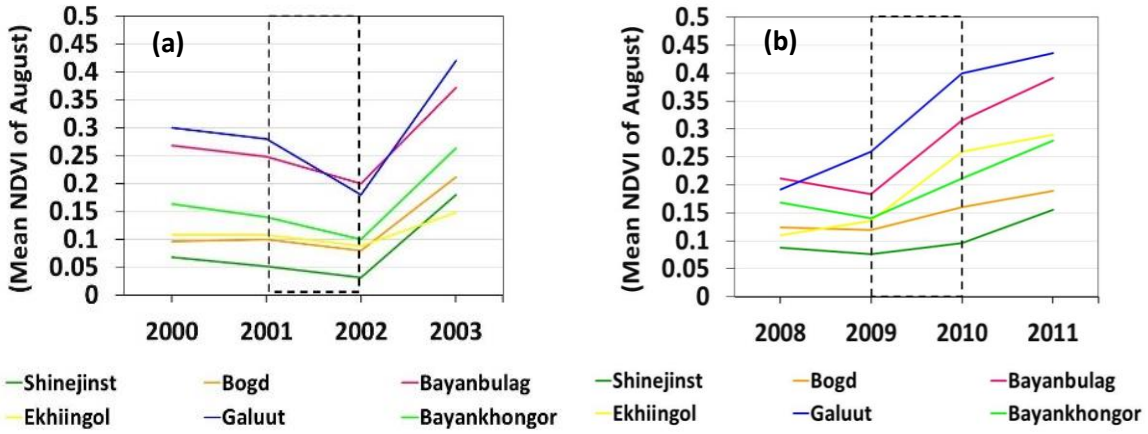

Figure 4.5 Mean NDVI of August vegetation trends caused by the (a) 2001/2002 and (b) 2009/2010 dzud events at different stations in the study area.

4.4.2 The Relationship between MODIS NDVI, Aridity Index ($_aAI_z$), and Seasonal Precipitation

To check how MODIS NDVI represents the spatial differences in vegetation, we examined the relationship between NDVI and the climate variables (adapted aridity index (aAIz) and seasonal precipitation; Figure 4.6). The results show that there is a significant relationship in the spatial patterns of NDVI; MODIS NDVI statistically significant ($p < 0.001$) correlated with aAIz and seasonal precipitation in the steppe regions with $R^2 = 0.64$ and $R^2 = 0.59$, respectively (Figure 4.6a, b). Furthermore, lower correlations were found in arid desert regions with $R^2 = 0.51$ and $R^2 = 0.56$, respectively (Figure 4.6c, d). The correlation for different vegetation types is higher between NDVI and aAIz than with NDVI and seasonal precipitation.

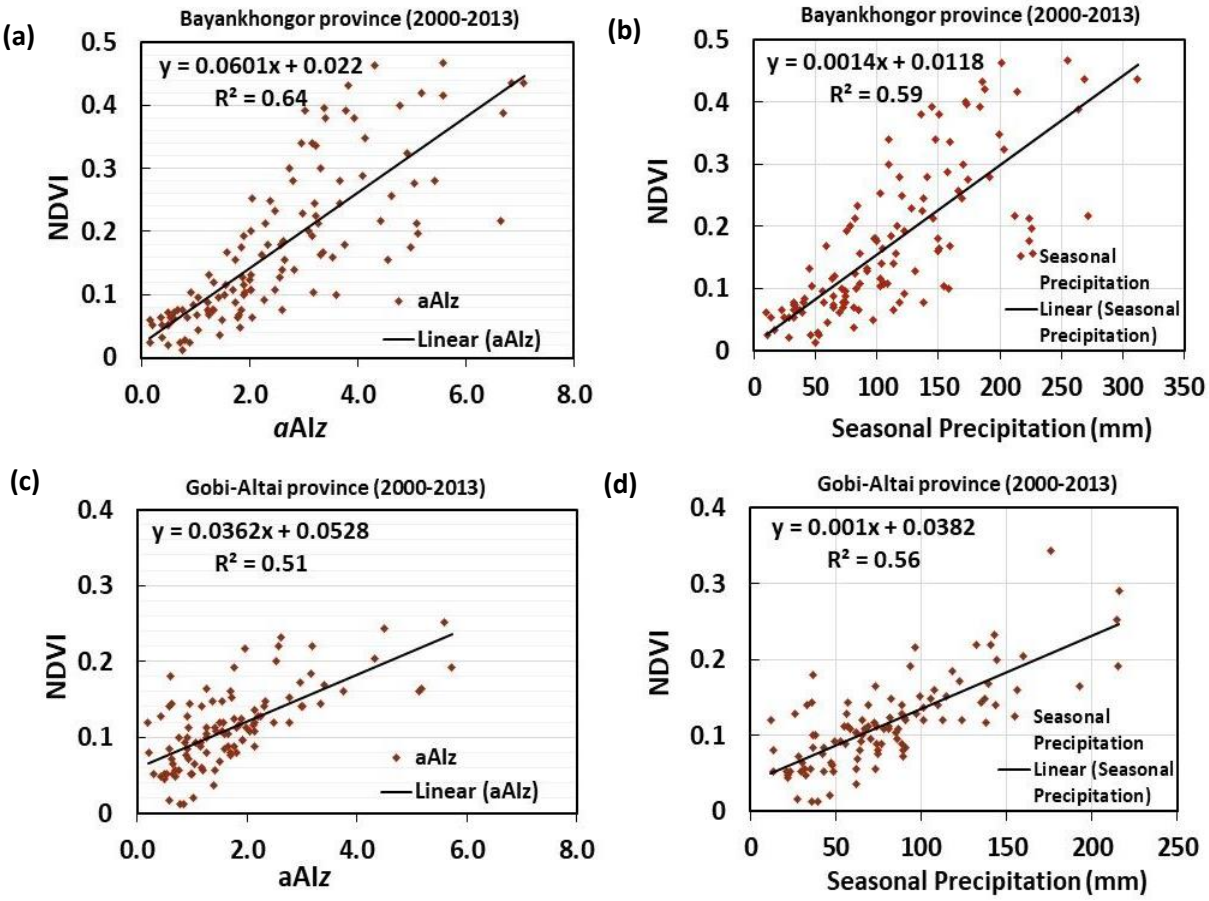

Figure 4.6 Scatter plot showing the mean August correlation values between NDVI and aridity index ($_aAI_z$); seasonal precipitation (mm) in (a,b) Bayankhongor and (c,d) Gobi-Altai.

The $_aAI_z$ performed as expected, highlighting drought years and *dzud* years. Droughts caused reduced biomass and led to a decrease in the amount of hay/forage (Nandintsetseg & Shinoda, 2013b). We compared drought occurrences with $_aAI_Z$ and created threshold criteria for the $_aAI_Z$ values. From 2000 to 2002, in particular, the effects of drought are apparent in these study regions. The dry years also contain massive *dzud* disasters, confirming the connection between the summer drought and the intensity of *dzud* events. The results of the developed $_aAI_Z$ index (with their accompanying stations) are represented from 1990 to 2013 in Table 4.3. When there were high rainfall totals during the growth period, the mean NDVI was 0.72 points above average. Therefore, a strong influence of July precipitation on the maximal growth phase in mid/late August should be evident.

Table 4.3 Summary of standardized aridity index ($_aAI_z$) values applied for drought risk analysis in this study.

no data: areas do not have enough data to calculate $_aAI_z$; (-) negative values indicate dry years and drought; (+) positive values indicate wet years; (<−1) indicate extremely dry years; (−0.5 to 0.5) indicate normal years; (>1) values indicate wet years;

		Bayankhongor						Gobi-Altai				
Station	**Bayanbulag**	**Bayankhongor**	**Bogd**	**Ekhiingol**	**Galuut**	**Shinejinst**	**Aj Bogd**	**Altai**	**Bugat**	**Khukhmorit**	**Tonkhil**	**Tooroi**
1990	1.0	1.0	1.3	0.1	1.1	1.1	-0.8	0.9	no data	no data	0.5	0.1
1991	0.8	-0.1	-1.0	-0.6	1.0	0.1	1.5	0.6	no data	no data	0.2	0.9
1992	-0.7	0.0	-0.9	0.1	0.6	-0.5	-0.2	0.8	no data	no data	-1.3	0.5
1993	2.3	1.9	1.2	2.1	1.7	1.6	no data	1.9	1.0	no data	2.4	no data
1994	-0.7	2.2	-0.3	-0.1	1.5	0.9	-0.7	1.5	2.3	no data	2.1	-0.9
1995	0.7	-0.5	-0.5	2.9	-0.5	-0.5	1.7	-0.1	0.3	no data	0.6	-0.5
1996	-0.1	-0.6	-0.4	1.2	0.0	0.3	0.4	-0.8	-0.7	no data	-0.6	0.7
1997	1.3	-0.1	0.0	0.4	-0.5	1.6	-0.6	-0.3	0.6	no data	-0.5	-0.3
1998	1.3	-0.8	-0.1	-0.8	-1.4	-1.1	-0.6	0.5	-0.3	no data	0.1	-0.5
1999	-0.2	1.0	0.3	0.1	1.1	1.7	-0.1	0.9	0.2	-0.3	0.3	-0.1
2000	-0.3	-1.0	-0.4	0.3	-1.2	-0.2	0.0	-0.9	-0.8	0.0	-0.6	0.3
2001	-1.0	-1.5	-1.4	-1.0	-1.2	-1.8	-0.7	-0.7	-1.5	-1.6	-1.2	-1.5
2002	-0.6	-1.3	-0.7	0.2	-1.4	-0.9	0.5	-1.8	-0.2	-0.3	-0.9	0.1
2003	1.1	2.3	2.2	0.0	0.2	1.9	3.1	1.4	2.5	2.7	2.5	3.4
2004	-0.6	-0.2	-1.2	-0.2	-0.8	-1.2	-0.5	-0.4	-0.4	0.2	-0.4	-0.6
2005	0.8	1.1	-1.4	-0.9	-0.5	-1.3	-0.5	1.3	0.0	-0.2	-0.2	0.7
2006	-0.8	-0.7	-0.4	-0.6	-1.1	0.0	-0.8	-0.6	-0.2	-0.4	-0.5	-0.6
2007	-0.5	0.6	0.9	2.4	-1.1	-0.2	-0.4	-1.2	0.3	0.5	-0.3	0.1
2008	-1.3	-1.2	1.4	-0.3	-1.7	-0.3	0.5	-1.3	-0.6	-0.2	-0.8	-1.0
2009	-1.5	-0.7	-1.2	-1.0	-0.4	-1.4	-1.5	-1.6	-0.9	-0.9	-0.5	-1.5
2010	0.1	-0.2	0.0	-0.1	0.0	-0.6	0.6	-0.1	0.1	0.6	0.0	0.0
2011	1.3	1.1	0.1	-0.3	1.3	0.5	-0.3	0.5	0.5	-1.1	-0.6	1.0
2012	0.1	-0.2	1.7	0.8	0.4	1.6	-0.2	-0.5	-1.3	0.4	-0.3	0.5
2013	-0.7	-0.3	-0.1	-0.6	0.0	-0.5	-1.0	0.3	-0.9	1.2	0.5	-0.7

Figure 4.7 compares the average MODIS NDVI of subsequent years (2000/2001, 2001/2002, and 2009/2010). NDVI decreased by approximately −0.09 from 2000 to 2001 in the northeast of Bayankhongor Province, from 2001 to 2002 in the central part of Bayankhongor Province, and from 2001 to 2002 in the southern part of Gobi-Altai (Figure 4.7a, b). However, NDVI increased in the steppe and mountain regions for most of the investigated areas (Figure 4.7c). The contribution of water supply in winter, a decrease of grazing pressure (due to livestock loss), and recovery in spring-summer rainfall played a minor role in vegetation regeneration in the semi-arid and desert regions.

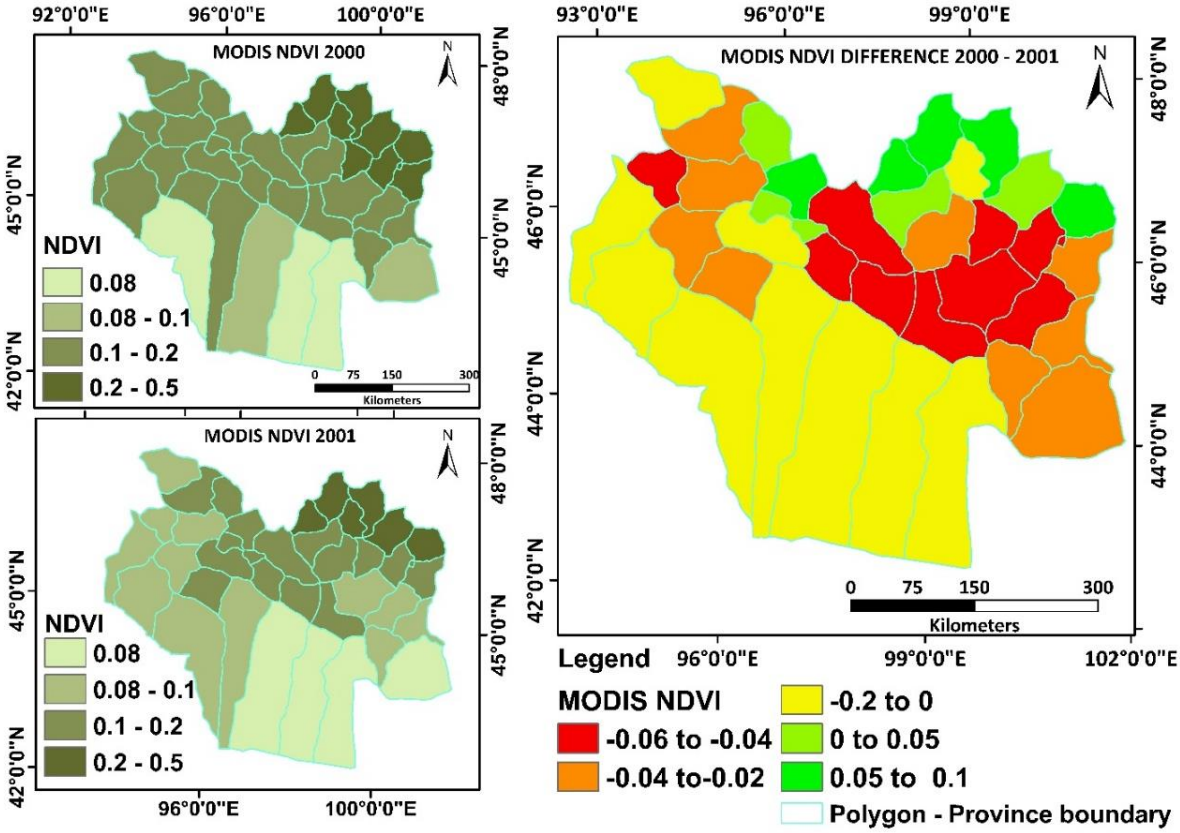

(a)

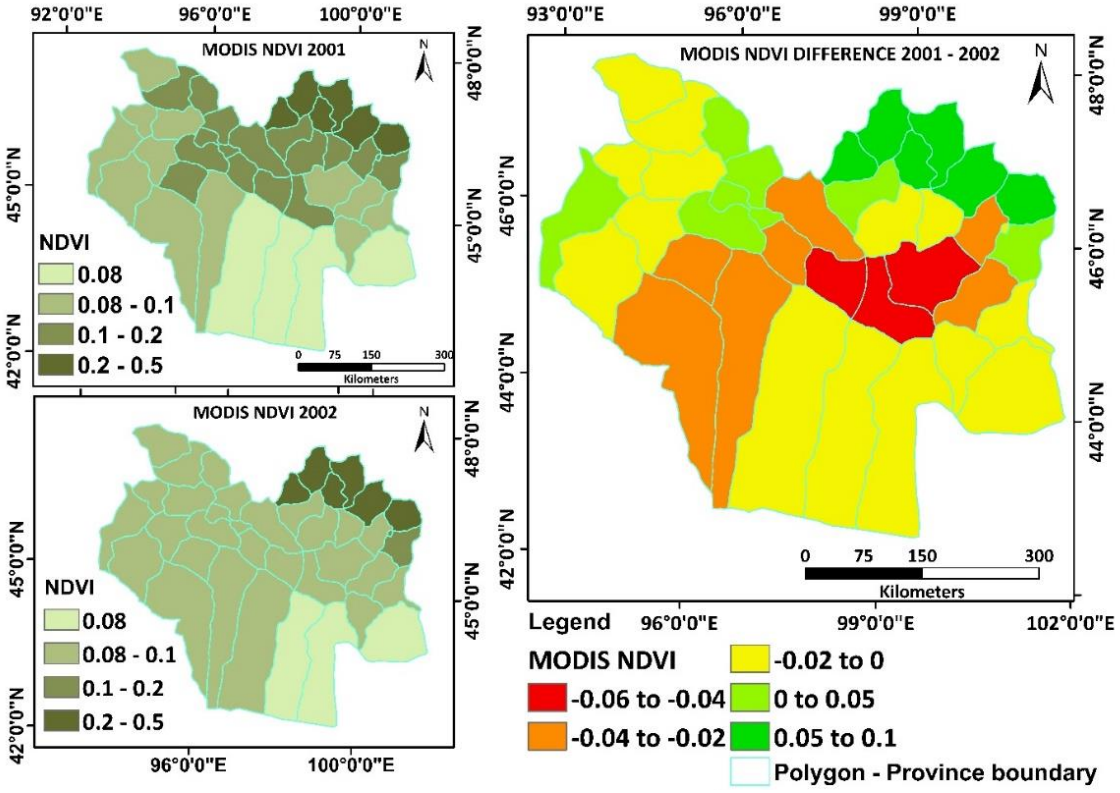

(b)

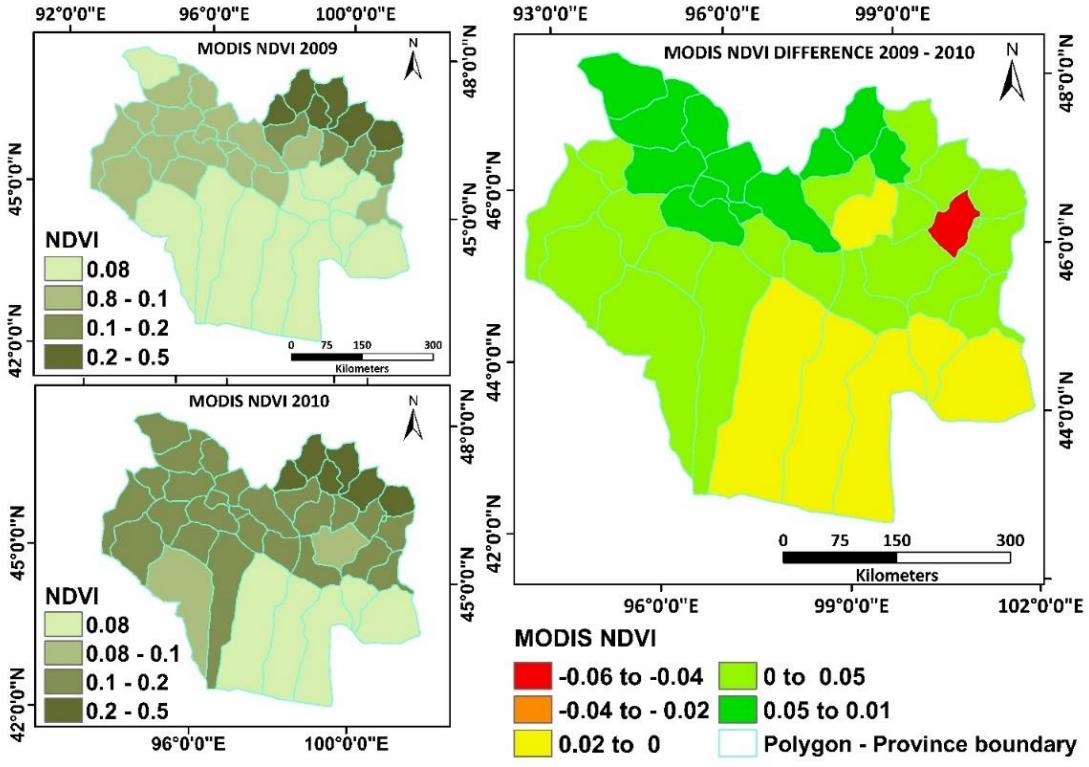

(c)

Figure 4.7 Spatial patterns of MODIS NDVI after dzud events (a) 2000/2001; (b) 2001/2002 and (c) 2009/2010.

4.4.3 Climate Condition Analysis

We examined the spatial distribution of CRU snow data during *dzud* events. Figure 4.8 shows the accumulated snow distribution maps during the *dzud* years of 1999/2000, 2000/2001, and 2009/2010. Observations were collected from November to March. Snow only accumulated in the northern section of the study area and increased during later years.

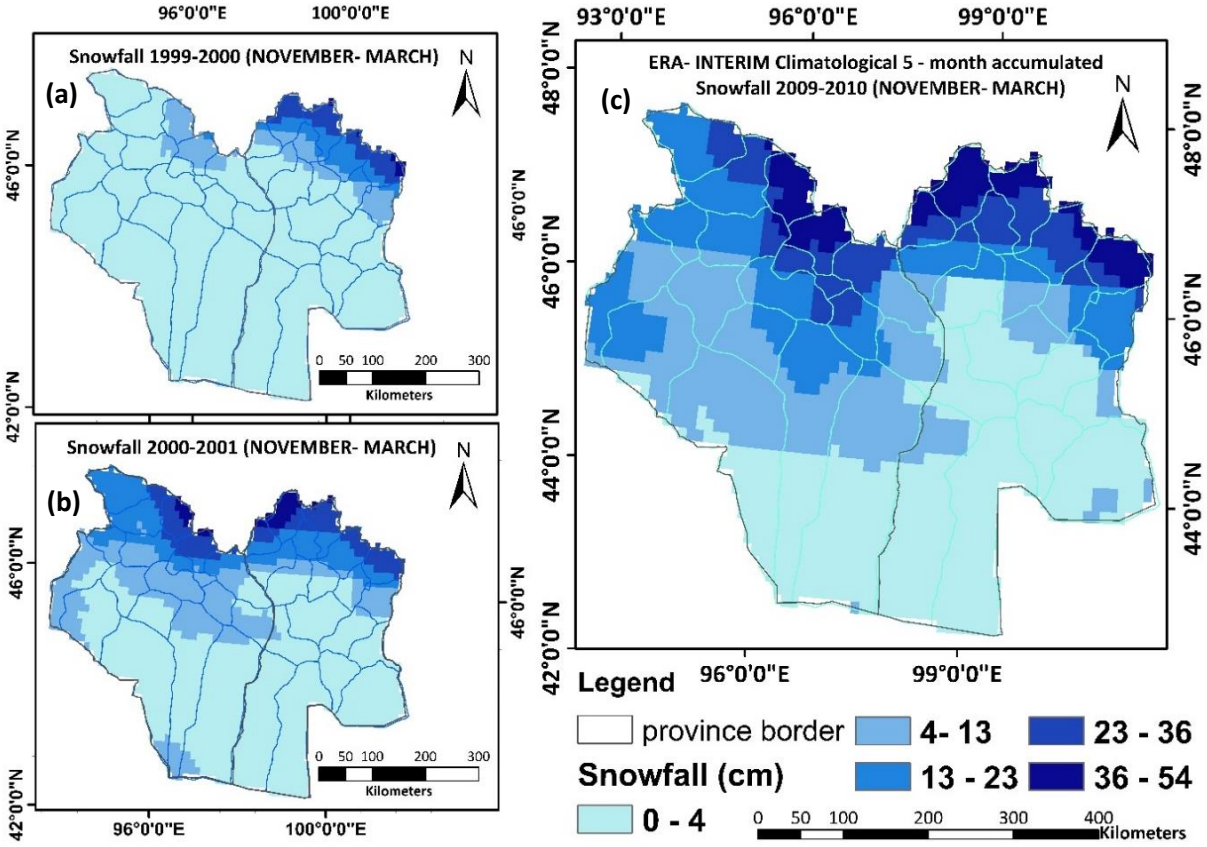

Figure 4.8 The spatial distribution of snowfall maps (between November and March), from (a) 1999/2000; (b) 2000/2001 and (c) 2009/2010.

We also examined the trends of annual mean precipitation and temperature as well as monthly precipitation and temperature. The mean annual precipitation and temperature differ significantly over the observation period. Figure 4.9 shows the time series of mean annual precipitation and temperature from 1985 to 2014 in Bayankhongor province and from 1990 to 2014 in Gobi-Altai province. Annual mean precipitation was 202 mm from 1985 to 2014, 226 mm from 1985 to 1999, and 179 mm from 2000 to 2014 in Bayankhongor province (Figure 4.9a, b). During the combined drought-*dzud* years, less precipitation was observed, i.e., 124.9 mm in 2000, 156 mm in 2001, and 128.6 mm in 2002 in Bayankhongor province. However, an increase in precipitation was observed in 1993, 1999, 2003, 2010, and 2011 (e.g., 233.8 mm in Bayankhongor province in 2011). For the Gobi-Altai province, the annual mean precipitation was 183.5 mm from 1990 to 2014, 205.7 mm from 1990 to 1999, and 168.7 mm from 2000 to 2014 (Figure 4.9c, d). During the combined drought-*dzud* years, the totals were 141.6 mm in 2000, 166.2 mm in 2001, and 108.3 mm in 2002. Hence, a peak in precipitation amount was observed in 1993, 2003, and 2010 in Gobi-Altai province (e.g., 215.3 mm in 2010).

As for temperature, a general trend towards a warmer climate was recognized in the period from 1985 to 2014. This result is consistent with (Klinge & Sauer, 2019).

(a)

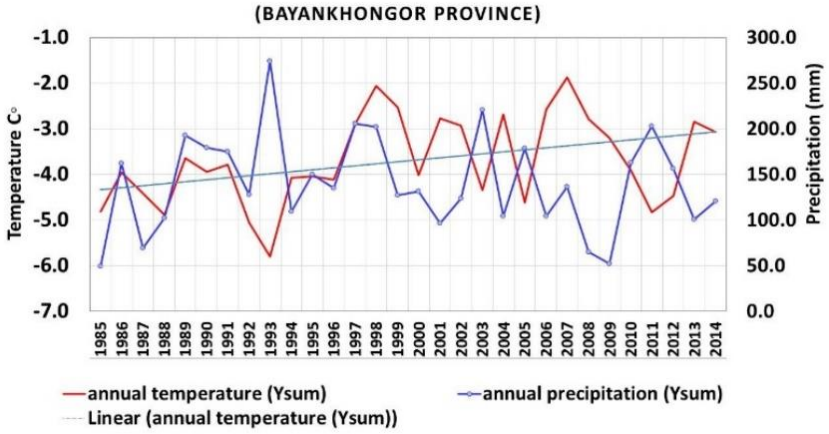

(b)

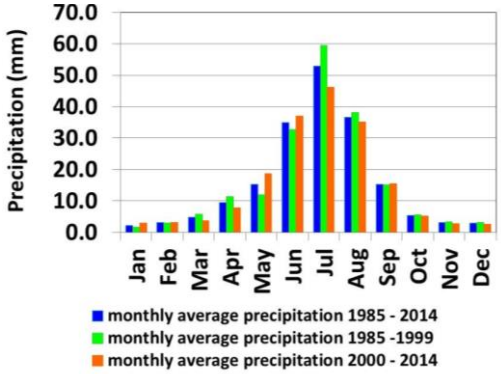

(c)

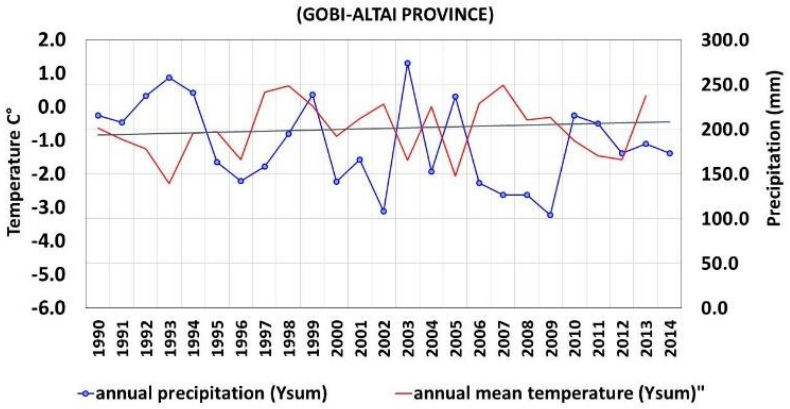

(d)

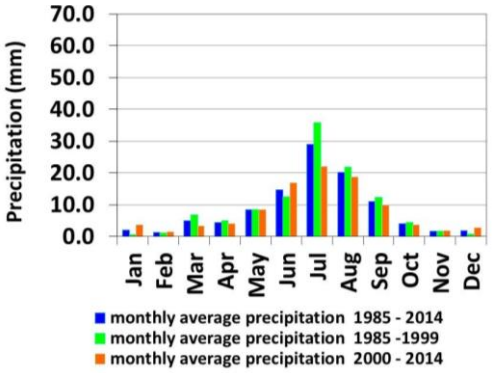

Figure 4.9 Comparison between mean annual precipitation and mean monthly precipitation (a,b) from 1985 to 2014 in Bayankhongor province and (c,d) from 1990 to 2014 in Gobi-Altai province.

Most stations during the last 15 years (2000 – 2014) are statistically drier than the previous 15 years (1985 – 1999). We determined the mean yearly precipitation during 2000–2014 is between 15 and 20% lower than 1985–1999. Contrary to the expected strong warming tendency in the winter months, the last 10 – 15 years showed a cooling in winter, which could be related to the Siberian cold high. This circumstance, coupled with the high drought intensity, was a fundamental factor in the occurrence of the consecutive *dzud*s from 2000 to 2002. The average annual temperature of the last 15 years (2000 – 2014) is higher than the temperature from 1985 to 1999. We detected the largest increase in annual temperature in the drier regions (southern area). The mean winter temperature from 2000 to 2014 (−3 to 2 °C) is cooler than the mean winter temperature from 1985 to 2014 (−0 to 9 °C). The summer season shows the biggest gain in temperature, while the gain during autumn is quite low. Several studies have discovered an increase in Eurasian snow cover over the past decades (J. L. Cohen et al., 2012; X. Wang et al., 2017) and increasing trends in anomalous fall melt events (Pan et al., 2019) through remote sensing.

4.4.4 Livestock Mortality Analysis

When considering the livestock mortality rate during consecutive *dzud* events, the most severe livestock loss was from 2000 to 2002, and from 2009 to 2010 (Figure 4.10). The highest livestock loss rate was nearly 60% in Bogd, Shinejinst, Ekhiingol, Bayankhongor, and Tooroi regions during the 2000/2002 *dzud* events. Regions further west in Mongolia contained the most mortality hotspots, with 80% of the total mortality (National Statistical Office of Mongolia, 2010). High mortalities indicate poor body conditions of the livestock-associated with adverse vegetation conditions due to drought or pasture degradation. During the 2010 *dzud*, the herds could not access pasture due to deep snow (Templer et al., 1993). The increase in pasture intensity reduces vegetation cover and it reinforced the effects of animal hooves (H. L. Zhao et al., 2005).

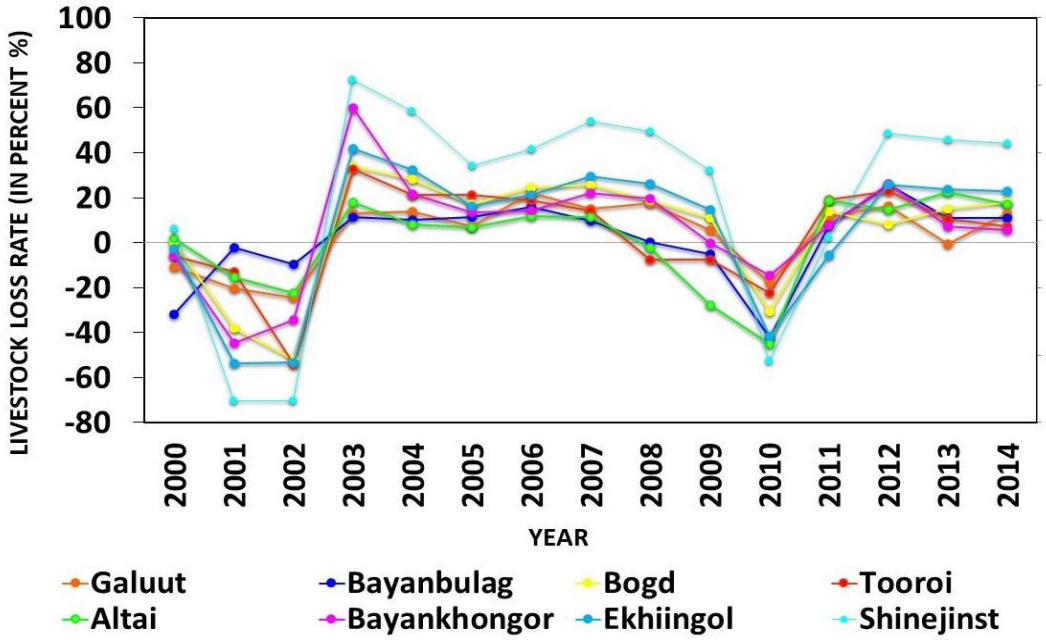

Figure 4.10 The livestock loss rate in percent from 2000 to 2014 (where negative values equal losses). Data: National Statistical Office of Mongolia.

4.4.5 Discussion

Our findings are consistent with other studies indicating that summer droughts and cold, snowy winters seem to be the major factors leading to *dzud* disasters (Mukund Palat et al., 2015a; Nandintsetseg, Shinoda, & Erdenetsetseg, 2018; Tachiiri et al., 2008). As other studies documented that Mongolia is facing severe economic damage and huge livestock losses (Appendix B) (e.g.,(Benson, 2011)) *dzud* might influence the vegetation phenology and livestock mortality. Our study finds that *dzud,* a combination of drought and harsh winter, contributes to the annual high livestock mortality in southwestern Mongolia, which is consistent with earlier studies (Begzsuren et al., 2004; Shestakovich, 2010). The climate projections show that these trends will be aggravated in the medium term and those extreme events, such as drought and *dzud,* will become more frequent and more intense, with severe environmental, social, and economic impacts (Mukund Palat et al., 2015a). Also, drought/dry years and lack of meltwater in the spring may cause high grazing pressure due to less vegetation resources for livestock. Moreover, reductions in vegetation cover due to high livestock grazing could negatively impact ecosystem function and increase vulnerability (Kakinuma et al., 2008; T. H. Oliver et al., 2015). We also noticed that livestock grazing is difficult after a cold *dzud* with a high snowfall that does not melt and covers the grassland during the entire winter. Vegetation is susceptible to the length of the rainy season. The years with low NDVI had very dry conditions during the following summer. Most investigated stations with dry conditions (minimum AI of −1) showed a low NDVI. We observed that the highest increase in annual temperature was found in the drier regions in the south of the study area, while stations in the northern parts of the study region exhibited a lower mean annual temperature due to lower temperatures during the winter. Years with drought risk and long dry periods heavily influence the local water budget by causing high evapotranspiration, increased capillary effect, and short-term soil salinization. This suggest that a low NDVI and the low soil moisture conditions can induce drought, and these impacts tend to be a precondition for *dzud*. Our adapted aridity index showed a considerable regional difference in NDVI from the climatic effects. The NDVI was closely correlated with ${}_{a}AI_{z}$, while seasonal precipitation showed a lower correlation with NDVI (Figure 4.6). In general, the maximum vegetation growth, irrespective of the annual precipitation conditions, remains stable. When there is a lack of snow cover, there is a lack of water available at the beginning of the growth phase. This is likely reducing the pasture growth due to water stress. For instance, a large amount of livestock died at a later time due to weakness or dehydration, as they were burdened during the winter due to weakened fodder supply. This is limited mainly by winter precipitation and the livestock loss rate, which has emerged as the most important condition of vegetation regeneration. Accumulated snow cover will increase the amount of soil moisture in spring and result in a positive effect on the vegetation cycle. We recognize that our study was limited to investigating recent climate related impacts on vegetation cover. Long-term climate trends were not assessed and may play a significant role, particularly if severe *dzud* events are becoming more frequent.

4.5 Conclusions

This study examined the spatiotemporal pattern in NDVI and the cycle of the growing season after different *dzud* events detected from MODIS data. Our analysis quantifies the understanding of different *dzud* mechanisms and their influence on vegetation and livestock grazing. Our results reveal spatiotemporal patterns of vegetation response to *dzud* and combined summer drought-*dzud*, and it can help assess the resilience of vegetation in different ecological zones. To clarify the role of *dzud* climate drivers, we assessed the relationship between the aridity index and summer NDVI (as a proxy for vegetation conditions) and found a significant correlation. The summer conditions represented by aridity index and drought risk have an impact on livestock mortality, which is heightened by *dzud*. The drought-associated *dzud* years corresponded with lower summer NDVI. Specifically, we assume that during dry winter conditions, the growth phase begins later due to water deficiency and leads to a weaker and slightly later vegetation growth peak. However, the *dzuds* from 2009 to 2010 coincide with greater livestock losses corresponded and higher summer NDVI. Alleviating the impacts of climatic stresses (drought and *dzud*) on vegetation will be a crucial challenge in the arid and semi-arid regions of Mongolia.

The consequences of changes in the frequency and intensity of environmental disasters have become a considerable issue for regional herders and the well-being of local communities. As a further study, the combined approach of herder's ecological knowledge and remote sensing is an opportunity to explore the speed of vegetation reaction to *dzud* and droughts.

Chapter 5 Development of a new Drought index using SMOS satellite soil moisture products: Case Study in Southwestern Mongolia

Oyudari Vova [1]*, Martin Kappas [1], Pavel Groisman [2], Tsolmon Renchin [3], Steven Fassnacht [1,4,5,6]

[1] Cartography, GIS and Remote Sensing Department, Institute of Geography, University of Göttingen, Goldschmidt Street 5, 37007 Göttingen, Germany;

[2] NC State University Research Scholar at National Centers for Environment Information, Federal Building, 151 Patton Avenue, Asheville, NC 28801, USA;

[3] Department of Physics, National University of Mongolia, Ulaanbaatar Mongolia, Ulaanbaatar 14200, Mongolia;

[4] Department of Ecosystem Science and Sustainability – Watershed Science, Colorado State University, Fort Collins, CO, United States, 80523-1476;

[5] Cooperative Institute for Research in the Atmosphere, CSU, Fort Collins, CO 80523-1375, USA

[6] Natural Resources Ecology Lab, Colorado State University, Fort Collins, CO 80523-1499, USA

* Correspondence Author

This chapter was submitted as a research article: Journal of Land, February 2021, 1122291, under review;

5.1 Abstract

A new drought index for meteorological and hydrological drought monitoring is presented, based on the integration of different remote sensing products and in situ observations. Due to a shortage of precipitation droughts reduces vegetation productivity, and thus, aggravate the impact of moisture stress on pastureland. Specifically, we examined a new composite Gobi drought index (GDI) based on the combination of Soil Moisture and Ocean Salinity (SMOS) Soil Moisture, several products from the MODIS satellite, and in situ Soil Moisture (SM) observations. Multiple linear regression method was used for estimation of GDI drought index. The former includes the surface soil moisture from the Soil Moisture and Ocean Salinity (SMOS) mission, the Moderate Resolution Imaging Spectroradiometer (MODIS) derived land surface temperature (LST), normalized difference vegetation index (NDVI), potential evapotranspiration (PET). The GDI drought index combines the soil moisture and temperature conditions while including the sensitive response of arid and semi-arid vegetation. The validation of the approach is based on the relationship between SPI and in-situ soil moisture (SM) observations, and their comparison to remote sensing (RS) – derived indices. The results show that the correlation was statistically significant between GDI and in-situ SM observations from the meteorological stations at 10 – 15 cm depths. The latter includes standardized precipitation index (SPI) from in-situ data. The correlation between GDI and SPI, as represented by the correlation coefficient (r) was 0.64. We also retrieved a subset of Soil Moisture Active/Passive (SMAP) soil moisture data and compared it with our GDI estimates. A high correlation between SMAP SM and GDI (0.85) is statistically significant at the 0.01 level and confirms that the GDI is a good overall tool for drought monitoring. The established new GDI index was retrieved at the 1 km spatial resolution for Southwest Mongolia from 2000 to 2018, and their two summer months (July, August) were used for monitoring drought and vegetation response to the varying soil/climatic conditions. Based on the assessment of drought severity, the new drought index allowed us to assess a large-scale spatial coherence of droughts across the Southwestern part of Mongolia.

Keywords: *drought; SMOS L2; MODIS products; in-situ soil moisture (SM); and multiple regression method*

5.2 Introduction

In recent years, the severity of various climatic hazards is expected to continue increasing due to climate change. Droughts have affected many regions of the world with the worst impact in the agricultural and livestock sectors (Mukund Palat et al., 2015b; *The impact of disasters and crises on agriculture and food security 2017 : FAO in Emergencies*). In our knowledge, when there is a lack of rainfall, drought occurs due to a deficiency of soil moisture and dryness. The lack of precipitation and other climatic factors (such as high temperatures, high winds, dust storms, low humidity, soil moisture) aggravate the severity of the drought event (Wilhite, 2000a). Droughts in Mongolia occur every 2-3 years; half of the country has been affected by a drought once every 4-5 years (Ulaanbaatar, 1998), and they always had significant socio-economic and environmental impacts. The largest droughts were in 2000, 2002, 2007, when most regions of the country were affected by extremely dry and hot weather (Bavuudorj, 2018; *Regional workshop on understanding the operational aspects of the drought observation system in Mongolia | United Nations ESCAP*). It is worth noting that the droughts have a dramatic effect on natural grassland. Thus, they may accelerate desertification processes together with destructive human activities (such as overgrazing), particularly in the arid and semi-arid regions of the Mongolian Plateau (Chang et al., 2017b). As reported by the UNCCD, desertification affects 64.7 % of the territory of Mongolia (*LAND DEGRADATION NEUTRALITY TARGET SETTING PROGRAMME NATIONAL REPORT ON VOLUNTARY TARGET SETTING TO ACHIEVE LAND DEGRADATION NEUTRALITY IN MONGOLIA National Committee on Combatting Desertification of Mongolia (NCCD)*, 2018). During the past 60 years, regional temperatures in Southern Mongolia have increased by 0.1 – 3.7 ˚C, spring precipitation has decreased by 17%, and summer precipitation has decreased by 11% (Karrouk, 2007). Climate changes are the likely causes that intensify droughts in the spring-and summer-time, especially during the growing season (*THIRD NATIONAL COMMUNICATION OF MONGOLIA Under the United Nations Framework Convention on Climate Change*; Oyudari Vova et al., 2020). The pastoral livelihoods are under pressure from the drought effects, while herders and herds often migrate 150-200 km from their usual camps in search of good pasture (Honeychurch & Honeychurch, 2015). It is very important to investigate the pasture responses to soil moisture deficit and to summer droughts that are crucial for the nation (Deng et al., 2020). Consequently, it is important to emphasize that accurate regional assessment of drought modeling must be based on realistic models (variables) and their current environmental conditions (Wilhite & Glantz, 1985b). For instance, in some studies, the strength of drought is defined depending on its area impact (Moreira et al., 2012; Szép et al., 2005).

Generally, there are recognized four types of drought: (1) meteorological drought, (2) agricultural drought, (3) hydrological drought, and (4) socio-economic drought (Heim, 2002). The meteorological drought refers to precipitation shortages, agricultural (or soil moisture) drought also accounts for soil moisture deficit, and hydrological drought is related to water resources (supply) in the forms of streamflow, groundwater, and/or evapotranspiration deficit. Socio-economic drought is linked with supply and demand economic aspects, related to other three types of drought (Dubrovsky et al., 2006). The meteorological and agricultural droughts occur when precipitation and available soil moisture

decrease, which can cause vegetation stress and adversely affect grassland (A. K. Mishra & Singh, 2010). Figure 5.1 displayed the simplified sketch of processes and drivers relevant for meteorological, agricultural, and hydrological droughts.

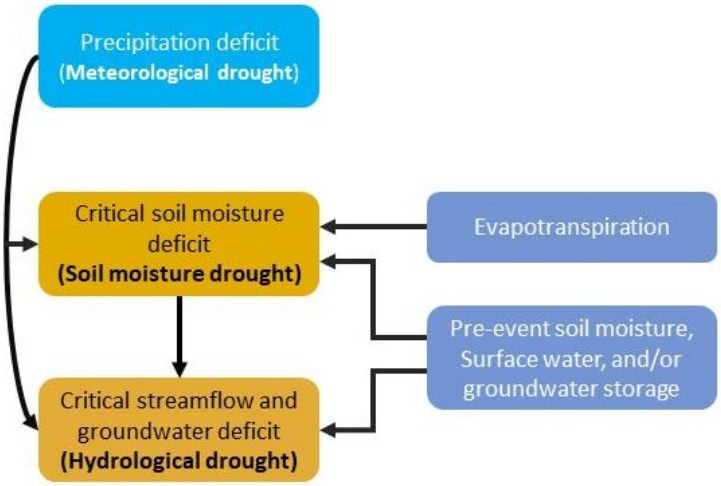

Figure 5.1 Drought types, causal processes, and their drivers of occurrences. Source: (Easterling et al., 2012)

In this context, soil moisture is considered a significant variable of agriculture drought in arid and semi-arid land. According to moisture conditions and deficiency of water for a specified area, drought indices classify as precipitation indices, water balance indices, soil moisture indices, and aridity indices (Nilda Sánchez et al., 2016b). There are currently a variety of studies that used drought indices to estimate the intensity of drought (Dubrovsky et al., 2006; A. K. Mishra & Singh, 2010; Shah & Mishra, 2020; Yihdego et al., 2019). The most well-known indices are the traditional Standardized Precipitation Index (SPI) and the Palmer Drought Severity Index (PDSI) (Alley, 1984; Mckee et al., 1993). The SPI and PDSI indices are used in long-term drought assessments. In Mongolia, six indexes were used for research, and two indexes such as PDSI, SPI indices were used for research and operational service goals (*Information And Research Institute Of Meteorology, Hydrology And Environment*). The above-mentioned six indices are Vegetation condition index (VCI), Vegetation Health index (VHI), Temperature Condition Index (TCI), Normalized Difference Drought index (NDDI), Normalized Difference Water Index (NDWI), and Vegetation Supply Water index (VSWI). They are provided by National Drought Watch System (*Satellite-based system to monitor droughts/dzuds handed over to Mongolia - Mongolia*).

Most of the drought monitoring approaches using satellite data are based on Normalized Difference Vegetation Index (NDVI), Vegetation Condition Index (VCI), and land surface temperature (LST) or brightness temperature. The NDVI is used to assess the vegetation condition to detect the greenness of vegetation canopy during the growing season affected by droughts (Hassan et al., 2018; Felix N. Kogan, 1997; Nanzad et al., 2019a; Berhan et al., 2011; Tucker & Choudhury, 1987). Among these variables, soil moisture indices (Martínez-Fernández et al., 2015), and some other hydrological aridity indices such as the Crop Moisture Index (W. C. Palmer, 1968), characterize the water deficit over a given area. Thus, several indicators are used jointly to get a full characterization of drought in a given area. It is noteworthy that the spatial distribution and the extent of drought events at the regional scale have become challenging. In this regard, the use of remote sensing data has the

advantage of providing temporal and spatial patterns of drought dynamics on large spatial scales. Hence, various remote-sensing indices were developed and proposed for global drought monitoring.

The soil moisture satellite products have offered a substantial advantage in terms of global coverage, temporal and spatial resolution, and has integrated into various drought monitoring programs (Z. Wan et al., 2004). Currently, there are two missions devoted to global surface soil moisture (SSM, top 0–5 cm) monitoring: the Soil Moisture and Ocean Salinity (SMOS) (Su et al., 2013) and the Soil Moisture Active and Passive (SMAP) (Entekhabi et al., 2010). These two missions opened a new perspective on drought monitoring by offering a 40 km global spatial resolution of soil moisture values every three days. Recent studies show that SMOS SM was successfully tested and can be used to characterize the pasture conditions in Mongolia (Oyudari Vova, Kappas, & Rafiei Emam, 2019). However, despite the availability of soil moisture data at a global scale, there is limited research using satellite soil moisture observations for drought analysis (Martínez-Fernández et al., 2016a; Scaini et al., 2015b). Agricultural and meteorological drought indices should integrate various parameters, like soil moisture, temperature, and evapotranspiration deficits to effectively monitor agricultural and meteorological drought (Mannava Sivakumar et al., 2010). In drought conditions, the soil moisture scarcity is often exacerbated by an increased heatwave. Therefore, integration of soil moisture, evapotranspiration, and vegetation status data offers an appropriate response variable to characterize vegetation conditions in the arid land.

Due to drought and desertification expansion in Mongolia, it is necessary to develop methods for large-scale vegetative drought assessment. The main objectives of the study were integrating the monthly average SMOS SM and the MODIS-based NDVI - LST - PET data using multiple linear regression (MLR) model to build an appropriate model for the drought assessment. Specifically: 1) to assess the GDI with other remote sensing indices (TCI, NMDI, VSWI, NDVI, NDWI, NDDI), and with the SPI index, 2) to evaluate GDI by verifying it using the in-situ SM observations from meteorological stations, and after verification 3) to apply the GDI to produce regional wide GDI 1 - km drought maps for summer months (July and August) from 2010 to 2018 across Southwestern Mongolia.

5.3 Study Area

This research was conducted in the Bayankhongor Province. The Province is located in the southwest of Mongolia and covers an area of 116,000 square kilometers. It includes the southern region of the Khangai Mountain Range, the eastern ridges of the Altai Mountains, and the unique Gobi Desert to the south Figure 5.2 (Ahearn, 2018). The Province climate is continental semi-arid with mean annual temperatures range from 0° to 7°C in the north and 0° to 8°C in the southern regions. As mentioned above, the region has experienced intense climatic change with the regional summer temperatures increased from 1984 to 2003 in the steppe, semi-desert, and desert areas. The Province suffers from a scarcity of water and has an average annual precipitation of 80 – 160 mm (Oyudari Vova et al., 2020). The vegetation growing season is short and depends on antecedent soil moisture and regional rainfall (Böhner, 2006; Hilker et al., 2014). Short grasses, semi-shrubs, and woody plants are the dominant vegetation (Bayarjargal et al., 2006). The soil type of the Province has a vertical distribution by elevation: white-loamy and sandy soil (below 1300 m), gray-stony soil (1300-2000 m), and dark brown soil (above 2000 m). In the Province, a wide range of anthropogenic environmental problems have emerged during the past several decades. These include increased livestock numbers (goats) and less seasonal movement of herds. Goats comprise approximately 81% of the herd, sheep – 16%, and the remaining 3% comprises camels, horses, and cattle (Fernández-Gimenez et al., 2012).

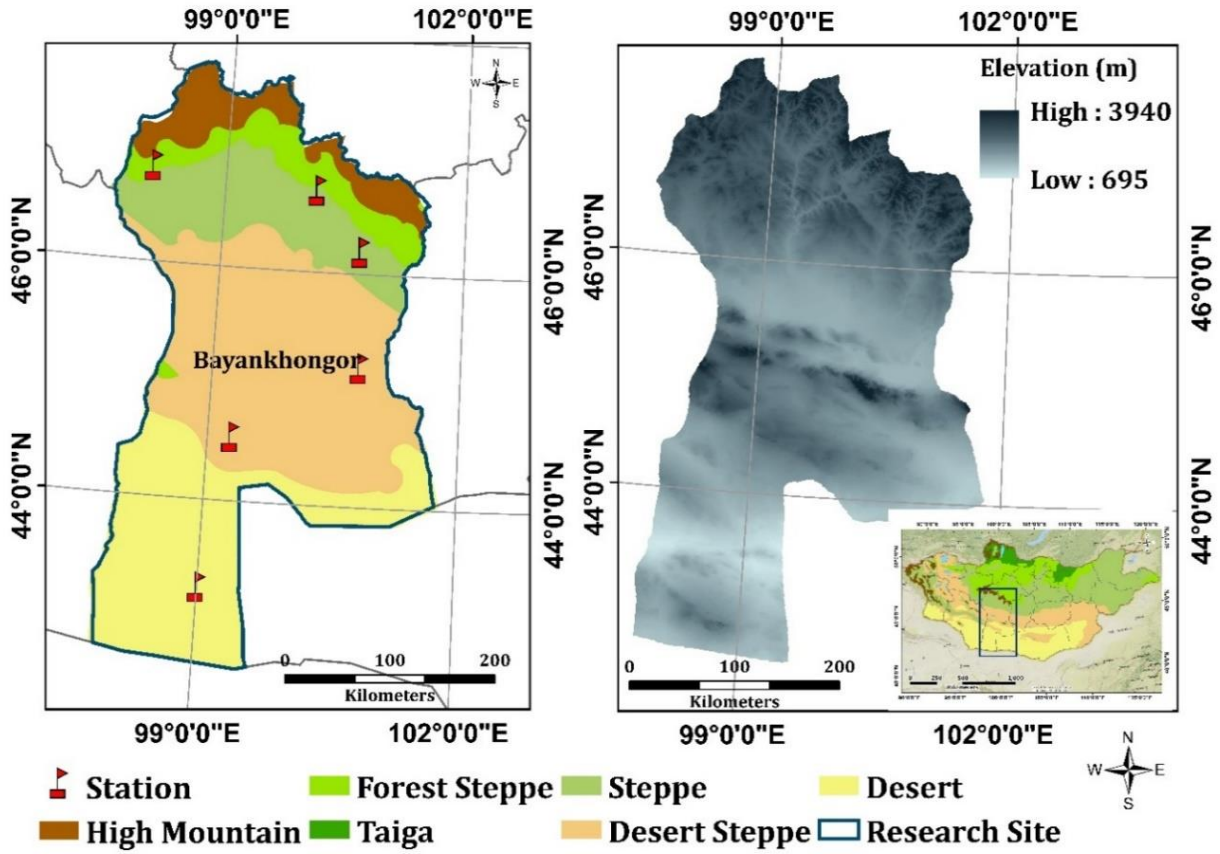

Figure 5.2 Geographical location and vegetation zone maps of Bayankhongor Province. (a) Meteorological station distribution and vegetation zones, data sourced from the Information and Research Institute of Meteorology, Hydrology, and Environment (IRIMHE) of Mongolia. (b) Digital Elevation Model (DEM) from SRTM (Shuttle Radar Topography Mission) data (USGS EROS Archive - Digital Elevation - SRTM Mission Summary).

The selected meteorological stations were representative of the surrounding geomorphologic and vegetation conditions. The climate datasets and maps of vegetation zones were provided by the Institute of Meteorology and Hydrology of Mongolia. The locations of the meteorological stations were categorized into three vegetation zones: steppe, semi-desert steppe, and desert (Table 5.1). These zones form belts of vegetation at different altitudes (from mountains to plains) and latitudes (from the north to south).

Table 5.1 Meteorological stations in the Bayankhongor and situ-measured SM data stations with location information, and vegetation zones.

Meteorological station	Province name	Vegetation zones	Latitude (N)	Longitude (E)	Elevation (M)
Bayanbulag	Bayankhongor	steppe	46° 49'32 N	98° 40'10 E	2398
Galuut	Bayankhongor	steppe	46° 43'30 N	100° 8'35 E	2102
Bayankhongor	Bayankhongor	steppe	46° 11'40 N	100° 42'2 E	1877
Bogd	Bayankhongor	semi-desert	45° 40'10 N	100° 7'75 E	1264
Shinejinst	Bayankhongor	semi-desert	44° 32'13 N	99° 17'34 E	2216
Ekhiingol	Bayankhongor	desert	43° 14'48 N	99° 21'14 E	1011

5.4 Data

The datasets that were used in this study include in-situ SM, meteorological, and remotely sensed data. In situ data included soil moisture, precipitation, and air temperature from the meteorological stations which were applied at the validation stage of this research. Table 5.2 shows a summary of the datasets that were used in this research.

Table 5.2 Summary of the datasets used in this research.

Name of Dataset	Implementation Year	Information/Resolution of Data	Source
Soil Moisture (in-situ SM) Precipitation (P)/ mm, Temperature (T)/ °C	2000-2015	Meteorological stations	Information and Research Institute of Meteorology, Hydrology, and Environment of Mongolia http://irimhe.namem.gov.mn/index.php
NDVI MOD13	2000-2018	MODIS/ TERRA (1 km resolution) Monthly NDVI	https://lpdaac.usgs.gov/products/mod13a3v006/
LST MOD11	2000-2018	MODIS/ TERRA 8 day, (1 km resolution)	https://lpdaac.usgs.gov/products/mod11a2v006/
PET MOD16	2000-2018	MODIS/ TERRA 8-day, 500 m (1 km resolution)	https://lpdaac.usgs.gov/products/mod16a3v006/
SMOS SM	2000-2015	SMOS L2 Daily composites to monthly (40 km resolution)	https://earth.esa.int/web/guest/missions/esa-operational-eo-missions/smos/content/-/asset_publisher/t5Py/content/how-to-obtain-data-7329
SMAP SM	2015-2018	SMAP L3 3-daily composite to monthly (9 km resolution)	https://nsidc.org/data/SPL3SMP_E/versions/3

- **SMOS products and (SM) data**

The SMOS Level 2 data (version 5.51) that we used, were provided by ESA's Soil Moisture and Ocean Salinity (SMOS) mission and projected on the Icosahedral Snyder equal-area hexagon Discrete Global Grid (DGG) with equally spaced nodes at ~ 15 km. The SMOS mission provides global soil moisture measurements with a 40 km spatial resolution and accuracy of 0.04 m^3/ m^{-3} (Yann H. Kerr et al., 2010). The datasets are provided ranging from regional to global scales and at a three days temporal resolution. The data available are daily values, decadal, and monthly averages. The snap toolbox program was used for data pre-processing, and daily composites were aggregated to monthly average values. The datasets between April and September from 2010 to 2015 were selected to create the new integrated methodology for drought indices and the consequent drought analysis. Since the SMOS satellite data cover a large spatial area, it appears more reasonable to use the monthly average values. To accomplish further analysis, SMOS SM measurements were provided by decades, i.e., three times per month (normally between the 29^{th} and 8^{th}, 9^{th} and 18^{th}, and 19^{th} and 28^{th} of each month) during the warm period of the year from April until the end of October. Afterward, daily composites were used to compute the monthly average composites for further analysis.

- **MODIS products (NDVI, LST, and PET)**

For this research, the Moderate Resolution Imaging Spectroradiometer MODIS input products were: NDVI MOD13 (MOD13A3)–a Normalized Difference Vegetation Index, LST MOD11 (MOD11A2)–a land surface temperature images, and PET MOD16 (MOD16A3) – a potential evapotranspiration data from the MODIS sensor aboard the Terra and Aqua satellites. They were used to calculate the drought indices from April to September 2010-2015. These remote sensing products are freely distributed by the U.S. Land Processes Distributed Active Archive Center (https://lpdaac.usgs.gov). The NDVI MOD13 is a 1 km spatial resolution monthly averaged daily product. LST MOD11 and PET MOD16 have an 8-day composite temporal resolution, which was recalculated to a monthly average value similar to the NDVI MOD13. The LST product has a spatial resolution of 1 km and the PET was aggregated to a 1 km spatial resolution. The 8-day data are adjusted to nadir and standard sun angles using bidirectional reflectance (BRDF) models (Justice et al., 2002; Vermote et al., 2002). The products have been processed for atmospheric and geometric corrections. The AppEEARS web tool was used for data download and pre-processing images. This tool provides users the data values as well as the associated data quality characteristics (https://lpdaacsvc.cr.usgs.gov/appeears). All MODIS individual images were downloaded, based on geographic coordinates. The LST values were in Kelvins are encoded in a 16-bit unsigned integer that ranges from 7500 to 65,535. The actual temperature values were derived using a multiplication factor of 0.02, as stated in the MODIS product manual. The NDVI values that were less than zero were excluded from analysis because the pixel values less than or equal to zero are assumed to represent the cloud or the presence of a water body. The PET values were in $kg/m^2/8day$ that range from -32767 to 32700, also actual PET values were calculated using a multiplication factor of 0.1. Further, MODIS spectral bands 2 and 6 are downloaded from April to September between 2000 and 2018 to calculate selected drought indices. The bands 2 and 6 were derived applying a multiplication factor of 0.0001 as it was stated in the guidance manual to MODIS products.

- **In-situ Soil Moisture (SM) data**

In-situ Soil Moisture (SM) measurements between April to September 2010-2015 from six different stations of the Bayankhongor Province were obtained from the Information and Research Institute of Meteorology, Hydrology, and Environment (IRIMHE) of Mongolia (Information And Research Institute Of Meteorology, Hydrology And Environment). The SM data are observed (by gravimetric methodology) as plant-available soil moisture (mm) in the upper 0–50 cm at monthly intervals (the 7^{th}, 17^{th}, and 27^{th} days of each month) from April to September due to seasonal conditions and were calculated as the actual total soil moisture minus the moisture content at the wilting point. At each SM station, the observations include one sample per month and the data are available in volumetric water content m^{-3}/ m^{-3}. In-situ measured SM data represent a 10-15 cm depth layer at a monthly average interval. This soil layer includes the major rooting zone of the grasses that dominate most of Mongolia. To account for spatial consistency between in-situ SM measurements and RS-derived drought indices, the corresponding nearest pixel value was used for each of the six soil moisture station locations.

- **Meteorological data**

Monthly precipitation totals (mm) and surface air temperature (°C) data are based on daily observation data from meteorological stations. The meteorological data (precipitation) has been used to estimate the Standardized Precipitation Index (SPI) which is the most widely used meteorological drought index, developed by (Mckee et al., 1993). The SPI estimates the standardized departure of

actual rainfall concerning a rainfall probability function. The SPI index was calculated using the monthly precipitation data from April to September 2000-2015 at the Information and Research Institute of Meteorology, Hydrology, and Environment (IRIMHE) of Mongolia. The seasonal SPI values are calculated to ascertain the influence of SPI values on vegetation conditions and the spatial patterns of soil moisture drought during the study period (Zargar et al., 2011). Specifically, the SPI is computed for shorter accumulation periods (e.g., 1 to 3 months); it is an indicator for immediate impacts of reduced soil moisture, snowpack, and flow in small creeks (*Copernicus European Drought Observatory (EDO*). The normalized SPI is an effective tool in analyzing wet and dry periods. The geographical locations of the six meteorological stations are displayed in Table 5.1.

5.5 Methods

A new integrated Gobi drought index (GDI) is developed based on the monthly average SMOS SM and NDVI / LST / PET - MODIS data. After all data processing, a multiple linear regression (MLR) model was applied to build this index. It allows users to quantify the drought intensity in their area and use GDI for a drought monitoring system in the future (A. K. Mishra & Singh, 2010).

Subsequently, the drought assessment based on the GDI was conducted in a three-stage process (Figure 5.3). Firstly, the assessment of the GDI model was performed by comparing the spatial-temporal evolution of GDI with other remote sensing indices (TCI, NMDI, VSWI, NDWI, NDDI), and with the SPI index, using the Pearson correlation coefficient (R). Secondly, in-situ SM observations and SMOS SM were correlated with the GDI to confirm the effectiveness of the drought model based on this index. Thereafter, the seasonal precipitation and temperature that are traditional characteristics of regional climate conditions were compared with the GDI behavior during the drought-occurred years. Finally, the developed drought model was applied to produce the regional wide GDI drought maps for the two-month seasons (July – August) from 2010 to 2018 with a spatial resolution of 1 km and temporal resolution of one month. The regional-wide monthly GDI drought distribution map has not yet been considered in previous studies in Southwestern Mongolia.

5.5.1 Development and comparison of drought indices

5.5.1.1 Integration method for remote sensing data of drought index (GDI)

Multiple linear regression analysis was conducted to develop the drought model which was named Gobi drought index (GDI). Multiple linear regression models have often been used in environmental and nature reserves studies. The model demonstrates how SMOS SM satellite data depends on NDVI, LST, and PET derived from the MODIS products. Multiple regression models were constructed to describe how the single response variable SMOS depends linearly on several predictor variables (Belsley et al., 2005; Murray et al., 2012). Basic descriptive statistics and regression coefficients are shown in Table 5.3. The six different drought indices (Table 5.5) were derived from the remote sensing (MODIS/TERRA) products, and the Standardized Precipitation Index (SPI) was computed as an alternative to verify the effectiveness and reliability of the GDI. Afterward, the remote sensing-based drought indices were tested in further comparative analysis. These drought indices are often applied for arid or semi-arid regions to represent the pasture conditions and drought monitoring (Chang et al., 2017c; Q. Liu et al., 2020; Zolotokrylin et al., 2016). We assume that the purposed drought index, GDI, is derived from satellite data and depends on NDVI, LST, and PET variables as in Equation (5.1).

GDI = *F* (NDVI, LST, PET) (5.1)

Under this assumption, a multidimensional linear regression model was selected:

$$y_i = \beta_0 + \beta_1 * x_{i1} + \beta_2 * x_{i2} + \beta_3 * x_{i3} \quad (5.2)$$

Here y_i is the dependent variable (GDI); β_0 is the intercept, $\beta_1 - \beta_3$ are the coefficients; x_i is the corresponding independent variables. Equation (5.2) represents the relationship between the dependent variable, GDI, and the independent variables as a weighted average in which the regression coefficients (β's) are the weight coefficients. The parameters of this model for all independent variables (NDVI, LST, and PET) and the characteristics of the goodness of fit are shown in Table 5.3.

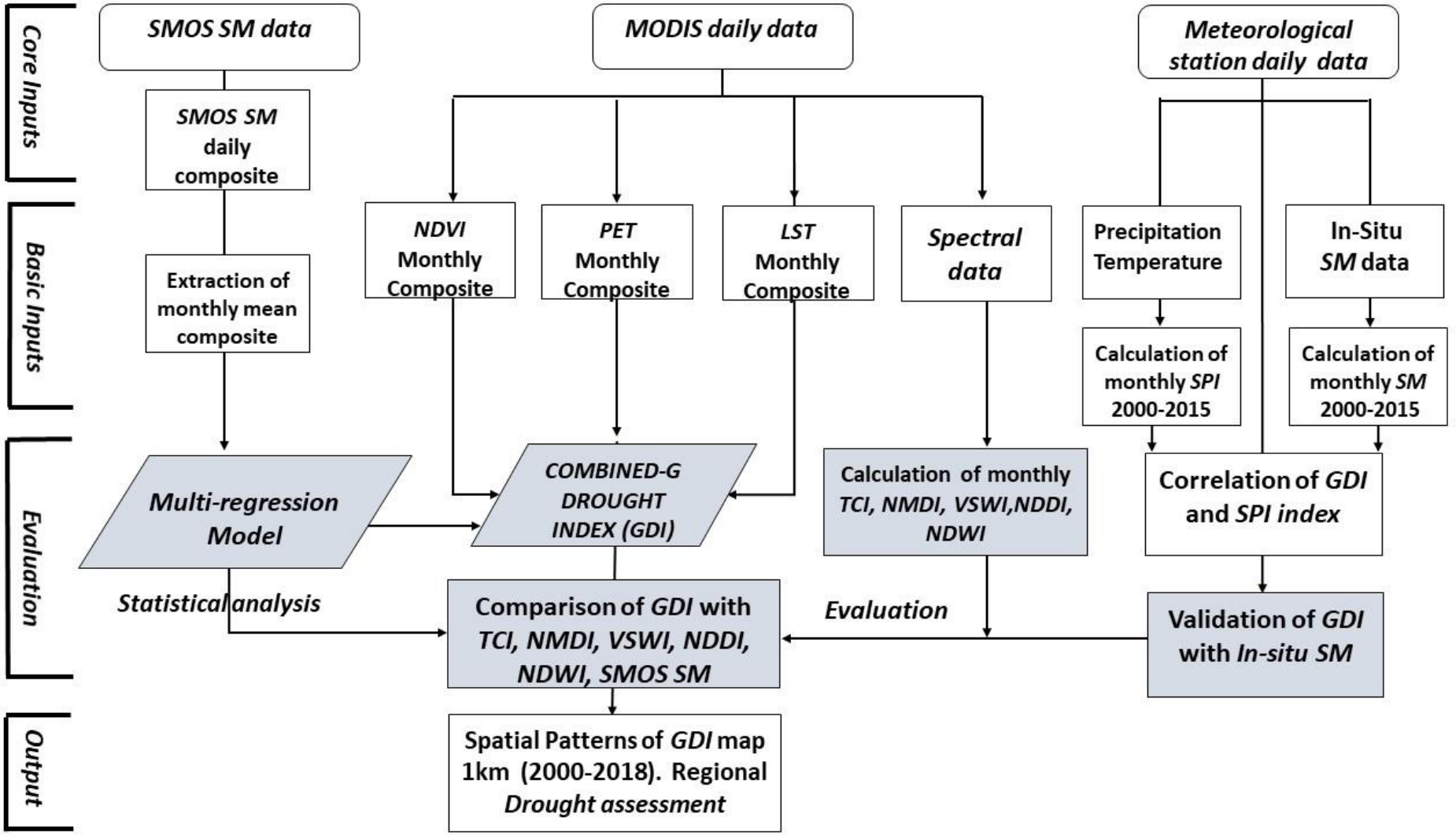

Figure 5.3 Flowchart of processing of the GDI drought model of this study

Table 5.3 Descriptive statistics of the multiple-regression model (5.2) used in this study for dependent Variable SMOS

Independent variables of the model	Regression Coefficient Estimates		t	Collinearity Statistics	
	β	Std. Error		Tolerance	VIF
(Constant)	-1.197	.040	-4.897		
NDVI	1.246	.132	9.454	.591	1.692
LST(Celsius)	-0.0008	.001	-.524	.781	1.280
PET	0.003	.001	4.490	.724	1.382

Here the variance inflation factor (VIF) is a measure of the goodness of fit and can be between 0 and 10 (J. Cohen et al., 2013; Hair et al., 1998); β are the regression estimates of coefficients in Eq. 5.2; Std. Error are the standard errors of these regression coefficients; t is the t-statistics for the β_i coefficients; Tolerance is the significance of the presence of individual independent variables in Eq. 5.2, and it ranges from 0 to 1 (R^2). Table 5.3 shows that there is no multicollinearity for this regression model.

A combination of ρ - value and VIF measures was used. The correlation analysis showed that there are no strong correlations between the independent variables as in Table 5.3. Likewise, the independent variables are normally distributed for the assumptions of the linear regression model.

Substituting β estimates from Table 5.3, we have a linear model for the integrated drought index (GDI, Equation 3):

$$\boldsymbol{GDI} = -1.197 + 1.246 * \boldsymbol{NDVI} - 0.0008 * \boldsymbol{LST} + 0.003 * \boldsymbol{PET} \qquad (5.3)$$

LST and NDVI alone cannot deliver an efficient characterization of the spatial patterns of water stress at an ecosystem level. The contribution of NDVI and PET in equation (5.3) can be interpreted as means to modulate soil water content through vegetation and temperature conditions. Thereby, the GDI seems to be more suitable to capture large-scale drought conditions in the arid land of the Southwest of Mongolia than each of these three independent variables in the right part of (5.3) separately. The drought classification used in this study is based on the U.S. Drought Monitor (Svoboda et al., 2002). Hence, the negative GDI values indicate relatively dry conditions, while the positive values are typical for more wet conditions. Six drought categories have been identified (Table 5.4).

Table 5.4 Intensity classification of GDI values (modified from the U.S. Drought Monitoring (Svoboda et al., 2002))

Drought intensity classes	GDI Ranges
Extreme drought	-0.5 to -0.3 or less
Severe drought	-0.3 to -0.2
Moderate drought	-0.2 to -0.1
Abnormally dry	-0.1 to 0
Normal	0.1 to 0.2
Abnormally wet	0.2 to 0.3 or above

Table 5.5 The Drought Indices definitions and their formula used in this research.

Drought index	Formula	Reference
SPI (Standardized Precipitation Index)	$g(x) = \frac{x^{a-1}\, e^{-\frac{x}{\beta}}}{\beta^{a}\, \Gamma(\alpha)} \quad for\ x > 0$ $\alpha > 0$ is a shape parameter $\beta > 0$ is a scale parameter χ is the precipitation amount $\Gamma(\alpha)$ is the gamma function	(Mckee et al., 1993 *Copernicus European Drought Observatory (EDO)*)
TCI (Temperature Condition Index)	$TCI = \frac{LST_{max} - LST_j}{LST_{max} - LST_{min}} * 100\%$ LST_{max} and LST_{min} are the maximum and minimum LST values for a given year	(F. N. Kogan, 1995b)
NMDI (Normalized Multi-Band Drought Index)	$NMDI = \frac{NIR - (SWIR1 - SWIR2)}{NIR - (SWIR1 + SWIR2)}$ NIR- Near-infrared band, Band 2 (841-876 nm); SWIR1 – shortwave infrared band; Band 6 (1628-1652); SWIR2 – shortwave infrared band, Band 7 (2105 – 2155 nm)	(L. Wang & Qu, 2007)
NDVI (Normalized Difference Vegetation Index)	$NDVI = \frac{NIR - Red}{NIR + Red}$ NIR- Near-infrared band, Band 2 (841 - 876 nm) Red – red band, Band 1 (620 – 670 nm)	(Huete et al., 2002)
VSWI (Vegetation Supply Water Index)	$VSWI = \frac{Ts}{NDVI}$ Ts – vegetation canopy temperature NDVI – normalized difference vegetation index	(T. N. Carlson et al., 1994; Toby N. Carlson et al., 1990)
NDDI (Normalized Difference Drought Index)	$NDDI = \frac{NDVI - NDWI}{NDVI + NDWI}$ NDVI – normalized difference vegetation index NDWI – normalized difference water index The NDDI was generated from NDVI and NDWI index	(Gu et al., 2007b)
NDWI (Normalized Difference Water Index)	$NDWI = \frac{NIR - SWIR}{NIR + SWIR}$ NIR - Near-infrared band, Band 2 (841-876 nm), SWIR - Short wave infrared	(Gao, 1996)

5.5.1.2 GDI drought index model validation

The GDI drought index was employed to assess the next step. Pearson correlation (*r*) (Sedgwick, 2012) values were applied for estimated GDI and with the SPI index and in-situ SM observations. The coefficients of the Pearson correlation (*r*) are in Equation (5.4):

$$\mathrm{r} = \frac{\sum_i^n=1 \, (X_i - \bar{X}) \, (Y_i - \bar{Y})}{\sqrt{\sum_i^n (X_i - \bar{X})^2} \sqrt{\sum_i^n \, (Y_i - \bar{Y})^2}} \tag{5.4}$$

Here X_i and Y_i are implies the individual derivations and measurements of variables X and Y, whereas $\bar{X}$ and $\bar{X}$ are implies the mean of X and Y, respectively. The correlation coefficient (*r*) ranges between – 1 and 1. If (*r*) is equal to zero, this implies that there is no linear association between the variables. When *r* equal to 1, there is indicate a perfect positive linear relationship between variables. When 0 < *r* < 1, indicates a positive linear relationship, the smaller the absolute *R*-value, the less well variable can be characterized by a single linear relationship. When *r* is positive and *r* values close to 1, it describes a significant relationship between variables (Puth et al., 2014). The Linear Pearson´s correlation (*r*) was verified at a monthly scale for the GDI and SPI other RS-derived drought indices, with in situ SM observations, and SMOS SM data.

5.5.1.3 Meteorological and RS-derived Drought Indices

To evaluate the effectiveness of the GDI, we compared it with several meteorological and satellite-derived drought indices. A correlation analysis was performed between GDI and seven drought indices: SPI, NDVI, NDWI, NDDI, NMDI, VSWI, and TCI. These seven indices have been widely used for agricultural, and meteorological drought monitoring over different land-cover types. The equations used for their estimation are provided in Table 5.5.

The monthly SPI index reflects short-term soil moisture and vegetation stress, especially during the vegetation growing season. The Standardized Precipitation Index (SPI) was widely used for the detection of meteorological drought and signified the precipitation deficit. The SPI estimates a standardized departure of actual precipitation concerning the precipitation probability distribution function (Svoboda et al., 2012). Drought, according to the SPI, starts when the SPI value is equal or below -1.0 and ends when its value becomes positive. Mean monthly SPI values were calculated between April to September from 2000 to 2015 and compared with the GDI values. We expected a negative SPI relation with GDI whereby the lower the SPI value would indicate precipitation deficit (dry year) and the greater SPI value indicates a wet year. Classification of the SPI index and further details about it can be found in (Mckee et al., 1993).

The effect of meteorological drought over large areas can be assessed by using a temperature condition index (TCI). The temperature condition index (TCI) is associated with both, the temperature-related vegetation stress and the vegetation stress caused by excessive wetness. TCI index characterizes the thermal soil condition and is based on the infra-red band soundings. These conditions are estimated relative to the maximum and minimum temperatures, and the TCI value ranges from 0 to 100. The TCI behavior is opposite to the NDVI, high temperatures indicate unfavorable or dry conditions while low temperature indicates mostly favorable vegetation conditions (F. N. Kogan, 1995b).

The normalized difference vegetation index (NDVI), is the normalized reflectance difference between the near-infrared (NIR) and visible red bands. NDVI is an indicator of vegetation phenology that captures the seasonal dynamics of vegetation and is used extensively in vegetation, ecosystem, and drought monitoring (Tucker, 1979b).

Normalized Difference Water Index (NDWI) is constructed from the near-infrared (NIR) and short-wave infrared (SWIR) bands and is a virtual indicator for vegetation liquid water content. It is less sensitive to atmospheric scattering effects than NDVI. NDWI is computed using the NIR and SWIR reflectance, which characterize sensitive changes in liquid water content and spongy mesophyll of vegetation canopies (Gao, 1996). The index has been successfully tested as a tool for drought indicators (Gu et al., 2007a, 2008b).

The normalized multi-band drought index (NMDI) is an alternative approach, which was used for soil and vegetation drought indicators (A. K. Mishra & Singh, 2010). The index is based on a combination of multiple near-infrared, and short-wave infrared channels (L. Wang & Qu, 2007). NMDI is well suited to monitor dry soil status: an increase of soil moisture is connected with a reduction of NMDI value. In extremely dry soil areas the NMDI values are around 0.15, and for wet soils, its values are higher than 0.3.

The Normalized Difference Drought Index (NDDI) is generated from NDVI and NDWI (Gu et al., 2007b). This index is relatively new. It was applied to the grassland study of the Great Plains in the United States by means of multi-date Landsat fused images (Renza et al., 2010), where it was shown that NDDI is a better indicator of drought compared to other indices.

The vegetation supply water index (VSWI), which was proposed by (T. N. Carlson et al., 1994), is based on the ratio between NDVI and land surface temperature (LST). The VSWI indicates the change in vegetation and soil moisture conditions using spectral reflectance of the visible bands. The VSWI index was consistently shown as an effective tool for the estimation of the water content status of soil and vegetation change (Hazaymeh & Hassan, 2016).

5.6 Results

- **Assessment of the GDI drought model**

5.6.1 Estimation of GDI from SMOS L2 SM product as a dependent variable

Recent studies have successfully validated the SMOS L2 product (Dall'Amico et al., 2012; Gherboudj et al., 2012) and used it to assess drought conditions (A. G. S. S. Souza et al., 2018). The use of the growing season data was sufficient because in this season soil moisture and vegetation dynamics are quite closely related. In the study area, the GDI index values were averaged monthly for each SMOS SM grid cell. The linear correlation between satellite SMOS SM data and the GDI was calculated from April to September (2010-2015). The correlation between SMOS SM and GDI, as represented by the correlation coefficient (r), was 0.77 and considered statistically significant (Figure 5.4). It is important to note that the satellite SMOS product shows a good agreement with the computed GDI during the entire seasonal cycle. The developed drought index can adequately reproduce the soil water balance dynamics in terms of soil water availability for plants. Overall, drought is related to the soil water availability for vegetation, and the water is stored not only in the surface layer as well in the root-zone layer. Thus, only satellite remote sensing data will be sufficient for future drought monitoring.

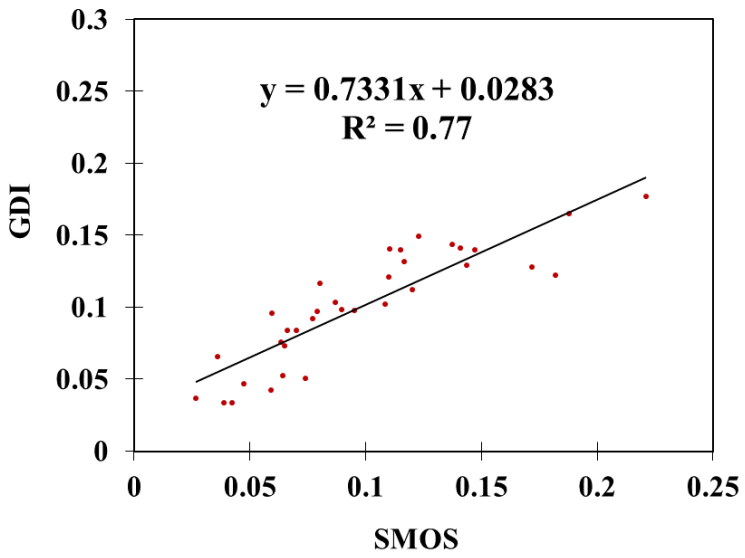

Figure 5.4 Relationship between GDI and SMOS SM calculated for monthly average data for the period from April to September 2010-2015.

5.6.2 Comparison of RS-derived drought indices and the SPI with GDI

To assess the reliability of the GDI, it was necessary to compare it with other RS well-known drought indices which are widely used globally for drought monitoring. While drought is a relative condition that differs widely between locations and climates, a standardized index such as SPI allows users to confidently compare historical and current droughts between different climatic and geographic locations. Generally, SPI is used since it is an appropriate indicator to assess the influence of precipitation or (drought conditions) in the growing season on the vegetation productivity period as well as in the temperature-driven drought areas where precipitation is relatively sufficient and high temperatures are the dominant factor in water stress areas. The comparison between GDI and seven computed drought indices, SPI, NMDI, VSWI, NDWI, NDVI, TCI, and NDDI was conducted from April to September during the 2010 – 2015 period. Correlation coefficients (*r*) were calculated at six Southwestern Mongolian stations (Table 5.6).

Table 5.6 The results of the comparison (Pearson correlation coefficient) between GDI, SPI, and RS-derived drought indices NMDI, VSWI, NDWI, NDVI, TCI, and NDDI (a); and between SPI and the same RS-derived drought indices (b). Stars (*) indicate the best correlations between specific RS-derived drought indices and GDI (SPI).

(a) Correlation coefficients *(r)* between GDI, SPI, and the RS-based drought indices	
SPI/GDI	0.64
NMDI/GDI	-0.91*
VSWI/GDI	0.97*
NDWI/GDI	0.81
NDVI/GDI	0.96*
TCI/GDI	0.68
NDDI/GDI	0.78*
(b) Correlation coefficients (*r)* between SPI and the RS-based drought indices	
SPI/NMDI	-0.48
SPI/VSWI	0.61*

SPI/NDWI	0.47
SPI/NDVI	0.62
SPI/TCI	0.69*
SPI/NDDI	0.38

Table 5.6 suggests that GDI showed the strongest positive correlation with VSWI (r = 0.97), followed by NDVI (r = 0.96), NMDI (r = -0.91), NDWI (r = 0.81), NDDI (r = 0.78), TCI (r = 0.68), and SPI (r = 0.64) respectively. NDVI is included in Eq. 5.3 and, therefore, its correlation with GDI is essential. The negative correlation between NMDI and GDI is due to different descriptions of drought by NMDI (with positive values indicating drought), and GDI (with negative values indicating drought conditions). These comparisons indicate that the VSWI demonstrated more consistency with the GDI than other examined RS drought indices. While we can see that the SPI has a weak correlation with NDDI (r = 0.38), and NMDI (r = - 0.48). However, the TCI and SPI (r = 0.69), NDVI and SPI (r = 0.62), VSWI and SPI (r = 0.61) were better correlated (Table 5.6b). This comparison in Table 5.6 suggests that GDI shows the greatest performance over diverse ecosystems compared to other RS-derived drought indices.

To check the relationship between monthly GDI and SPI, a scatter plot and correlation coefficients were calculated between SPI and GDI for all six stations for the 2010 - 2015 period (Figure 5.5 and Table 5.6). Figure 5.5 shows a satisfactory agreement between GDI and SPI over the entire study area (for all vegetation types and grasslands).

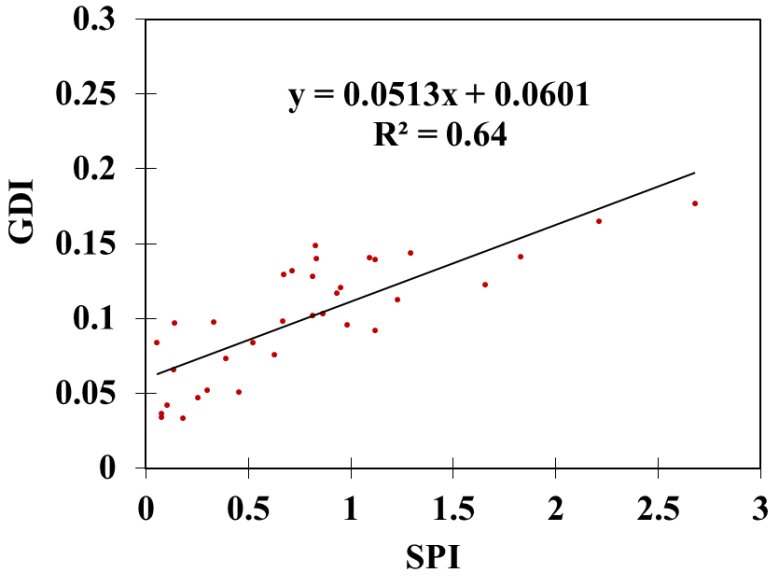

Figure 5.5 Scatter plot of the GDI and the SPI index.

Similarly, correlation analyses conducted for each year separately show statistically significant correlations between SPI and GDI ranging from 0.53 to 0.91 (Table 5.7) except for the moderate drought year of 2014.

Table 5.7 Year-wise correlation between the VSWI and GDI, NMDI and GDI, NDDI and GDI. Stars (*) indicate the best interannual correlations between VSWI, NMDI, NDDI, and reference GDI for individual years from April to September.

VSWI and the GDI Index [correlation coefficient (*r)*]						
VSWI – GDI (*r*)	0.95	0.96	**0.99 ***	0.98	0.97	**0.99 ***
NMDI and the GDI Index [correlation coefficient (*r)*]						
NMDI – GDI (*r*)	-0.43	-0.95	**-0.97 ***	-0.96	-0.94	**-0.98 ***
NDDI and the GDI Index [correlation coefficient (*r)*]						
NDDI – GDI (*r*)	**0.89 ***	0.88	**0.90 ***	0.81	0.55	0.65

The linear correlations show the reliability of the GDI compared toRS–derived drought indices. Table 5.7 shows high statistically significant coefficient correlations between three RS-derived indices and the GDI. These results imply that the GDI is not only closely related to SPI but it also quantifies the past normal years and appropriately captures different responses of summer rainfall and seasonal drought conditions. Among them, the VSWI and the GDI demonstrate the best interrelation. The VSWI, NMDI, NDDI, and the GDI correlation results suggest that the GDI appropriately captures the inter-annual variability of drought intensity, particularly in 2012, 2013, and 2015 at the 0.05 significance level.

Figure 5.6 show the dynamics of the spatially averaged GDI, and SPI (a), and two of the RS-derived drought indices, TCI (b), and NDDI (c). The comparative dynamics of the explored drought indices overlap well with the GDI and show a remarkable seasonal similarity. During the observation period, droughts occurred in the spring months of April, May, and in the summer period from July and August. The drought during August was especially severe in the southeastern areas. When the water demand in August to September is critical for pastures in the dry steppe, this period is more drought-prone, especially in the dryland. However, the drought conditions were weakened from June to July.

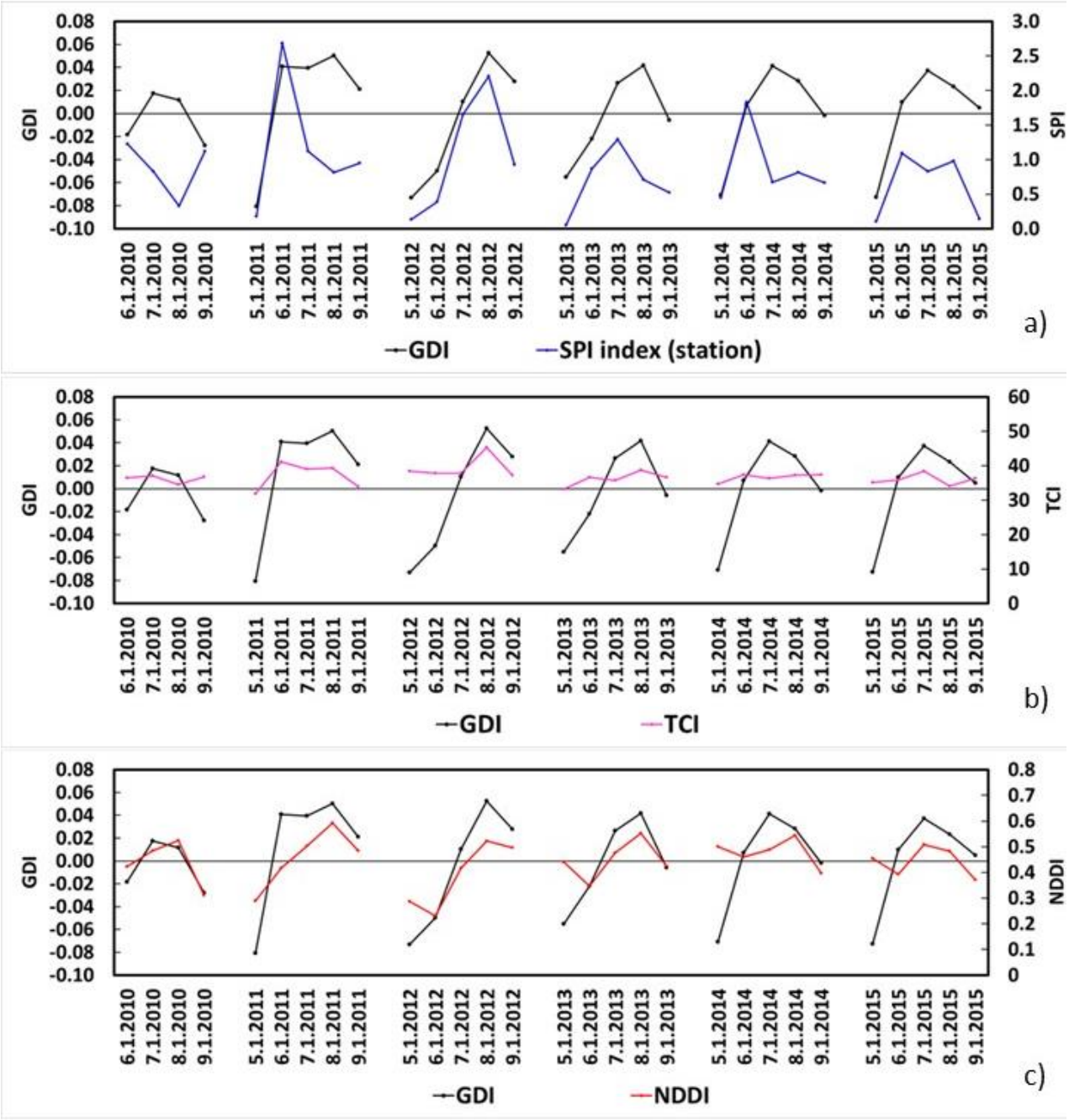

Figure 5.6 Dynamics of the spatially averaged GDI and SPI (a), two of the RS-derived drought indices TCI (b), and NDDI (c). Time series span from April to September during the 2010-2015 period.

5.6.3 Validation of the GDI drought index by the in-situ SM observations

Finally, the effectiveness of the GDI drought index was assessed by validation with in-situ SM measurements at six meteorological stations over the study region. Correlation coefficients between in-situ SM measurements and the GDI show a relatively strong relationship with in-situ SM observations in the study area across different vegetation zones (Table 5.8).

Table 5.8 Correlations between in-situ SM and GDI at each province station from north to south. Stars (*) indicate the best year correlations between in–situ SM measurements and GDI.

In-situ SM and the GDI Index [correlation coefficient (*r*)]						
Station	Bayanbulag	Galuut	Bayankhngor	Bogd	Shinejinst	Ekhiingol
In-Situ SM – GDI (*r*)	0.65	0.78*	0.80 *	0.74*	0.55	0.83 *

Figure 5.7 presents monthly variations of the in – situ SM observations and the GDI from April to September during the 2010 – 2015 period. The figure shows that the GDI has successfully captured the seasonal difference of the in - situ SM observations. When in-situ SM observations are substantially lower in April, May, and August, the GDI values are increased. Thus, the GDI recognizes both spring and summer droughts, which is helpful for agrometeorological drought early warnings.

However, the point-derived data on soil moisture only reflects information from a small region, while the drought extent by satellite data over a large area and long periods are pixel values. Errors and uncertainties can occur in both data series because of limited observed SM data in the study area.

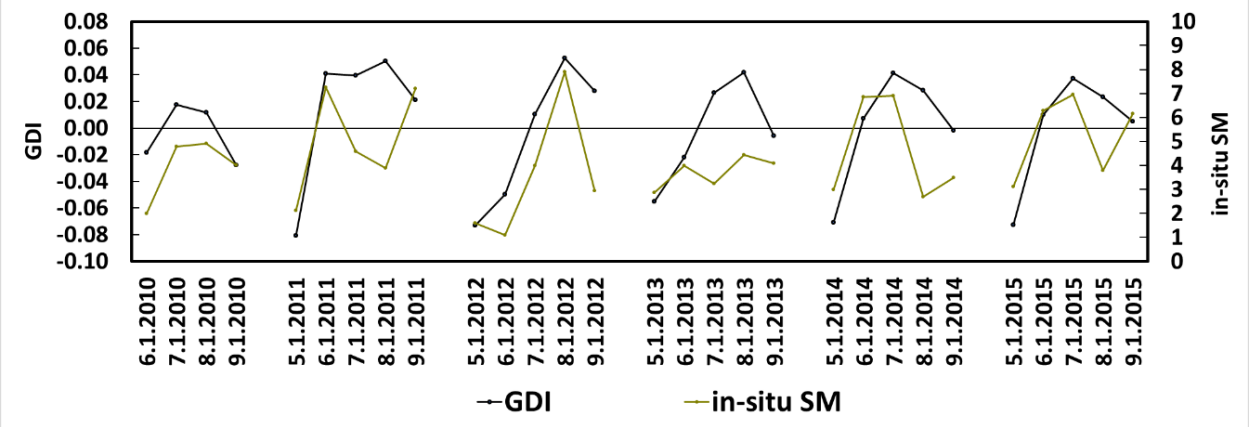

Figure 5.7 Spatial and temporal variations of monthly averaged in-situ SM observations and the GDI at six stations in Bayankhongor Province.

5.6.4 The spatial relationship between the GDI, precipitation, and temperature.

The rising temperature and lack of precipitation associated with global warming are likely to increase the intensity of drought events in the Mongolian Plateau (P Batima et al., 2005). Thus, we assume that observed climate conditions in the drought-occurred years would certainly manifest themselves in the GDI. The precipitation and temperature data over the five years from six meteorological stations in the Bayankhongor Province were used to assess the linear relationship between GDI and these meteorological variables.

Table 5.9 depicts Pearson correlation coefficients in different years between the GDI and precipitation. Significant high correlations were found only during 2011, 2012, and 2013 years. Droughts in this area were mainly caused by summer precipitation deficit. By contrast, wet weather

accompanies higher rainfall and lower temperature, such as in the years 2011, 2012, and 2013. These years were comparatively wet in the Gobi areas of Mongolia (Dorjsuren et al., 2016).

Table 5.9 Year-wise correlation between annual precipitation and the GDI. Stars (*) indicate the best year correlations between precipitation and GDI.

Precipitation and the GDI Index [correlation coefficient (*r*)]						
Year	2010	2011	2012	2013	2014	2015
Precipitation (mm) – GDI (*r*)	- 0.19	0.81	0.82 *	0.86 *	0.50	0.60

Figure 5.8 panels show the scatter correlation plots between GDI and precipitation and between GDI and temperature at six stations from April to September during the 2010 to 2015 period. Pearson correlation coefficients 0.53 and 0.49 are statistically significant with $p < 0.001$. The summer season of 2010 had high temperatures and little rainfall, which resulted in heavy droughts in this region. Intensive droughts were observed during the periods of 2001 to 2002, and 2010. The temperature rise, no effective precipitation, soil water depletion, and plant transpiration increase caused the drought conditions well caught by the GDI.

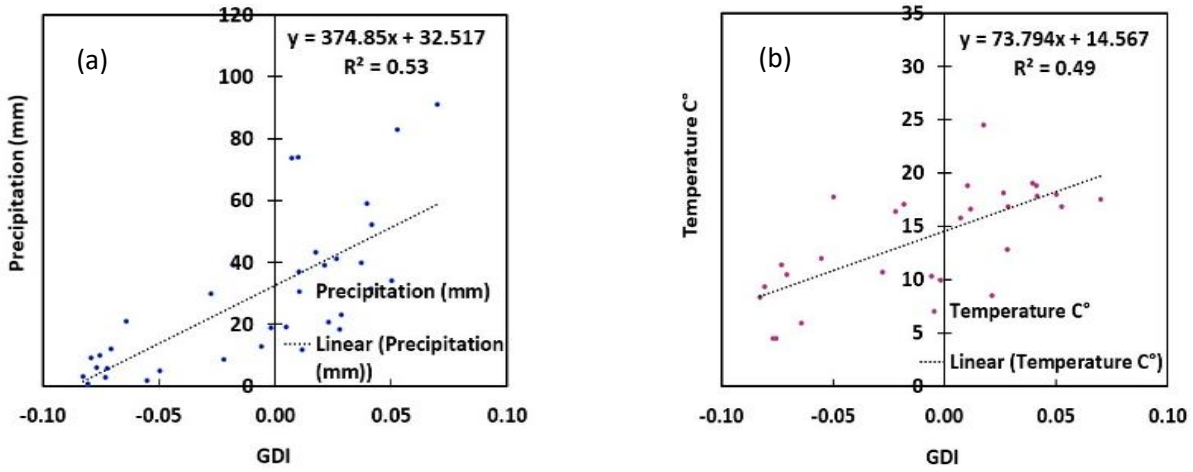

Figure 5.8 Scatter plots of the GDI with (a) monthly Precipitation and (b) monthly Temperature.

5.6.5 Spatial and Temporal Patterns of Drought intensity

The spatial distribution GDI maps were produced for July and August, which have the highest vegetation growth and play a major role during the grazing season. The new integrated drought index can help to monitor pasture conditions while potentially may serve as an early warning to take proper drought management actions and to help herder's wellbeing. Figure 5.9 shows the spatial pattern of GDI anomalies for July and August from 2000 to 2018 across the Bayankhongor Province. From 1999 to 2002, the worst drought events had occurred in the consecutive summers across the country, and in 2009 and 2010 drought happened again throughout entire Mongolia. According to the spatial-temporal pattern of GDI shown in Figure 5.9a, moderate to severe drought occurred in some areas of southern and central Bayankhongor, especially in 2001 and 2002. In 2001, the drought mainly occurred in southwestern Bayankhongor, and in years 2007 and 2009 in July in northwestern Bayankhongor

(Figure 5.9b). The intensity of drought was high in July 2001 and August 2002, which was consistent with the findings of the National Drought Monitoring (*Information And Research Institute Of Meteorology, Hydrology And Environment*).

The vegetation with a relatively fast response to lack of precipitation during the dry season is mainly concentrated in the northwestern steppe and is nearly absent in the southern desert zone of the Province. In our study, severe to extreme drought conditions concentrated in central and southwestern areas of the Province in July 2007, July 2009, and in July 2017. In August 2010, July 2001, July 2002, and August 2007, both GDI and SPI (not shown) indicate moderate to severe meteorological and soil moisture droughts in this region. Meanwhile, wet weather conditions with higher precipitation and lower temperature (for example, July 2003 with the SPI +2.0, July 2011 with SPI +2.1, and August 2012 with + 2.3), generate in the Gobi Desert a relatively wet year. These findings correspond well with a study by Dorjsuren et al. (Dorjsuren et al., 2016).

(a)

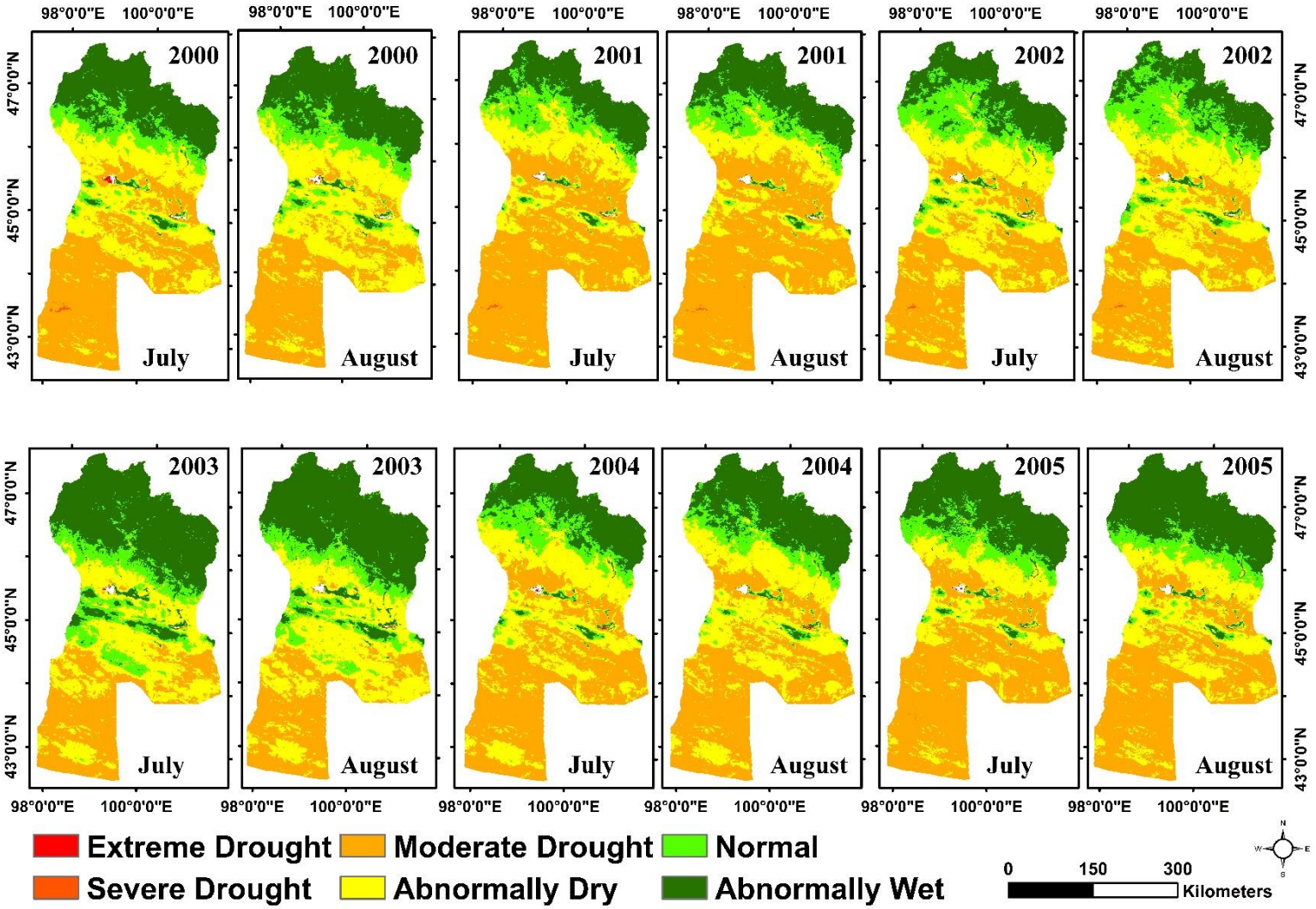
98°0'0"E
100°0'0"E
47°0'0"N
45°0'0"N
43°0'0"N
2000
July
2000
August
2001
July
2001
August
2002
July
2002
August
2003
July
2003
August
2004
July
2004
August
2005
July
2005
August
Extreme Drought
Moderate Drought
Normal
Severe Drought
Abnormally Dry
Abnormally Wet
0
150
300
Kilometers

(b)

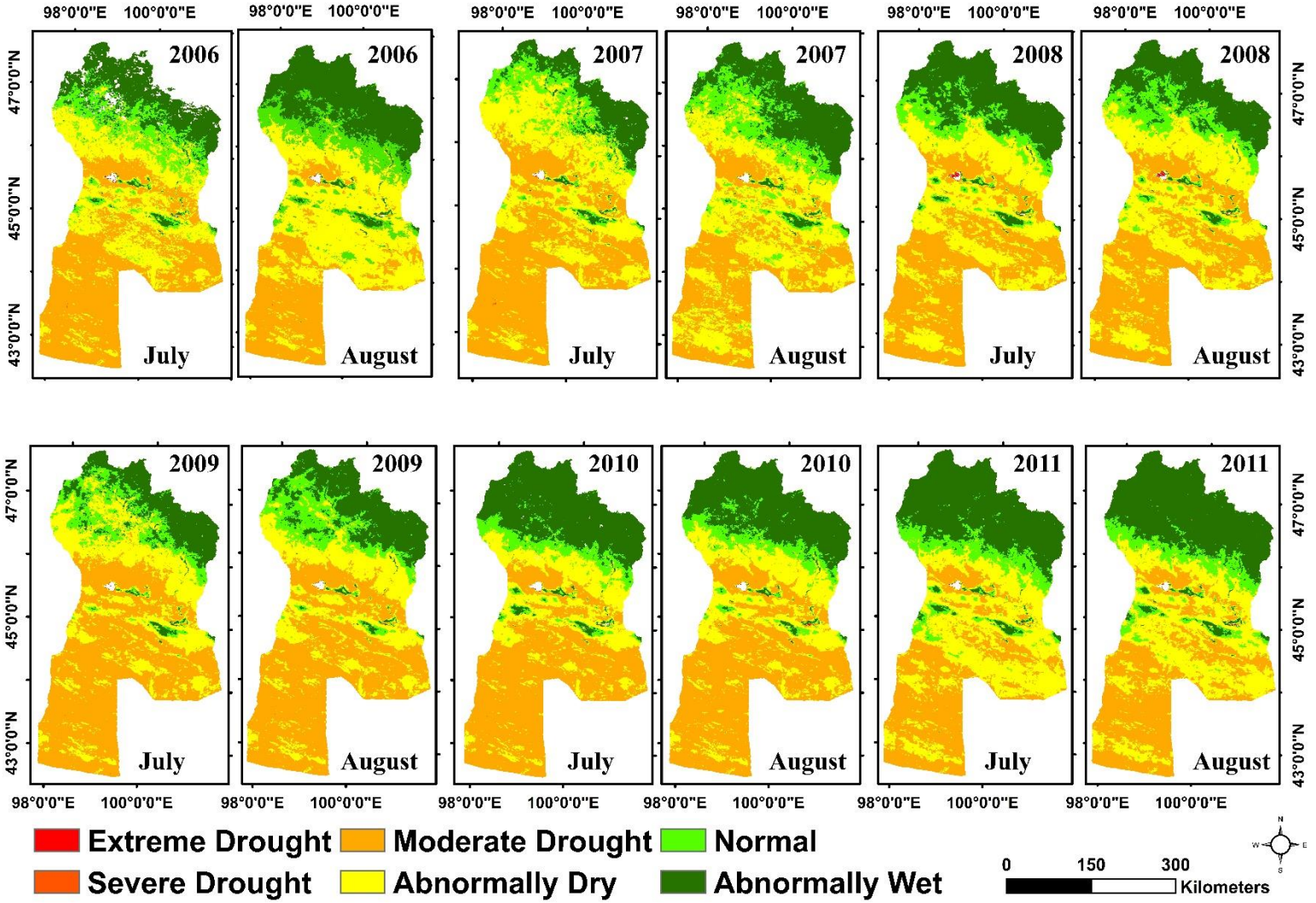
98°0'0"E
100°0'0"E
47°0'0"N
45°0'0"N
43°0'0"N
2006
July
2006
August
2007
July
2007
August
2008
July
2008
August
2009
July
2009
August
2010
July
2010
August
2011
July
2011
August
Extreme Drought
Moderate Drought
Normal
Severe Drought
Abnormally Dry
Abnormally Wet
0
150
300
Kilometers

(c)

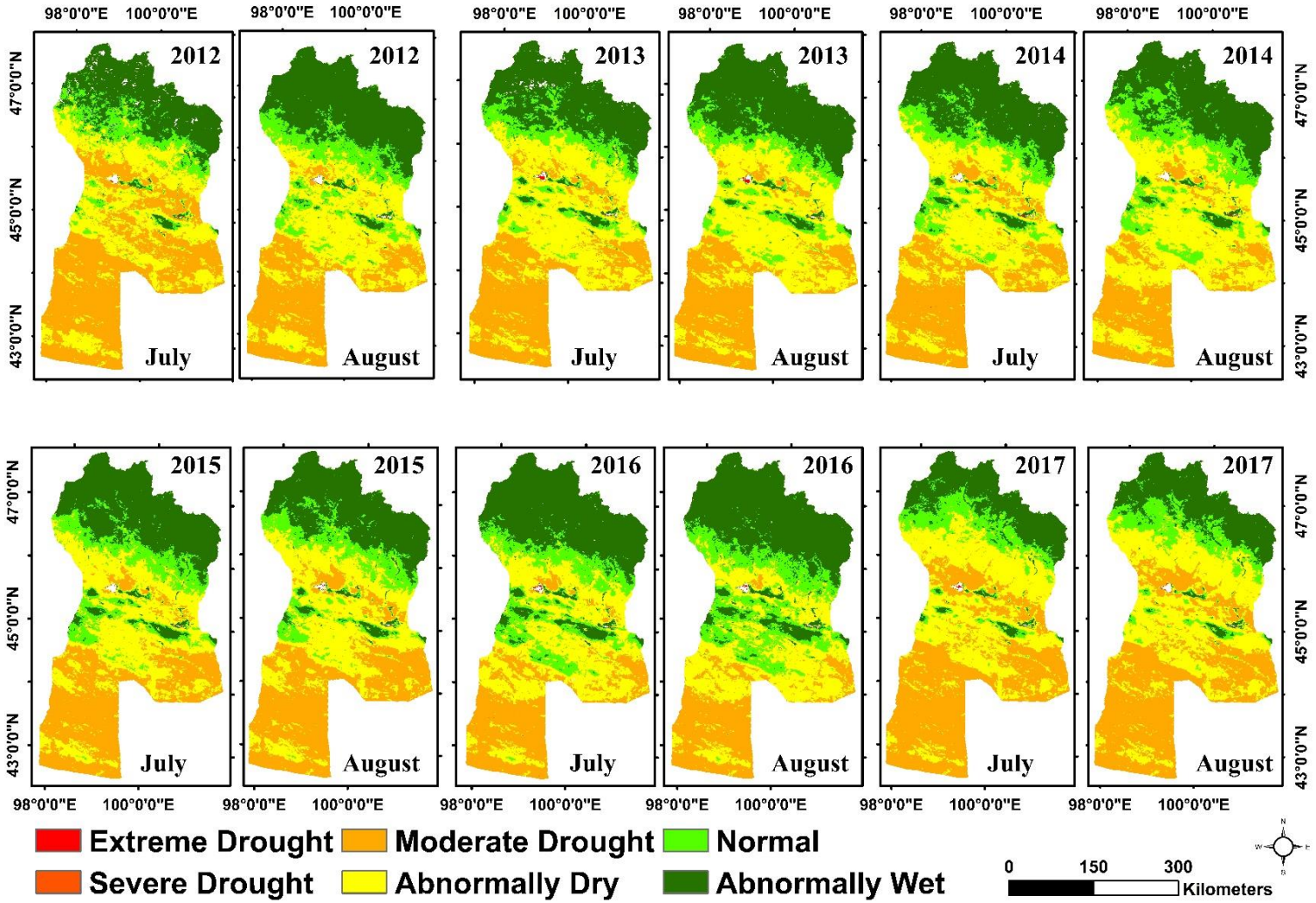
98°0'0"E
100°0'0"E
47°0'0"N
45°0'0"N
43°0'0"N
2012
July
2012
August
2013
July
2013
August
2014
July
2014
August
2015
July
2015
August
2016
July
2016
August
2017
July
2017
August
Extreme Drought
Moderate Drought
Normal
Severe Drought
Abnormally Dry
Abnormally Wet
0
150
300
Kilometers

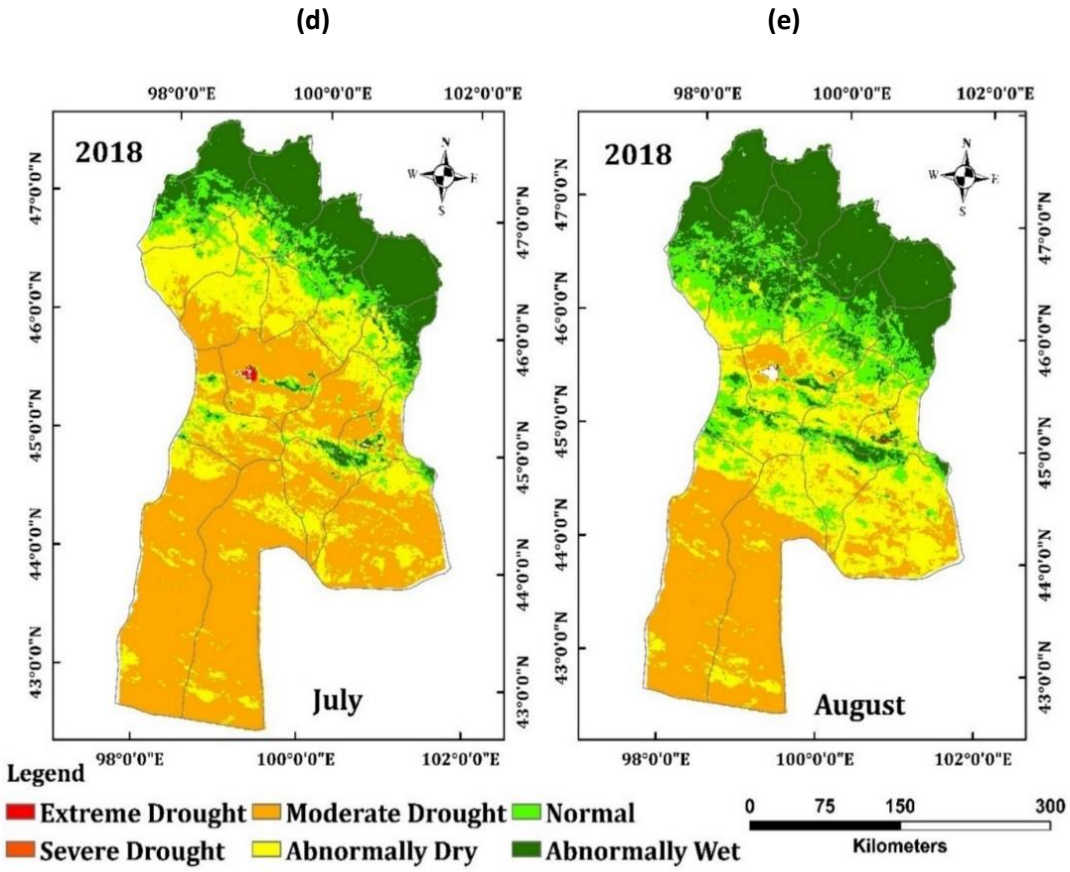

Figure 5.9 Spatiotemporal drought severity GDI maps, calculated for July and August month for each of the years from 2000 to 2018 in Bayankhongor Province.

The drought severity (moderate, severe, and extreme droughts) for different drought periods is shown in Figure 5.10. Here, changes in drought severity are computed as the percentage of the variance of change (as a percentage of change/magnitude). We see a large variability in the changes in drought intensity. The heaviest drought event in the Bayankhongor Province was observed in 2001 when 50.28 % of the total area was identified as an area with moderate drought and 22% of the region was quantified as abnormally dry.

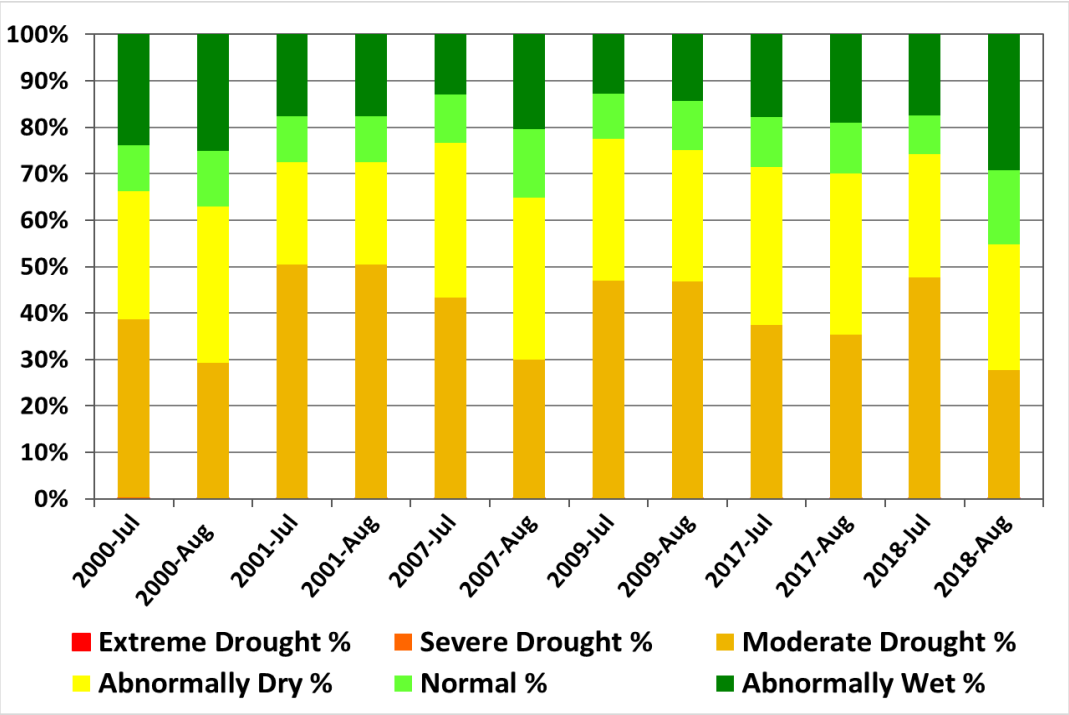

Figure 5.10 GDI changes in drought intensity (in % of the Province area). Percent of the grassland drought areas are shown as moderate (orange) abnormal dry (yellow), normal (light green), and wet (dark green). Prominent drought years were 2000, 2001, 2002, 2007, 2009, 2017, and 2018.

5.7 Discussion

A need to reduce the impacts of future drought events is paramount being a part of the national development strategy and climate change adaptation plan in Mongolia (*THIRD NATIONAL COMMUNICATION OF MONGOLIA Under the United Nations Framework Convention on Climate Change*). A substantial part of this research was to recognize soil moisture as an important parameter for monitoring meteorological and hydrological droughts. The deficit of soil moisture is an appropriate indicator of regional agrometeorological drought assessments (Vyas et al., 2015). The new proposed drought index GDI was derived from SMOS and LST, PET, and NDVI products. We evaluated the GDI performance by comparing it to other RS-derived drought indices, and in-situ SM observations. Presented integrated drought index, GDI has a maximum of benefits for description both, real-time vegetation conditions and soil moisture deficit.

A comparative analysis with other works that have used different approaches becomes now obligatory (Aghakouchak et al., 2015). There are only a few studies that compared traditional drought indices with the RS-derived drought indices and in-situ soil moisture observations (Scaini et al., 2015c; Vicente-Serrano et al., 2012). In the earlier work, the soil water scarcity index (SWDI), which was calculated from in-situ soil moisture data (0 - 5 cm), and SMOS soil moisture series, showed a high agreement with the surface layer observations (Martínez-Fernández et al., 2016b). Comparison of the SMOS products with in-situ observations has been performed earlier (Dall'Amico et al., 2012; N Sánchez et al., 2012). Positive results of this comparison support an idea that the SMOS L2 could be directly used for agricultural and hydrological drought monitoring (Chakrabarti et al., 2014). Champagne et al., 2015 (Champagne et al., 2015) used SMOS SM anomalies for analyzing agricultural drought risks, and Martinez-Fernandez et al. (Martinez-Fernandez et al., 2015) applied the agriculture

drought index SWDI (soil water deficit) and also found high relation between these indices and crop yields. We hypothesize that in-situ SM data in the different vegetation zones should be sufficient for validation of the GDI drought index. Our integrated drought index was able to satisfactorily capture the temporal variations of the in-situ observations in both desert and semi-desert areas and accurately reproduced the rainfall seasonality shown in Figure 5.7 (Y. H. Kerr et al., 2016; Molero et al., 2016). Figure 5.9 confirms that at shorter time scales (~month) GDI reproduces temporal and spatial variability of meteorological droughts (Lorenzo-Lacruz et al., 2010). However, semi-arid zone phenology is more dependent on moisture than temperature. We assume that temperature variations are responsible for the seasonal drought pattern whereas the drought severity is controlled by moisture supply. This argument is supported by the results shown in (Figures 5.6a and 5.8a). In arid lands, the rainfall is seasonal and directly affects vegetation. Thus, precipitation controls both the moisture-stress and thermal-stress of vegetation in the arid ecosystem (Bhuiyan et a., 2008).

SPI is known to exhibit a reasonable performance in replication the soil moisture variability on a global and regional scales (Halwatura et al., 2016; Li et al., 2020; Z. Liu et al., 2019a; Nepal S. et al., 2020; Sternberg et al., 2009b). SPI and GDI series are compared at given selected locations of the Bayankhongor Province of Mongolia. In these locations, monthly precipitation (July and August) has similar tendencies as the GDI series (Figure 5.6a and 5.8a), which confirms that GDI variations at the monthly time scale were mainly caused by regional precipitation. The Student´s t-test was applied to all correlation estimates to verify that our results were statistically significant. Indeed, Figure 5.5 shows that GDI and SPI were statistically significantly correlated, with a p-value greater than 0.05. We hypothesized that for the summer season, drought conditions represented by the GDI are equally trustworthy when they are represented by the SPI. However, the SPI is based on in situ data and for a sparse network of the study area and cannot document all peculiarities of drought patterns. Considering the GDI comparison to other RS-derived indices, VSWI (r = 0.97), NDVI (r = 0.96), NMDI (r = - 0.91), and NDWI (r = 0.81) had the closest correlations with our Gobi Drought Index (Table 5.6a).

In dry and hot climate zones the water evaporates faster, thus considering jointly evaporation (PET), vegetation (NDVI), temperature (LST) as reference data, the GDI was able to detect sufficiently steady the drought conditions in the Gobi region. With an integration of a vegetation condition and the surface evaporation, the grassland droughts were detected efficiently by the GDI. At high potential evapotranspiration and heatwaves, the loss of soil moisture will be intensified (Rind et al., 1990; Um et al., 2020). Since NDDI, NDWI, NMDI, and TCI are describing the vegetation condition and the temperature anomalies, which is may more suitable for the monitoring of droughts in the steppe than the semi-desert zone. A previous study highlights that the TCI is suitable for the forest zone, and the NDWI and VSWI are suitable for the steppe zone and the NMDI cannot accurately reflect grassland drought condition in Mongolia (Chang et al., 2017a).

However, the spatiotemporal patterns of NDDI, NDWI, VSWI drought indices were comparable to the results from other studies conducted in the Southwest of Mongolian grasslands (Erdenetuya et al., 2010). We noticed that the spatial changes in the monthly averaged NDVI, NDDI, NDWI, and VSWI during the 2000-2018 period across the Bayankhongor Province are strongly associated with the general distribution of GDI drought maps in Figure 5.9. Also, spatial patterns of NDVI, NDDI, NDWI, and VSWI drought characteristics highlight strong spatial links of droughts that occurred during the years 2001, 2002, 2007, 2009, 2010, 2017, and 2018 across the Province (Figure 5.9). Particularly, the droughts during the 2000 – 2002 period were severe and extreme across the entire Mongolian Plateau (Z. Liu et al., 2019b; Sternberg et al., 2009a). Moreover, 2004, 2005, 2007, and 2009 years were also

highly affected by droughts throughout Mongolia (Nanzad et al., 2019b; Tuvdendorj et al., 2019). Let us note that the global-widespread drought stress was also intensified during this period. We can see that the dynamics of NDWI and VSWI are quite similar, hence these dynamics remain quite stable (Figure 5.11) and is consistent with the results of previous studies (Renza et al., 2010). Nevertheless, there are still discrepancies among different drought indices regarding the drought onset, persistence, and severity (Erdenetuya et al., 2010) and (National Remote Sensing Center of Mongolia).

New Soil Moisture Active/Passive (SMAP) data products have become available since March 31st, 2015, and cover the entire global land areas with about 3-day time step (Entekhabi, D. et al., 2010). These products (e.g. Enhanced SMAP L3) have a spatial resolution of about ~9 km that is higher than the SMOS SM data spatial resolution used in our study (O'Neill, J.C et al., 2019). However, they characterize the soil moisture content only in the upper 5 cm soil layer. The L3 SMAP data product is unique to SMAP and is possible given that the SMAP radar and radiometer share the same antenna and data acquisition strategy. The L3 SMAP accuracy is equal to or better than 0.04 $cm^3\ cm^{-3}$ (1-sigma) for regions with volumetric water content below ~5 $kg\ m^{-2}$, which is typical for the Gobi Desert areas. We retrieved a subset of SMAP (SPL3SMP_E.003) monthly average soil moisture data for our study area (https://nsidc.org/data/SPL3SMP_E/versions/3) and compared it with our GDI estimates. A high correlation between SMAP SM and GDI (+0.85) is statistically significant at the 0.01 level and confirms that the GDI still is a good overall tool for drought monitoring in the Mongolian Drylands against new emerging remote sensing tools.

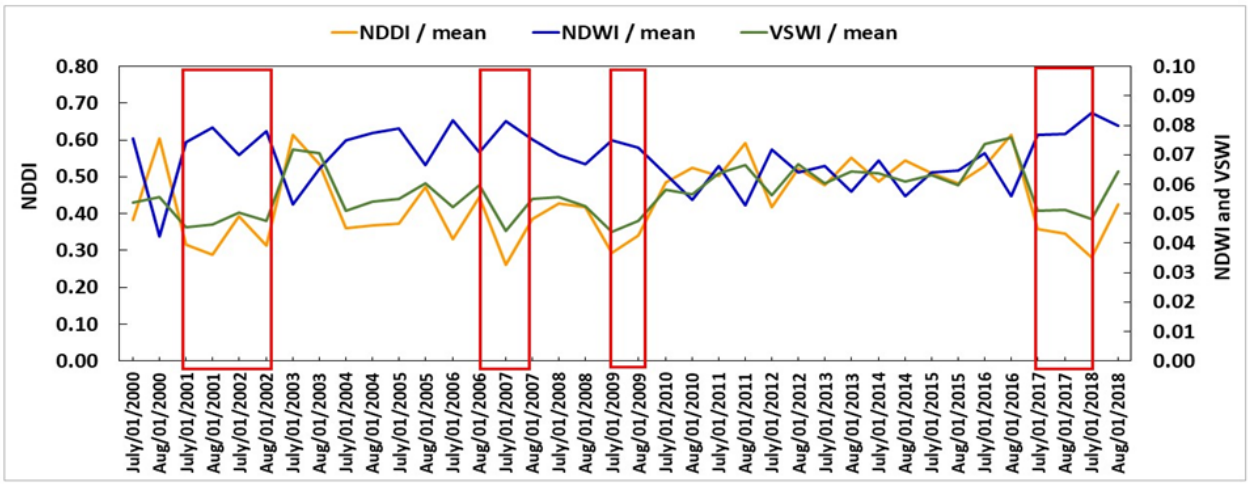

Figure 5.11 Time series of the spatially averaged July and August NDDI, NDWI, and VSWI drought indices from 2000 to 2018. The drought years are highlighted by red columns.

5.8 Conclusions

The multiple linear regression analysis was used to develop an integrated drought index, GDI, derived from SMOS and LST, PET, and NDVI of MODIS products. Our results provide experimental evidence about the usefulness of the integrated GDI for drought monitoring in the semi-arid study region. The integrated GDI can incorporate both, the meteorological and soil moisture drought patterns and sufficiently well represent overall drought conditions in the arid lands. The GDI assessment based on the SMOS SM product presented in this paper is one of the first such assessments

accomplished in Mongolia at the regional level. We tested which drought index has a high relationship with the integrated GDI and validated it with the in-situ SM observations. Specifically,

- Monthly GDI and 1-month SPI show significant correlations and both are useful for drought monitoring in semi-arid lands. Strong correlations of monthly GDI with VSWI, NDDI, NDWI, and in-situ SM demonstrate the effectiveness of the GDI in drought monitoring.
- Comparison of these drought indices with the GDI allowed assessing the drought coincidence in time from several angles and quantified better their intensity.
- We conclude that the GDI model can play a key role in the monitoring and assessment of agrometeorological and hydrological droughts.

The integrated GDI was able to detect the drought events which have been underestimated by the National Drought Watch System in Mongolia. The integrated GDI can be beneficial for vegetation stress characterization due to drought with the help of satellite, climatological, and geophysical data. Thus, the proposed drought index could serve as an independent and complementary drought monitoring index. Furthermore, the integrated GDI is an important source of information for assessing drought conditions that are typically quantified using climate indices on the regional scale. Our GDI can be used as an extra tool for rangeland managers, who are developing a local monitoring system, as well as for researchers in countries with similar climates and ecosystems. The future application of the GDI can be extended to monitor potential impacts on water resources and agriculture in Mongolia, which have been impacted by long periods of drought. However, the multiple linear regression model of the proposed new drought index should be enhanced and readjusted in different ecological and climate regions.

Chapter 6 General conclusions, limitations, and recommendations

6.1 Summary findings

In this work, we have accomplished three main objectives:

- evaluated of the spatial and temporal patterns of soil moisture,
- estimated the effects of climate extremes on vegetation growth cycle, and
- developed and assessed a new drought index.

Below the dissertation is summarized in the form of its goals:

We believe that our work is the first assessment step toward examining not only the consistency of remote sensing SMOS SM data based on the in-situ SM observations, and the spatial pattern of SM in the selected area, but also a useful tool for grassland drought monitoring in a rapidly changing climate and region.

Future projections of climate extremes warn us to be prepared for them. However, studies over Mongolia have shown substantial limitations of methods on downscaling of coarse-scale remote sensing soil moisture products. Thus, a technical method of analysis of comparison ground and remote sensing data can be quite useful. Examined for Southwestern Mongolia, the bias correction technique and downscaling procedure resulted in significant improvements in the correlation of in-situ SM measurements and related vegetation patterns (NDVI). This work allows identifying the relationships between the regional climate factors and soil moisture depletion on one side, and resulting vegetation patterns on the other side.

- The bias correction approach resulted in significant improvements in the accuracy and spatial resolution of the averaged SMOS SM during the 2010 – 2015 period.
- Based on the recognized SMOS SM pattern, we identified the areas that are potentially threatened by drought stress and dryness.
- After bias correction of SMOS SM data, NDVI has shown a relationship with both, SM and precipitation data.
- An insufficient water supply from the soil and soil moisture deficit due to drought and dryness are highly likely to increase the frequency of *dzud* events and impact the vegetation growth cycle.
- Regional droughts are likely prolonged in cold seasonal climates by insufficient snow accumulation in winter and by low precipitation and high evapotranspiration during the warm season.
- Generally, much less is known about the impacts of climate extremes change on soil moisture and ecological droughts, particularly in drylands.

In chapter 3 the bias-corrected SMOS L2 SM product was validated against a situ SM measurement in the four provinces Arkhangai, Uvurkhangai, Bayankhongor, and Gobi-Altai in central-southwestern Mongolia. The bias correction method was used for comparing the Spatio-temporal characteristics of the SMOS SM to the in-situ SM measurements. An area of 1822 km × 684 km was examined, consisting of 918 SMOS L2 data pixels. Furthermore, we found that the bias-corrected SMOS SM distributions for the entire study area were similar to those of NDVI and had similar dynamics. This was particularly true in open shrub-lands, where NDVI values are low. Here, the NDVI dynamics show good compatibility and strong correlations with the bias-corrected SMOS SM in the seasonal cycle.

Noticeably, the spatial distribution of SM depends on soil parameters that are not distributed homogeneously across the area. This indicates, in general, that SM in dry steppe areas could change very rapidly in the topsoil layer.

The distribution patterns of bias-corrected SMOS SM correctly reproduced the relatively humid season from June to July as well as the drying out period starting in October. Significant rainfall in July 2011 caused an increase in SM, which was recorded in both the bias-corrected SMOS SM data and the precipitation records. In 2011 and 2012, the maximum SM (in July) depended strongly on precipitation. In Gobi-Altai province (desert/high mountain region) the wettest year was 2011, however, while the highest SM value was detected in June, the SM had already decreased in July 2011. The lower than average rainfall during this rainy season was the main cause of the SM reduction in late July. These findings could indicate that SM conditions during the early plant growth stage critically impact the vegetation condition. When there is a lack of rainfall in drylands (Bayankhongor, Gobi-Altai), higher temperatures reduce further SM, which is precipitation driven in these areas. Our results showed that the small seasonal changes in the bias-corrected SMOS SM and situ measurements were generally similar throughout the study area during the three phases of observed vegetation growth (i.e., warm spring, summer recharging, and autumn drying season). The study region lies in a zone that transitions between steppe, forest-steppe, and desert. The lowest correction between SMOS SM and in situ SM was observed in the dry, lowland regions.

In chapter 4 the results about *dzud* showed that a combination of drought and harsh winter, that lead to annual high livestock mortality in southwestern Mongolia. The climate projections indicate that these tendencies trends will be aggravated in the medium term and the extreme events, such as drought and *dzud,* will become more frequent and more intense, accompanied by severe environmental, social, and economic impacts. We applied the seasonal aridity index ${}_aAI_z$, and found that at the stations with dry conditions (minimum ${}_aAI_z$ of −1) a low NDVI is observed. We noticed that drought/dry years and lack of meltwater in the spring may cause high grazing pressure due to less vegetation resources for livestock. The reductions in vegetation cover due to high livestock grazing could negatively impact ecosystem function and increase vulnerability. We noticed that livestock grazing is difficult after a cold *dzud* with a high snowfall that does not melt and covers the grassland during the entire winter. The years with low NDVI had very dry conditions during the following summer. We found the highest increase in annual temperature in the drier regions at the south of the study area, while stations in the northern parts of the study region exhibited a lower mean annual temperature due to lower temperatures during the winter. Years with drought risk and long dry periods heavily influence the local water budget by causing high evapotranspiration, increased capillary effect, and short-term soil salinization. Vegetation is susceptible to the length of the rainy season. Our results suggest that low NDVI and low soil moisture conditions can induce drought, and these impacts tend to be a precondition for *dzud*. The modified seasonal aridity index showed

considerable regional differences in NDVI due to climatic effects. The NDVI was closely correlated with $_aAI_z$, while seasonal precipitation showed a lower correlation with NDVI. Overall, the seasonal aridity index $_aAI_z$ approach was beneficial from a meteorological aspect to determine and characterize the interconnection between water deficit and dzud effects on grassland drought.

Long-term meteorological data and CRU snow data were used to characterize the climate conditions during dzud and drought years and the spatial distribution of snow cover during *dzud* events. Specifically, we examined trends of annual mean precipitation and temperature as well as monthly precipitation and temperature. Our results showed that in most stations during the last 15 years (2000 – 2014), there was statistically drier than during the previous 15 years (1985 – 1999). We found that the mean yearly precipitation during 2000–2014 is by 15 to 20% lower than during the 1985–1999 period. Contrary to the expected strong warming tendency in the winter months, the last 10 – 15 years showed a winter cooling, which could be related to the Siberian cold high shift. This circumstance, coupled with the high drought intensity, was a fundamental factor in the occurrence of the consecutive *dzud*s from 2000 to 2002. The average annual temperature of the last 15 years (2000 – 2014) is higher than the temperature from 1985 to 1999. We detected the largest increase in annual temperature in the drier regions (southern area). The mean winter temperature from 2000 to 2014 (−3 to 2 °C) was colder than the mean winter temperature from 1985 to 2014 (−0 to 9 °C). The summer season shows the largest gain in temperature, while the same gain during autumn is quite low.

In chapter 5 we developed the Gobi drought index (GDI) is based on the combination of Soil Moisture and Ocean Salinity (SMOS) Soil Moisture and several products from the MODIS satellite. It was validated by the in-situ Soil Moisture (SM) observations. The GDI allowed us to characterize coherently the spatial and temporal drought expansion and map the droughts at the 1 km spatial resolution for Southwest Mongolia from 2000 to 2018. This mapping for two summer months (July, August) was conducted for monitoring the grassland drought and vegetation response to varying soil/climatic conditions. The comparison between the latest SM product (SMAP) and GDI has shown a high correlation (0.85) that is statistically significant at the 0.01 level.

The proposed GDI associates the soil moisture and temperature conditions with a sensitive response of arid and semi-arid grassland conditions. Generally speaking, our GDI has the following benefits: (a) few data are required for its computation; (b) it can be transferable and scalable over most of the globe areas; (c) it is a useful model in the areas with scarce gauge coverage; and (d) it is an affordable tool since it can identify both, meteorological and hydrological droughts. The GDI assessment based on the SMOS SM product presented in this work is one of the first assessments accomplished in Mongolia at the regional level.

As a result, the integrated GDI was able to detect the drought events which have been underestimated by the National Drought Watch System in Mongolia. Our integrated drought index can be beneficial for vegetation stress characterization due to drought with the help of satellite, climatological, and geophysical data. Thus, the proposed drought index could serve as an independent and complementary drought monitoring index. To the advantage of this research, we can say that the GDI can substitute several different remote sensing drought indices and help to monitor the vegetation condition and soil moisture status in different ecosystem drylands.

6.2 Limitations

A list of the drought-affected area and regional grassland drought assessment reports is missing and/or is still under development.

An insufficient database on drought impact on the environment and socio-economic conditions, such as the vegetation growth cycle, crop plants, and state of soil moisture, and the surface water level is still a considerable problem for the local studies in Mongolia.

The framework for hydrological and meteorological drought modeling is still under investigation and the experience is limited. We did not consider the dependence between vegetation and soil characteristics, because aquifer characteristics had a much more significant effect on hydrological and meteorological drought and then vegetation and soil characteristics (Van Lanen et al., 2013).

6.3 Recommendations

Our study demonstrated the use of an integrated drought index, GDI, for assessing the severity of droughts at a large scale in the Southwestern region of Mongolia. The proposed drought model will be useful as a tool for national drought management and future Gobi ecosystem assessments. These assessments may include mapping of pasture conditions, desertification, hydrological and meteorological droughts.

This work can be useful for planners and policymakers, who are actively engaged in drought mitigation and preparedness. Based on current and past observed drought states, e. g. on the state of soil moisture, temperature, precipitation, the vegetation conditions, and their cumulative effects, the planners can use the projections of climate and future human activity jointly with our results to predict the future states of environment and drought variations in Mongolia.

For example, investigating the vegetation reaction on drought impact may help us to determine (to plan) the plant resistance to drought and develop irrigation systems that will reduce the consequences for Mongolia of moisture deficit and its changes. Our study emphasizes and describes intensifications of seasonal patterns of drought. These tendencies could affect temperate dryland plant conditions and the services they provide. Knowledge of these tendencies and proper prevention measures that address groundwater resources protection, soil conservation, and efficient agriculture practices can help to keep the Gobi ecosystem stable.

The future application of the GDI can be extended to monitor potential impacts on water resources and agriculture in Mongolia, which have been impacted by long periods of drought. However, the multiple linear regression model of the proposed new drought index should be enhanced and readjusted in different ecological climate regions.

The results and methods of the Ph.D. thesis are based on already freely available satellite data products from existing satellites. The development of new satellites and methods is a rapidly developing field of research. Future satellites such as EnMAP or innovative data products such as SIF will make new environmental data available at higher spatial and spectral resolution. For example, the Environmental Mapping and Analysis Program (EnMAP scheduled to be launched at the end of 2021) is a German hyperspectral satellite mission that aims at monitoring and characterizing Earth's environment on a global scale. It measures the dynamic processes of Earth's ecosystems by extracting geochemical, biochemical, and biophysical parameters that provide information on the status and evolution of various terrestrial ecosystems. The use of Solar Induced Fluorescence (SIF) to Assess Vegetation

Change and Vulnerability will have a new impact on ecological studies and could be integrated into our GDI-approach. The SIF is a relatively new emerging satellite product, which provides information on photosynthetic activity versus NDVI, which is a greenness index. It serves as a direct and strong proxy to gross primary production (GPP), capturing dynamic responses of vegetation to environmental stressors such as drought and high-temperature anomalies. Due to the dynamics in the development of remote sensing, new data with enhanced quality (e.g. hyperspectral data) will be available in the near future. Further development is also taking place in the radar area, where in the future we will be using much higher spatial resolution data and frequencies (e.g. the ESA Biomass Earth Explorer mission, which will carry the first P-band synthetic aperture radar, able to deliver accurate maps of tropical, temperate and boreal biomass). Observations from these new missions will support and also will lead to a better insight into the rates of habitat loss and, therefore, on the effects that this loss may have on the environmental biodiversity.

ACKNOWLEDGEMENTS

The Ph.D. study was supported by the European Commission under Project Number E1606. First, I would like to express my sincere gratitude to my "everyday" supervisor Prof. Dr. Martin Kappas for his endless guidance, patience, motivation, and support. His constructive comments and the mentoring throughout this whole journey were always very valuable for me. Without his constant encouragement, this work would never have been successful. I also deeply appreciate the support and guidance of Prof. Dr. Tsolmon Renchin from the National University of Mongolia (Department of Physics), who has been contributed to developing the proposal for this research. My special thanks to Prof. Dr. Daniela Sauer (Department of Physical Geography, University of Göttingen) for her guidance and for taking over the co-supervision on my thesis.

Besides, I would like to thank the rest of my thesis committee: Prof. Dr. Daniela Sauer, Prof. Dr. Heiko Faust, Prof. Tsolmon Renchin, Dr. Pavel Groisman, and Dr. Daniel Wyss for their insightful comments and encouragement.

I especially thank Dr. Pavel Groisman, who also supports within the context of this thesis, for his valuable comments, contribution, and excellent teamwork.

This work would not have been possible without the support of many people for supporting and assisting me spiritually and academically during my Ph.D. journey, namely: Dr. Jan Degener, Dr. Ammar Rafiei Emmam, Dr. Stefan Erasmi, Dr. Daniel Wyss, Dr. Phan Thanh Noi, Nguyen Trong Hung, Nguyen The Dung, Pham Thi Nhung, Elbeck Erdanaev, Holger Vogt and all former colleagues at the Department of Cartography, GIS, and Remote Sensing, University of Göttingen. My sincere thanks to the secretary Mrs. Martina Beck, for her endless encouragement, motivation, friendship, and assistance. I also thank my colleagues at the Human Geography Department, particularly Katharina Najork and Sammy Idrus. My great thanks to all my former colleagues.

I sincerely thank Dr. Ammar Rafiei Emmam, and Dr. Steven Fassnacht for their valuable ideas and productive discussions, and excellent teamwork for chapters 3 and 4.

Special thanks to the long-lasting friends Enkhjargal, Gunsmaa, Ammar, Baku, Khulan, Irina, Robert, and friends from the National University of Mongolia.

Finally, and most importantly, I want to thank my family, this work would not have been possible without the abundant love and continuous support of my mother Tserenlkham, and my lovely beautiful daughter Misheel, my lovely sister Ariundari and her family, my sweet nieces Indra, Inga, and Ariana, auntie Oyunchimeg, brother Zolzaya, and Tungalagdolgion for their constant emotional support and encouragement. My deep gratitude to all my friends for their love and motivation, and support through my Ph.D. study.

To my lovely father VOVA, to whom I promised to dedicate this dissertation before he left this world.

Appendix to Chapter 3

Appendix A

Table A 1. Summary and general characteristics of SM sensors in the last and current decade.

Sensor/Space mission	Operation period	Frequency (GHz)	Resolution (km)	Incidence angle (°)
SSMR/Nimbus-7	1978-1988	6.6, 10.7, 18, 21, 37	150 (at 6.6 GHz)	50
SSM/I/DMSP	1987-	19.3, 22.3, 37, 85.5	25 (at 19.3 GHz)	53
TMI/TRMM	1997-2015	10.65, 19.35, 21.3, 37, 85.5	50 (at 10.65 GHz)	53
AMSR-E/EOS PM-1	2002-2011	6.9, 10.7, 18.7, 23.8, 36.5, 89	56 (at 6.9 GHz)	55
AMSR2/GCOM-W1	2012	6.92, 7.3, 10.65, 18.7, 23.8, 36.5, 89	10 (at 6.92 GHz)	55
MIRAS/SMOS	2009	1.42	25 to 40	0 to 55
Aquarius/SAC-D	2011-2015	1.41	76×94, 84×120, 96×156	29, 38, 46
SMAP/SMAP	2015-	1.43	40	40

Source: (Baghdadi. N; Mehrez. Z, 2016), SSMR = Scanning Multi-channel Microwave Radiometer; SSM/I/DMSP = Special Sensor Microwave Imager/Defense Meteorological Satellite Program; TMI/TRMM = Microwave Imager/Tropical Rainfall Measuring Mission; AMSR-E/EOS PM-1 = Advanced Microwave Scanning Radiometer – EOS; MIRAS/SMOS = Microwave Imaging Radiometer using Aperture Synthesis/Soil Moisture Ocean Salinity; Aquarius/SAC-D = Aquarius/Satélite de Aplicaciones Científicas-D; SMAP = Soil Moisture Active Passive

Appendix to Chapter 4

Appendix A

Table A 2. The Dzud events on the Mongolian plateau in the past 70 years.

Year	Extreme Event	Livestock Mortality/NSO
1944–1945	*dzud*+drought	No data
1954–1955	*dzud*	-
1956–1957	*dzud*	-
1967–1968	*dzud*+drought	-
1976–1977	*dzud*	3294.30
1986–1987	*dzud*	1635.10
1993–1994	*dzud*	2342.12
1996–1997	*dzud*	1203.50
1999–2000	*dzud*+drought	4291.30
2000–2001	*dzud*+drought	8249.90
2001–2002	*dzud*+drought	7676.50
2009–2010	*dzud*+drought	12,052.81

*Source: (*Fernández-Giménez et al., 2012b*).*

Appendix B

Table A 3. Economic loss caused by drought and Dzuds in Mongolia.

***Dzud* and Drought Information**	**1999–2002 Drought and *Dzud* Years.**	**2009–2010 White *Dzud* Years.**
Drought and *Dzud* severity range	Drought and *Dzud* continued 3 consecutive years and covered around 90% of the total territory.	Covered 80.9 % of the total territory, 17 provinces and 175soums/administrative unit
Mortality	Not enough information /not clear	17 people between the ages of 12 and 89 died
Livestock loss	11 million livestock	8.8 million livestock
Financial loss (the exchange rate is during that period)	91.7 billion MNT (Mongolian Tugrik)	360 billion MNT
The number of households left without livestock	2369 households	8711 households
The number of households left with livestock	Over 10,000 households were left with less than 100 livestock	32,756 households lost more than 50% of their livestock

Source: (Benson, 2011).

REFERENCES

Abbaspour, K. C., Faramarzi, M., Ghasemi, S. S., & Yang, H. (2009). Assessing the impact of climate change on water resources in Iran. *Water Resources Research*, *45*(10), 1–16. DOI: https://doi.org/10.1029/2008WR007615

AghaKouchak, A., Farahmand, A., Melton, F. S., Teixeira, J., Anderson, M. C., Wardlow, B. D., and Hain, C. R. (2015), Remote sensing of drought: Progress, challenges and opportunities, *Rev. Geophys.*, 53, 452– 480. DOI: 10.1002/2014RG000456

Ahearn, A. (2018). Herders and hazards: covariate dzud risk and the cost of risk management strategies in a Mongolian subdistrict. *Natural Hazards*, *92*(1), 165–181. DOI: https://doi.org/10.1007/s11069-017-3128-4

Ahmadalipour, A., Moradkhani, H., Yan, H., & Zarekarizi, M. (2017). Remote sensing of drought: vegetation, soil moisture, and data assimilation. In *Remote sensing of hydrological extremes* (pp. 121–149). Springer

Al-Yaari, A., Wigneron, J.-P., Ducharne, A., Kerr, Y. H., Wagner, W., De Lannoy, G., Reichle, R., Al Bitar, A., Dorigo, W., Richaume, P., & Mialon, A. (2014). Global-scale comparison of passive (SMOS) and active (ASCAT) satellite based microwave soil moisture retrievals with soil moisture simulations (MERRA-Land). *Remote Sensing of Environment*, *152*, 614–626. DOI: https://doi.org/10.1016/J.RSE.2014.07.013

Albergel, C., Rüdiger, C., Carrer, D., Calvet, J.-C., Fritz, N., Naeimi, V., Bartalis, Z., & Hasenauer, S. (2009). An evaluation of ASCAT surface soil moisture products with in-situ observations in Southwestern France. *Hydrology and Earth System Sciences*, *13*(2), 115–124

Alley, W. M. (1984). The Palmer Drought Severity Index: limitations and assumptions. *Journal of Climate & Applied Meteorology*, *23*(7), 1100–1109. DOI: https://doi.org/10.1175/1520-0450(1984)023<1100:TPDSIL>2.0.CO;2

Anderson, M. C., Norman, J. M., Mecikalski, J. R., Otkin, J. A., & Kustas, W. P. (2007). A climatological study of evapotranspiration and moisture stress across the continental United States based on thermal remote sensing: 1. Model formulation. *Journal of Geophysical Research: Atmospheres*, *112*(D10). DOI: https://doi.org/10.1029/2006JD007506

Anshuka, A., van Ogtrop, F. F., & Willem Vervoort, R. (2019). Drought forecasting through statistical models using standardised precipitation index: a systematic review and meta-regression analysis. In *Natural Hazards* (Vol. 97, Issue 2, pp. 955–977). Springer Netherlands. DOI: https://doi.org/10.1007/s11069-019-03665-6

Awe, G. O., Reichert, J. M., Timm, L. C., & Wendroth, O. O. (2015). Temporal processes of soil water status in a sugarcane field under residue management. *Plant and Soil*, *387*(1–2), 395–411. DOI: https://doi.org/10.1007/s11104-014-2304-5

Bannari, A., Morin, D., Bonn, F., & Huete, A. R. (1995). A review of vegetation indices. *Remote Sensing Reviews*, *13*(1–2), 95–120. https://doi.org/10.1080/02757259509532298

Bao, G., Qin, Z., Bao, Y., Zhou, Y., Li, W., & Sanjjav, A. (2014). NDVI-Based Long-Term Vegetation Dynamics and Its Response to Climatic Change in the Mongolian Plateau. *Remote Sensing*, *6*(9), 8337–8358. https://doi.org/10.3390/rs6098337

Batima P, Gombluudev, N. L., & Erdenetsetseg B. (2005). *OBSERVED CLIMATE CHANGE IN MONGOLIA*. www.aiaccproject.org

Batima, P, Natsagdorj, L., Gombluudev, P., & Erdenetsetseg, B. (2005). Observed Climate Change in Mongolia. *AIACC Working Paper*

Batima, Punsalmaa. (2006). Climate change vulnerability and adaptation in the livestock sector of Mongolia. *International START Secretariat: Washington DC*, 204–209

Batima, Punsalmaa, Natsagdorj, L., & Batnasan, N. (2013). Vulnerability of Mongolia's pastoralists to climate extremes and changes. In *Climate Change and Vulnerability*. DOI: https://doi.org/10.4324/9781315067179

Batkhishig, O. (2013). Chapter 12. Human Impact and Land Degradation in Mongolia. In *Dryland East Asia: Land Dynamics a mid-Social and Climate Change*. DOI: https://doi.org/10.1515/9783110287912.265

Bavuudorj, G. (2018). *Agriculture and Drought In Mongolia Regional workshop on understanding the operational aspects of the drought observation system in Mongolia*

Bayarjargal, Y., Karnieli, A., Bayasgalan, M., Khudulmur, S., Gandush, C., & Tucker, C. J. (2006). A comparative study of NOAA-AVHRR derived drought indices using change vector analysis. *Remote Sensing of Environment*, *105*(1), 9–22. DOI: https://doi.org/10.1016/j.rse.2006.06.003

Bayissa, Y. A. (2018). Developing an impact-based combined drought index for monitoring crop yield anomalies in the Upper Blue Nile Basin. *Developing an Impact-Based Combined Drought Index for Monitoring Crop Yield Anomalies in the Upper Blue Nile Basin*

Bedunah, D. J., & Schmidt, S. M. (2000). Rangelands of Gobi Gurvan Saikhan National Conservation Park, Mongolia. *Rangelands*, *22*(4), 18–24. DOI: https://doi.org/10.2458/azu_rangelands_v22i4_bedunah

Begzsuren, S., Ellis, J. E., Ojima, D. S., Coughenour, M. B., & Chuluun, T. (2004). Livestock responses to droughts and severe winter weather in the Gobi Three Beauty National Park, Mongolia. *Journal of Arid Environments*, *59*(4), 785–796. DOI: https://doi.org/10.1016/j.jaridenv.2004.02.001

Belsley, D., Kuh, E., & Welsch, R. (2005). *Regression diagnostics: Identifying influential data and sources of collinearity*

Beniston, M., Stephenson, D. B., Christensen, O. B., Ferro, C. A. T., Frei, C., Goyette, S., Halsnaes, K., Holt, T., Jylhä, K., & Koffi, B. (2007). Future extreme events in European climate: an exploration of regional climate model projections. *Climatic Change*, *81*(1), 71–95

Benson, C. (2011). *Dzud Disaster Financing and Response in Mongolia Paper prepared for World Bank study on Structuring Dzud Disaster Preparation, Financing and Response to Increase Resilience of Herder Households to Climatic Risk in Mongolia*. World Bank, Washington, DC

Bento, V., Trigo, I., Gouveia, C., & DaCamara, C. (2018). Contribution of Land Surface Temperature (TCI) to Vegetation Health Index: A Comparative Study Using Clear Sky and All-Weather Climate Data Records. *Remote Sensing*, *10*(9), 1324. DOI: https://doi.org/10.3390/rs10091324

Bhuiyan, C. (2008). Desert vegetation during droughts: response and sensitivity. *Int. Arch. Photogramm. Remote Sens. Spat. Inf. Sci*, *37*, 907-912. DOI: http://citeseerx.ist.psu.edu/viewdoc/summary?doi=10.1.1.184.2599

Bhuiyan, C., Singh, R. P., & Kogan, F. N. (2006). Monitoring drought dynamics in the Aravalli region (India) using different indices based on ground and remote sensing data. *International Journal of Applied Earth Observation and Geoinformation*, *8*(4), 289–302. DOI: https://doi.org/10.1016/j.jag.2006.03.002

Bircher, S., Balling, J. E., Skou, N., & Kerr, Y. H. (2012). Validation of SMOS Brightness Temperatures During the HOBE Airborne Campaign, Western Denmark. *IEEE Transactions on Geoscience and Remote Sensing*, *50*(5), 1468–1482. DOI: https://doi.org/10.1109/TGRS.2011.2170177

Bohner, J. (2008). General climatic controls and topoclimatic variations in Central and High Asia. *Boreas*, *35*(2), 279–295. DOI: https://doi.org/10.1111/j.1502-3885.2006.tb01158.x

Bolten, J. D., & Crow, W. T. (2012). Improved prediction of quasi-global vegetation conditions using remotely-sensed surface soil moisture. *Geophysical Research Letters*, *39*(19)

Bulygina, O. N., Razuvaev, V. N., & Korshunova, N. N. (2009). *Changes in snow cover over Northern Eurasia in the last few decades*. *4*, 6. DOI: https://doi.org/10.1088/1748-9326/4/4/045026

Bulygina, O.N., P.Ya. Groisman, V.N. Razuvaev, and N.N. Korshunova (2011) Changes in Snow Cover Characteristics over Northern Eurasia since 1966. *Environ. Res. Lett*., **6**, 045204, DOI: doi:10.1088/1748-9326/6/4/045204 (10pp)

Carlson, T. N., Gillies, R. R., & Perry, E. M. (1994). A method to make use of thermal infrared temperature and NDVI measurements to infer surface soil water content and fractional vegetation cover. *Remote Sensing Reviews*, *9*(1–2), 161–173. DOI: https://doi.org/10.1080/02757259409532220

Carlson, Toby N., Perry, E. M., & Schmugge, T. J. (1990). Remote estimation of soil moisture availability and fractional vegetation cover for agricultural fields. *Agricultural and Forest Meteorology*, *52*(1–2), 45–69. DOI: https://doi.org/10.1016/0168-1923(90)90100-K

Centre for Environmental Data Analysis. (2015). *Centre for Environmental Data Analysis*.

Chakrabarti, S., Bongiovanni, T., Judge, J., Zotarelli, L., & Bayer, C. (2014). Assimilation of SMOS soil moisture for quantifying drought impacts on crop yield in agricultural regions. *IEEE Journal of Selected Topics in Applied Earth Observations and Remote Sensing*, *7*(9), 3867–3879. DOI: https://doi.org/10.1109/JSTARS.2014.2315999

Champagne, C., Davidson, A., Cherneski, P., L'Heureux, J., & Hadwen, T. (2015). Monitoring agricultural risk in Canada using L-band passive microwave soil moisture from SMOS. *Journal of Hydrometeorology*, *16*(1), 5–18. DOI: https://doi.org/10.1175/JHM-D-14-0039.1

Champagne, C., Rowlandson, T., Berg, A., Burns, T., L'Heureux, J., Tetlock, E., Adams, J. R., McNairn, H., Toth, B., & Itenfisu, D. (2016). Satellite surface soil moisture from SMOS and Aquarius: Assessment for applications in agricultural landscapes. *International Journal of Applied Earth Observation and Geoinformation*, *45*, 143–154. DOI: https://doi.org/10.1016/J.JAG.2015.09.004

Chang, S., Chen, H., Wu, B., Nasanbat, E., Yan, N., & Davdai, B. (2021). A Practical Satellite-Derived Vegetation Drought Index for Arid and Semi-Arid Grassland Drought Monitoring. *Remote Sensing*, *13*(3), 414. DOI: https://doi.org/10.3390/rs13030414

Chang, S., Wu, B., Yan, N., Davdai, B., & Nasanbat, E. (2017). Suitability Assessment of Satellite-Derived Drought Indices for Mongolian Grassland. *Remote Sensing*, *9*(7), 650. DOI: https://doi.org/10.3390/rs9070650

Cheng, S., & Huang, J. (2016). Enhanced soil moisture drying in transitional regions under a warming climate. *Journal of Geophysical Research*, *121*(6), 2542–2555. DOI: https://doi.org/10.1002/2015JD024559

Climatic Research Unit. *(1901-2013). CEDA Data Server, Index of CRU TS 3.22 data*

Cohen, J., Cohen, P., West, S., & Aiken, L. (2013). *Applied multiple regression correlation analysis for the behavioral sciences*

Cohen, J. L., Furtado, J. C., Barlow, M. A., Alexeev, V. A., & Cherry, J. E. (2012). Arctic warming, increasing snow cover and widespread boreal winter cooling. *Environmental Research Letters*, *7*(1), 014007

Collow, T. W., Robock, A., Basara, J. B., & Illston, B. G. (2012). Evaluation of SMOS retrievals of soil moisture over the central United States with currently available in situ observations. *Journal of Geophysical Research: Atmospheres*, *117*(D9)

Copernicus European Drought Observatory (EDO). (n.d.). Retrieved November 23, 2020, from https://edo.jrc.ec.europa.eu/

Crocetti, L., Forkel, M., Fischer, M., Jurečka, F., Grlj, A., Salentinig, A., Trnka, M., Anderson, M., Ng, W. T., Kokalj, Ž., Bucur, A., & Dorigo, W. (2020). Earth Observation for agricultural drought monitoring in the Pannonian Basin (southeastern Europe): current state and future directions. In *Regional Environmental Change* (Vol. 20, Issue 4, pp. 1–17). Springer Science and Business Media Deutschland GmbH. DOI: https://doi.org/10.1007/s10113-020-01710-w

D'Odorico, P., Caylor, K., Okin, G. S., & Scanlon, T. M. (2007). On soil moisture-vegetation feedbacks and their possible effects on the dynamics of dryland ecosystems. *Journal of Geophysical Research: Biogeosciences*, *112*(G4), n/a-n/a. DOI: https://doi.org/10.1029/2006JG000379

Dagvadorj, D., Natsagdorj, L., Dorjpurev, J., & Namkhainyam, B. (2009). *Mongolia assessment report on climate change 2009*. Ministry of Nature, Environment and Tourism

Dai, A., & Zhao, T. (2017). Uncertainties in historical changes and future projections of drought. Part I: Estimates of historical drought changes. *Climatic Change*, *144*(3), 519–533

Dall'Amico, J. T., Schlenz, F., Loew, A., & Mauser, W. (2012). First results of SMOS soil moisture validation in the upper danube catchment. *IEEE Transactions on Geoscience and Remote Sensing*, *50*(5 PART 1), 1507–1516. DOI: https://doi.org/10.1109/TGRS.2011.2171496

Davi, N., Jacoby, G., Fang, K., Li, J., D'Arrigo, R., Baatarbileg, N., & Robinson, D. (2010). Reconstructing drought variability for Mongolia based on a large-scale tree ring network: 1520-1993. *Journal of Geophysical Research-Atmospheres*, *115*(22). DOI: https://doi.org/10.1029/2010JD013907

Davi, N. K., Jacoby, G. C., Curtis, A. E., & Baatarbileg, N. (2006). Extension of drought records for central Asia using tree rings: West-central Mongolia. *Journal of Climate*, *19*(2), 288–299

de Beurs, K. M., Henebry, G. M., Owsley, B. C., & Sokolik, I. (2015). Using multiple remote sensing perspectives to identify and attribute land surface dynamics in Central Asia 2001–2013. *Remote Sensing of Environment*, *170*, 48–61. DOI: https://doi.org/10.1016/J.RSE.2015.08.018

De Rosnay, P., Drusch, M., Vasiljevic, D., Balsamo, G., Albergel, C., & Isaksen, L. (2013). A simplified extended Kalman filter for the global operational soil moisture analysis at ECMWF. *Quarterly Journal of the Royal Meteorological Society*, *139*(674), 1199–1213

Deng, Y., Wang, S., Bai, X., Luo, G., Wu, L., Chen, F., Wang, J., Li, C., Yang, Y., Hu, Z., Tian, S., & Lu, Q. (2020). Vegetation greening intensified soil drying in some semi-arid and arid areas of the world. *Agricultural and Forest Meteorology*, *292–293*, 108103. DOI: https://doi.org/10.1016/j.agrformet.2020.108103

Didan, K. (2015). MOD13Q1 MODIS/Terra Vegetation Indices 16-Day L3 Global 250m SIN Grid V006. NASA EOSDIS Land Processes DAAC. In *USGS* (Vol. 5, pp. 2002–2015). DOI: https://doi.org/10.5067/MODIS

Didan, Kamel, Barreto Munoz, A., Solano, R., & Huete, A. (2015). *MODIS Vegetation Index User's Guide (MOD13 Series)*

Dorigo, W. A., Zurita-Milla, R., de Wit, A. J. W., Brazile, J., Singh, R., & Schaepman, M. E. (2007). A review on reflective remote sensing and data assimilation techniques for enhanced agroecosystem modeling. *International Journal of Applied Earth Observation and Geoinformation*, *9*(2), 165–193

Dorjsuren, M., Liou, Y.-A., & Cheng, C.-H. (2016). Time Series MODIS and in Situ Data Analysis for Mongolia Drought. *Remote Sensing*, *8*(6), 509. DOI: https://doi.org/10.3390/rs8060509

Downing, T. E. (1991). Vulnerability to hunger in Africa: A climate change perspective. *Global Environmental Change*, *1*(5), 365–380

Draper, C. S., Reichle, R. H., De Lannoy, G. J. M., & Liu, Q. (2012). Assimilation of passive and active microwave soil moisture retrievals. *Geophysical Research Letters*, *39*(4)

Du, L., Tian, Q., Yu, T., Meng, Q., Jancso, T., Udvardy, P., & Huang, Y. (2013). A comprehensive drought monitoring method integrating MODIS and TRMM data. *International Journal of Applied Earth Observation and Geoinformation*, *23*, 245–253

Dubrovsky, M., Svoboda, M., Trnka, M., Hayes, M., Wilhite, D., Zalud, Z., & Hlavinka, P. (2006). Application of Relative Drought Indices in Assessing Climate-Change Impacts on Drought Conditions in Czechia. *Drought Mitigation Center Faculty Publications*

Easterling, D., Rusticucci, M., Semenov, V., Alexander, L. V, Allen, S., Benito, G., Cavazos, T., Nicholls, N., Easterling, D., Goodess, C., Kanae, S., Kossin, J., Luo, Y., Marengo, J., McInnes, K., Rahimi, M., Reichstein, M., Sorteberg, A., Vera, C., Midgley, P. (2012). *3 - Changes in Climate Extremes and their Impacts on the Natural Physical Environment*. Cambridge University Press

Emam, A. R., Kappas, M., & Hosseini, S. Z. (2015). Assessing the impact of climate change on water resources, crop production, and land degradation in a semi-arid river basin. *Hydrology Research*, *46*(6), nh2015143. DOI: https://doi.org/10.2166/nh.2015.143

Enenkel, M., Steiner, C., Mistelbauer, T., Dorigo, W., Wagner, W., See, L., Atzberger, C., Schneider, S., & Rogenhofer, E. (2016). A combined satellite-derived drought indicator to support humanitarian aid organizations. *Remote Sensing*, *8*(4), 340

Engman, E. T. (1991). Applications of microwave remote sensing of soil moisture for water resources and agriculture. *Remote Sensing of Environment*, *35*(2–3), 213–226. DOI: https://doi.org/10.1016/0034-4257(91)90013-V

Entekhabi, D., Njoku, E. G., O'Neill, P. E., Kellogg, K. H., Crow, W. T., Edelstein, W. N., Entin, J. K., Goodman, S. D., Jackson, T. J., Johnson, J., Kimball, J., Piepmeier, J. R., Koster, R. D., Martin, N., McDonald, K. C., Moghaddam, M., Moran, S., Reichle, R., Shi, J. C., … Van Zyl, J. (2010). The soil moisture active passive (SMAP) mission. *Proceedings of the IEEE*, *98*(5), 704–716. DOI: https://doi.org/10.1109/JPROC.2010.2043918

Erdenetuya, M., Bulgan, D., & Erdenetsetseg, B. (2010). Drought monitoring and assessment using multi satellite data in Mongolia. In *32nd Asian Conference on Remote Sensing (2011), TSI-Climate change, ISBN* (pp. 978-1)

FAO. (2017). *World Food Programme S P E C I A L R E P O R T FAO/WFP CROP AND LIVESTOCK ASSESSMENT MISSION TO MONGOLIA*. www.fao.org/publications

FAO. (2010). *FAO´s Role in the Mongolia Dzud Appeal*

Farkas, O., & Kempf, B. (2002). *Reinventing the Dzud: Livestock Famine in Twenty-First-Century Mongolia*

Fassnacht, S., Allegretti, A., Venable, N., Fernández-Giménez, M., Tumenjargal, S., Kappas, M., Laituri, M., Batbuyan, B., & Pfohl, A. (2018). Merging Indigenous Knowledge Systems and Station Observations to Estimate the Uncertainty of Precipitation Change in Central Mongolia. *Hydrology*, *5*(3), 46. DOI: https://doi.org/10.3390/hydrology5030046

Fekade Mekuria, E. (2012). *SPATIAL AND TEMPORAL ANALYSIS OF RECENT DROUGHT USING VEGETATION TEMPERATURE CONDITION INDEX Case of Somali regional state of Ethiopia SPATIAL AND TEMPORAL ANALYSIS OF RECENT DROUGHT YEARS USING VEGETATION TEMPERATURE CONDITION INDEX Case of Somali regional state, Ethiopia*

Fernandez-Gimenez, M. (2000). The role of Mongolian nomadic pastoralists' ecological knowledge in rangeland management. *Ecol Appl*, *10*, 1318–1326. DOI: https://doi.org/10.1890/1051-0761(2000)010[1318:tromnp]2.0.co

Fernández-Gimenez, M. E., Batjav, B., & Baival, B. (2012a). *Lessons from the Dzud: Adaptation and Resilience in Mongolian Pastoral Social-Ecological Systems*

Fernández-Giménez, M. E., Batkhishig, B., & Batbuyan, B. (2012b). Cross-boundary and cross-level dynamics increase vulnerability to severe winter disasters (dzud) in Mongolia. *Global Environmental Change*, *22*(4), 836–851. DOI: https://doi.org/10.1016/j.gloenvcha.2012.07.001

Fernández-Giménez, M. E., Batkhishig, B., Batbuyan, B., & Ulambayar, T. (2015). Lessons from the Dzud: Community-Based Rangeland Management Increases the Adaptive Capacity of Mongolian Herders to Winter Disasters. *World Development*, *68*(1), 48–65. DOI: https://doi.org/10.1016/j.worlddev.2014.11.015

Fernández-Giménez, M. E., Venable, N. H., Angerer, J., Fassnacht, S. R., Reid, R. S., & Khishigbayar, J. (2017). Exploring linked ecological and cultural tipping points in Mongolia. In *Anthropocene* (Vol. 17, pp. 46–69). Elsevier Ltd. DOI: https://doi.org/10.1016/j.ancene.2017.01.003

Gang, C., Wang, Z., Zhou, W., Chen, Y., Li, J., Chen, J., Qi, J., Odeh, I., & Groisman, P. Y. (2016). Assessing the spatiotemporal dynamic of global grassland water use efficiency in response to climate change from 2000 to 2013. *Journal of Agronomy and Crop Science*, *202*(5), 343–354

Gao, B. C. (1996). NDWI - A normalized difference water index for remote sensing of vegetation liquid water from space. *Remote Sensing of Environment*, *58*(3), 257–266. DOI: https://doi.org/10.1016/S0034-4257(96)00067-3

Georgi, B. et al. (2012). *Urban adaptation to climate change in Europe Challenges and opportunities for cities together with supportive national and European policies*. Rep. No. 2/2012. DOI:10.2800/41895

Gherboudj, I., Magagi, R., Goïta, K., Berg, A. A., Toth, B., & Walker, A. (2012). Validation of SMOS data over agricultural and boreal forest areas in Canada. *IEEE Transactions on Geoscience and Remote Sensing*, *50*(5 PART 1), 1623–1635. DOI: https://doi.org/10.1109/TGRS.2012.2188532

González-Zamora Ángel A4 - Sánchez, Nilda A4 - Martínez-Fernández, José A4 - Wagner, Wolfgang, Á. A.-G.-Z. (2016). Root-zone plant available water estimation using the SMOS-derived soil water index. *Advances in Water Resources*, *v. 96*, 339-353–2016 v.96. DOI: https://doi.org/10.1016/j.advwatres.2016.08.001

González-Zamora, A., Sánchez, N., Gumuzzio, A., Piles, M., Olmedo, E., & Martínez-Fernández, J. (2015). VALIDATION OF SMOS L2 AND L3 SOIL MOISTURE PRODUCTS OVER THE DUERO BASIN AT DIFFERENT SPATIAL SCALES. *ISPRS - International Archives of the Photogrammetry, Remote Sensing and Spatial Information Sciences*, *XL-7/W3*, 1183–1188. DOI: https://doi.org/10.5194/isprsarchives-XL-7-W3-1183-2015

Groisman, P.Y., and A.J. Soja, (2009) Ongoing climatic change in Northern Eurasia: Justification for expedient research. *Environ. Res. Lett*., **4**, doi:10.1088/1748-9326/4/4/045002 (7 pp.).

Groisman, P. Y., Bulygina, O. N., Yin, X., Vose, R. S., Gulev, S. K., Hanssen-Bauer, I., & Førland, E. (2016). Recent changes in the frequency of freezing precipitation in North America and Northern Eurasia. *Environmental Research Letters*. DOI: https://doi.org/10.1088/1748-9326/11/4/045007

Groisman, P. Y., Clark, E. A., Kattsov, V. M., Lettenmaierb, D. P., Sokolik, I. N., Aizen, V. B., Cartus, O., Chen, J., Conard, S., Katzenberger, J., Krankina, O., Kukkonen, J., Machida, T., Maksutov, S., Ojima, D., Qi, J., Romanovsky, V. E., Sanotoro, M., Schmullius, C. C., … Wood, E. F. (2009). The Northern Eurasia Earth Science Partnership: An example of science applied to societal needs. *Bulletin of the American Meteorological Society*, *90*(5), 671–688. DOI: https://doi.org/10.1175/2008BAMS2556.1

Gu, Y., Brown, J. F., Verdin, J. P., & Wardlow, B. (2007). A five-year analysis of MODIS NDVI and NDWI for grassland drought assessment over the central Great Plains of the United States. *Geophysical Research Letters*, *34*(6). DOI: https://doi.org/10.1029/2006GL029127

Gu, Y., Hunt, E., Wardlow, B., Basara, J. B., Brown, J. F., & Verdin, J. P. (2008). Evaluation of MODIS NDVI and NDWI for vegetation drought monitoring using Oklahoma Mesonet soil moisture data. *Geophysical Research Letters*, *35*(22). DOI: https://doi.org/10.1029/2008GL035772

Guan, X., Huang, J., Guo, R., Yu, H., Lin, P., & Zhang, Y. (2015). Role of radiatively forced temperature changes in enhanced semi-arid warming in the cold season over east Asia. *Atmospheric Chemistry and Physics*, *15*(23), 13777–13786

Gunin, P. D., Vostokova, E. A., Dorofeyuk, N. I., Tarasov, P. E., & Black, C. C. (1999). Strategies for Nature Management and Vegetation Conservation. In *Vegetation Dynamics of Mongolia* (pp. 165–202). Springer Netherlands. DOI: https://doi.org/10.1007/978-94-015-9143-0_6

Gutman, G., Chen, J., Henebry, G. M., & Kappas, M. (Eds.). (2020). *Landscape Dynamics of Drylands across Greater Central Asia: People, Societies and Ecosystems* (Vol. 17). Springer International Publishing. DOI: https://doi.org/10.1007/978-3-030-30742-4

Hair, J. F., Black, W. C., Babin, B. J., Anderson, R. E., & Saddle River Boston Columbus San Francisco New York Indianapolis London Toronto Sydney Singapore Tokyo Montreal Dubai Madrid Hong Kong Mexico City Munich Paris Amsterdam Cape Town, U. (1998). *MULTIVARIATE DATA ANALYSIS A Global Perspective*

Halwatura, D., McIntyre, N., Lechner, A., & Arnold, S. (2016). Reliability of meteorological drought indices for predicting soil moisture droughts. *Hydrology and Earth System Sciences Discussions*, 1–25. DOI: https://doi.org/10.5194/hess-2016-467

Hansen, J., Ruedy, R., Sato, M., & Lo, K. (2010). GLOBAL SURFACE TEMPERATURE CHANGE. *Reviews of Geophysics*, *48*(4), RG4004. DOI: https://doi.org/10.1029/2010RG000345

Hassan, M., Smith, A., Walker, K., Rahman, M., & Southworth, J. (2018). Rohingya Refugee Crisis and Forest Cover Change in Teknaf, Bangladesh. *Remote Sensing*, *10*(5), 689. DOI: https://doi.org/10.3390/rs10050689

Hazaymeh, K., & Hassan, Q. K. (2016). *Remote sensing of agricultural drought monitoring: A state of the art review*. DOI: https://doi.org/10.3934/environsci.2016.4.604

Heim, R. R. (2002). A Review of Twentieth-Century Drought Indices Used in the United States. *Bulletin of the American Meteorological Society*, *83*(8), 1149–1166. DOI: https://doi.org/10.1175/1520-0477-83.8.1149

Herzschuh, U. (2006). Palaeo-moisture evolution in monsoonal Central Asia during the last 50,000 years. *Quaternary Science Reviews*. DOI: https://doi.org/10.1016/j.quascirev.2005.02.006

Hessl, A. E., Anchukaitis, K. J., Jelsema, C., Cook, B., Byambasuren, O., Leland, C., Nachin, B., Pederson, N., Tian, H., & Hayles, L. A. (2018). Past and future drought in Mongolia. *Science Advances*, *4*(3), e1701832. DOI: https://doi.org/10.1126/sciadv.1701832

Hilker, T., Natsagdorj, E., Waring, R. H., Lyapustin, A., & Wang, Y. (2014). Satellite observed widespread decline in Mongolian grasslands largely due to overgrazing. *Global Change Biology*, *20*(2), 418–428. DOI: https://doi.org/10.1111/gcb.12365

Hillel, D. (1998). *Environmental soil physics: Fundamentals, applications, and environmental considerations*

Honeychurch, W., & Honeychurch, W. (2015). The Heartland of Inner Asia: Mongolia and Steppe Pastoral Nomadism. In *Inner Asia and the Spatial Politics of Empire* (pp. 79–108). Springer New York. DOI: https://doi.org/10.1007/978-1-4939-1815-7_4

Huang, J., Li, Y., Fu, C., Chen, F., Fu, Q., Dai, A., Shinoda, M., Ma, Z., Guo, W., Li, Z., Zhang, L., Liu, Y., Yu, H., He, Y., Xie, Y., Guan, X., Ji, M., Lin, L., Wang, S., … Wang, G. (2017a). Dryland climate change: Recent progress and challenges. *Reviews of Geophysics*, *55*(3), 719–778. DOI: https://doi.org/10.1002/2016RG000550

Huang, J, Yu, H., Dai, A., Wei, Y., & Kang, L. (2017b). Potential threats over drylands behind 2 C global warming target. *Nat Clim Change*, *7*, 417–422

Huang, Jianping, Yu, H., Guan, X., Wang, G., & Guo, R. (2016). Accelerated dryland expansion under climate change. *Nature Climate Change*, *6*(2), 166–171. DOI: https://doi.org/10.1038/nclimate2837

Huete, A., Didan, K., Miura, T., Rodriguez, E. P., Gao, X., & Ferreira, L. G. (2002). *Overview of the radiometric and biophysical performance of the MODIS vegetation indices*. *Remote Sensing of Environment*, *83*(1-2), 195-213. https://doi.org/10.1016/S0034-4257(02)00096-2

Information And Research Institute Of Meteorology, Hydrology, And Environment. (n.d.). Retrieved November 12, 2020, http://irimhe.namem.gov.mn/

Islam, M. Q., & Tiku, M. L. (2005). Multiple Linear Regression Model Under Nonnormality. *Communications in Statistics - Theory and Methods*, *33*(10), 2443–2467. DOI: https://doi.org/10.1081/STA-200031519

Ivits, E., Horion, S., Fensholt, R., & Cherlet, M. (2014). Drought footprint on European ecosystems between 1999 and 2010 assessed by remotely sensed vegetation phenology and productivity. *Global Change Biology*, *20*(2), 581–593

Jackson, T. J., Bindlish, R., Cosh, M. H., Zhao, T., Starks, P. J., Bosch, D. D., Seyfried, M., Moran, M. S., Goodrich, D. C., & Kerr, Y. H. (2011). Validation of Soil Moisture and Ocean Salinity (SMOS) soil moisture over watershed networks in the US. *IEEE Transactions on Geoscience and Remote Sensing*, *50*(5), 1530–1543

Janssen, M. A. (1994). *Atmospheric remote sensing by microwave radiometry*

Ji, L., & Peters, A. J. (2003). Assessing vegetation response to drought in the northern Great Plains using vegetation and drought indices. *Remote Sensing of Environment*, *87*(1), 85–98

John, R., Chen, J., Lu, N., Guo, K., Liang, C., Wei, Y., Noormets, A., Ma, K., & Han, X. (2008). Predicting plant diversity based on remote sensing products in the semi-arid region of Inner Mongolia. *Remote Sensing of Environment*, *112*(5), 2018–2032. DOI: https://doi.org/10.1016/j.rse.2007.09.013

Johnston, C. A. (1992). Landscape boundaries: consequences for biotic diversity and ecological flows. *Quantitative Methods for Studying Landscape Boundaries*

Jonard, F., Bircher, S., Demontoux, F., Weihermüller, L., Razafindratsima, S., Wigneron, J.-P., & Vereecken, H. (2018). *remote sensing Passive L-Band Microwave Remote Sensing of Organic Soil Surface Layers: A Tower-Based Experiment*. *10*, 304. DOI: https://doi.org/10.3390/rs10020304

Jung, M., Reichstein, M., Ciais, P., Seneviratne, S. I., Sheffield, J., Goulden, M. L., Bonan, G., Cescatti, A., Chen, J., de Jeu, R., Dolman, A. J., Eugster, W., Gerten, D., Gianelle, D., Gobron, N., Heinke, J., Kimball, J., Law, B. E., Montagnani, L., … Zhang, K. (2010). The recent decline in the global land evapotranspiration trend due to limited moisture supply. *Nature*, *467*(7318), 951–954. DOI: https://doi.org/10.1038/nature09396

Justice, C. O., Townshend, J. R. G., Vermote, E. F., Masuoka, E., Wolfe, R. E., Saleous, N., Roy, D. P., & Morisette, J. T. (2002). An overview of MODIS Land data processing and product status. *Remote Sensing of Environment*, *83*(1–2), 3–15. DOI: https://doi.org/10.1016/S0034-4257(02)00084-6

Kakinuma, K., Ozaki, T., Takatsuki, S., & Chuluun, J. (2008). How Pastoralists in Mongolia perceive vegetation changes caused by grazing. *Nomadic Peoples*, *12*(2), 67–73. DOI: https://doi.org/10.3167/np.2008.120205

Kakinuma, K., Yanagawa, A., Sasaki, T., Rao, M. P., & Kanae, S. (2019). Socio-ecological Interactions in a Changing Climate: A Review of the Mongolian Pastoral System. *Sustainability*, *11*(21), 5883. DOI: https://doi.org/10.3390/su11215883

Kala, J., De Kauwe, M. G., Pitman, A. J., Medlyn, B. E., Wang, Y.-P., Lorenz, R., & Perkins-Kirkpatrick, S. E. (2016). Impact of the representation of stomatal conductance on model projections of heatwave intensity. *Scientific Reports*, *6*(1), 1–7

Kang, L., Han, X., Zhang, Z., & Sun, O. J. (2007). Grassland ecosystems in China: a review of current knowledge and research advancement. *Philosophical Transactions of the Royal Society of London. Series B, Biological Sciences*, *362*(1482), 997–1008. DOI: https://doi.org/10.1098/rstb.2007.2029

Karlsen, S. R., Tolvanen, A., Kubin, E., Poikolainen, J., Høgda, K. A., Johansen, B., Danks, F. S., Aspholm, P., Wielgolaski, F. E., & Makarova, O. (2008). MODIS-NDVI-based mapping of the length of the growing season in northern Fennoscandia. *International Journal of Applied Earth Observation and Geoinformation*, *10*(3), 253–266. DOI: https://doi.org/10.1016/j.jag.2007.10.005

Karnieli, A., Agam, N., Pinker, R. T., Anderson, M., Imhoff, M. L., Gutman, G. G., Panov, N., & Goldberg, A. (2010). Use of NDVI and land surface temperature for drought assessment: Merits and limitations. *Journal of Climate*, *23*(3), 618–633

Karrouk, M.-S. (2007). *Climate Change and its Impacts in Morocco*. 253–267. DOI: https://doi.org/10.1007/978-1-4020-6429-6_18

Kawamura, K., Akiyama, T., Yokota, H., Tsutsumi, M., Yasuda, T., Watanabe, O., & Wang, S. (2005). Quantifying grazing intensities using geographic information systems and satellite remote sensing in the Xilingol steppe region, Inner Mongolia, China. *Agriculture, Ecosystems & Environment*, *107*(1), 83–93. DOI: https://doi.org/10.1016/J.AGEE.2004.09.008

Kerr, Y. H., Al-Yaari, A., Rodriguez-Fernandez, N., Parrens, M., Molero, B., Leroux, D., Bircher, S., Mahmoodi, A., Mialon, A., Richaume, P., Delwart, S., Al Bitar, A., Pellarin, T., Bindlish, R., Jackson,

T. J., Rüdiger, C., Waldteufel, P., Mecklenburg, S., & Wigneron, J. P. (2016). Overview of SMOS performance in terms of global soil moisture monitoring after six years in operation. *Remote Sensing of Environment*, *180*, 40–63. DOI: https://doi.org/10.1016/j.rse.2016.02.042

Kerr, Yann H., Waldteufel, P., Wigneron, J. P., Delwart, S., Cabot, F., Boutin, J., Escorihuela, M. J., Font, J., Reul, N., Gruhier, C., Juglea, S. E., Drinkwater, M. R., Hahne, A., Martin-Neira, M., & Mecklenburg, S. (2010). The SMOS L: New tool for monitoring key elements ofthe global water cycle. *Proceedings of the IEEE*, *98*(5), 666–687. DOI: https://doi.org/10.1109/JPROC.2010.2043032

Kerr, Yann H, Member, S., Waldteufel, P., Richaume, P., Pierre Wigneron, J., Ferrazzoli, P., Mahmoodi, A., Al Bitar, A., Cabot, F., Gruhier, C., Enache Juglea, S., Leroux, D., Mialon, A., Delwart, S., Kerr, Y. H., Richaume, P., Al Bitar, A., Cabot, F., Gruhier, C., Wigneron, J. P. (2012). The SMOS Soil Moisture Retrieval Algorithm. *IEEE TRANSACTIONS ON GEOSCIENCE AND REMOTE SENSING*, *50*(5). DOI: https://doi.org/10.1109/TGRS.2012.2184548

Kerr, Yann H, Waldteufel, P., Wigneron, J.-P., Martinuzzi, J.-M., Font, J., & Berger, M. (2001). Soil Moisture Retrieval from Space: The Soil Moisture and Ocean Salinity (SMOS) Mission. In *IEEE TRANSACTIONS ON GEOSCIENCE AND REMOTE SENSING* (Vol. 39, Issue 8)

Kim, H., & Choi, M. (2015). An Inter-comparison of active and passive satellite soil moisture products in East Asia for dust-outbreak prediction. *Journal of the Korean Society of Hazard Mitigation*, *15*(4), 53–58

Kim, S. W., Jung, D., & Choung, Y.-J. (2020). Development of a Multiple Linear Regression Model for Meteorological Drought Index Estimation Based on Landsat Satellite Imagery. *Water*, *12*(12), 3393

Klinge, M., & Sauer, D. (2019). The spatial pattern of Late Glacial and Holocene climatic and environmental development in Western Mongolia - A critical review and synthesis. *Quaternary Science Reviews*, *210*, 26–50. DOI: https://doi.org/10.1016/j.quascirev.2019.02.020

Kogan, F. N. (1995). Application of vegetation index and brightness temperature for drought detection. *Advances in Space Research*, *15*(11), 91–100. DOI: https://doi.org/10.1016/0273-1177(95)00079-T

Kogan, F., Stark, R., Gitelson, A., Jargalsaikhan, L., Dugrajav, C., & Tsooj, S. (2004). Derivation of pasture biomass in Mongolia from AVHRR-based vegetation health indices. *Taylor & Francis*, *25*(14), 2889–2896. DOI: https://doi.org/10.1080/01431160410001697619

Kogan, Felix N. (1997). Global Drought Watch from Space. *Bulletin of the American Meteorological Society*, *78*(4), 621–636. DOI:https://doi.org/10.1175/1520-0477(1997)078<0621:GDWFS>2.0.CO;2

Kolassa, J., Reichle, R., Liu, Q., Cosh, M., Bosch, D., Caldwell, T., Colliander, A., Holifield Collins, C., Jackson, T., Livingston, S., Moghaddam, M., & Starks, P. (2017). Data Assimilation to Extract Soil Moisture Information from SMAP Observations. *Remote Sensing*, *9*(11), 1179. DOI: https://doi.org/10.3390/rs9111179

Koren, V., Moreda, F., & Smith, M. (2008). Use of soil moisture observations to improve parameter consistency in watershed calibration. *Physics and Chemistry of the Earth, Parts A/B/C*, *33*(17–18), 1068–1080

Kornelsen, K. C., & Coulibaly, P. (2014). Design of an optimum soil moisture monitoring network using SMOS. *2014 IEEE Geoscience and Remote Sensing Symposium*, 3206–3209

Natsagdorj L. Munkhbat B. and Gomboluudev P. (2019). Climate biocapacity of Mongolia and its change. *Proceedings of the Mongolian Academy of Sciences*, 54–70. DOI: https://doi.org/10.5564/pmas.v59i2.1219

LAND DEGRADATION NEUTRALITY TARGET SETTING PROGRAMME NATIONAL REPORT ON VOLUNTARY TARGET SETTING TO ACHIEVE LAND DEGRADATION NEUTRALITY IN MONGOLIA (2018). *National Committee on Combatting Desertification of Mongolia (NCCD)*.

Lehmkuhl, F., Grunert, J., Hülle, D., Batkhishig, O., & Stauch, G. (2018). Paleolakes in the Gobi region of southern Mongolia. In *Quaternary Science Reviews* (Vol. 179, pp. 1–23). Elsevier Ltd. DOI: https://doi.org/10.1016/j.quascirev.2017.10.035

Li, W., Duan, L., Wang, W., Wu, Y., Liu, T., Quan, Q., Chen, X., Yin, H., & Zhou, Q. (2020). Spatiotemporal characteristics of drought in a semi-arid grassland over the past 56 years based on the Standardized Precipitation Index. *Meteorology and Atmospheric Physics*, 1–14. DOI: https://doi.org/10.1007/s00703-020-00727-4

Lindroth, A., Grelle, A., & Moren, A.-S. (1998). Long-term measurements of boreal forest carbon balance reveal large temperature sensitivity. *Global Change Biology*, *4*(4), 443–450. DOI: https://doi.org/10.1046/j.1365-2486.1998.00165.x

Liu, Q., Zhang, S., Zhang, H., Bai, Y., & Zhang, J. (2020). Monitoring drought using composite drought indices based on remote sensing. *Science of the Total Environment*, *711*, 134585. DOI: https://doi.org/10.1016/j.scitotenv.2019.134585

Liu, Y. Y., Evans, J. P., McCabe, M. F., de Jeu, R. A. M., van Dijk, A. I. J. M., Dolman, A. J., & Saizen, I. (2013). Changing Climate and Overgrazing Are Decimating Mongolian Steppes. *PLoS ONE*, *8*(2), e57599. DOI: https://doi.org/10.1371/journal.pone.0057599

Liu, Z., Yao, Z., Huang, H., Batjav, B., & Wang, R. (2019). Evaluation of extreme cold and drought over the Mongolian Plateau. *Water (Switzerland)*, *11*(1). DOI: https://doi.org/10.3390/w11010074

Lorenzo-Lacruz, J., Vicente-Serrano, S. M., López-Moreno, J. I., Beguería, S., García-Ruiz, J. M., & Cuadrat, J. M. (2010). The impact of droughts and water management on various hydrological systems in the headwaters of the Tagus River (central Spain). *Journal of Hydrology*, *386*(1–4), 13–26. DOI: https://doi.org/10.1016/j.jhydrol.2010.01.001

LP DAAC : NASA Land Data Products and Services

LP DAAC - MOD13Q1. https://lpdaac.usgs.gov/products/mod13q1v006/

Ma, H., Mater, H. Z.-I. L., & U. (2018). Memorandum of Understanding Between the Conference of the Parties To the United Nations Convention To Combat Desertification in Those Countries Experiencing Serious Drought and/or Desertification, Africa and the Council of the Global Environment

MARCC- Mongolia: Assessment Report on Climate Change (2009). Ministry of Environment of Mongolia

Mannava Sivakumar., Raymond P Motha., Donald A Wilhite., Deborah A Wood. (2010). *Agricultural Drought Indices. Proceedings of an Expert Meeting Murcia, Spain*. World Meteorological Organization

Marczewski, W., & Łukowski, M. (2014). Comparison of Surface Soil Moisture from SMOS Satellite and Ground Measurements. *International Agrophysics*. 28, 359-369. DOI: 10.2478/intag-2014-0026

Martínez-Fernández, J., González-Zamora, A., Sánchez, N., & Gumuzzio, A. (2015). A soil water based index as a suitable agricultural drought indicator. *Journal of Hydrology*, *522*, 265–273. DOI: https://doi.org/10.1016/j.jhydrol.2014.12.051

Martínez-Fernández, J., González-Zamora, A., Sánchez, N., Gumuzzio, A., & Herrero-Jiménez, C. M. (2016). Satellite soil moisture for agricultural drought monitoring: Assessment of the SMOS derived Soil Water Deficit Index. *Remote Sensing of Environment*, *177*, 277–286. DOI: https://doi.org/10.1016/j.rse.2016.02.064

Martinez-Fernandez, J., Sanchez, N., Gonzalez-Zamora, A., Gumuzzio-Such, A., & Herrero-Jimenez, C. M. (2015). Feasibility of the SMOS soil moisture for agricultural drought monitoring: Assessment with the Soil Water Deficit Index. *International Geoscience and Remote Sensing Symposium (IGARSS), 2015-November*, 976–979. DOI: https://doi.org/10.1109/IGARSS.2015.7325931

Mckee, T. B., Doesken, N. J., & Kleist, J. (1993). THE RELATIONSHIP OF DROUGHT FREQUENCY AND DURATION TO TIME SCALES. In *Eighth Conference on Applied Climatology*

Miao, L., Li, S., Zhang, F., Chen, T., Shan, Y., & Zhang, Y. (2020a). Future Drought in the Dry Lands of Asia Under the 1.5 and 2.0 °C Warming Scenarios. *Earth's Future*, *8*(6), 0–13. DOI: https://doi.org/10.1029/2019EF001337

Mishra, A. K., & Singh, V. P. (2010). A review of drought concepts. In *Journal of Hydrology* (Vol. 391, Issues 1–2, pp. 202–216). DOI: https://doi.org/10.1016/j.jhydrol.2010.07.012

Mishra, B. K., Rafiei Emam, A., Masago, Y., Kumar, P., Regmi, R. K., & Fukushi, K. (2018). Assessment of future flood inundations under climate and land-use change scenarios in the Ciliwung River Basin, Jakarta. *Journal of Flood Risk Management*, *11*, S1105–S1115. DOI: https://doi.org/10.1111/jfr3.12311

Molero, B., Merlin, O., Malbéteau, Y., Al Bitar, A., Cabot, F., Stefan, V., Kerr, Y., Bacon, S., Cosh, M. H., Bindlish, R., & Jackson, T. J. (2016). SMOS disaggregated soil moisture product at 1 km resolution: Processor overview and first validation results. *Remote Sensing of Environment*, *180*, 361–376. DOI: https://doi.org/10.1016/j.rse.2016.02.045

Moreira, E. E., Mexia, J. T., & Pereira, L. S. (2012). Are drought occurrence and severity aggravating? A study on SPI drought class transitions using log-linear models and ANOVA-like inference. *Hydrology and Earth System Sciences*, *16*(8), 3011–3028. DOI: https://doi.org/10.5194/hess-16-3011-2012

Moriasi, D. N., J. G. Arnold, J. G., M. W. Van Liew, M. W. Van, R. L. Bingner, R. L., R. D. Harmel, R. D., & T. L. Veith, T. L. (2007). Model Evaluation Guidelines for Systematic Quantification of Accuracy in Watershed Simulations. *Transactions of the ASABE*, *50*(3), 885–900. DOI: https://doi.org/10.13031/2013.23153

Morinaga, Y., Tian, S.-F., & Shinoda, M. (2003). Winter snow anomaly and atmospheric circulation in Mongolia. *International Journal of Climatology*, *23*(13), 1627–1636. DOI: https://doi.org/10.1002/joc.961

Mukund Palat, R., Nicole, K. D., Rosanne, D. D., Jerry, S., Baatarbileg, N., Caroline, L., Bradfield, L., Shih-Yu, W., & Oyunsanaa, B. (2015a). Dzuds, droughts, and livestock mortality in Mongolia. *Environmental Research Letters*, *10*(7), 74012. DOI: https://doi.org/10.7916/d8q81d7s

Munkhtsetseg, E., Kimura, R., Wang, J., & Shinoda, M. (2007). Pasture yield response to precipitation and high temperature in Mongolia. *Journal of Arid Environments*, *70*(1), 94–110. DOI: https://doi.org/10.1016/j.jaridenv.2006.11.013

Murray, L., Nguyen, H., Lee, Y.-F., Remmenga, M. D., & Smith, D. W. (2012). VARIANCE INFLATION FACTORS IN REGRESSION MODELS WITH DUMMY VARIABLES. *Conference on Applied Statistics in Agriculture*. DOI: https://doi.org/10.4148/2475-7772.1034

Musolino, D., De Carli, A., & Massarutto, A. (2017). Evaluation of the socio-economic impacts of the drought events: The case of the Po river basin. *European Countryside*, *9*(1), 163–176. DOI: https://doi.org/10.1515/euco-2017-0010

Nandintsetseg, B., & Shinoda, M. (2011). Seasonal change of soil moisture in Mongolia: its climatology and modeling. *International Journal of Climatology*, *31*(8), 1143–1152. DOI: https://doi.org/10.1002/joc.2134

Nandintsetseg, B., & Shinoda, M. (2013). Assessment of drought frequency, duration, and severity and its impact on pasture production in Mongolia. *Natural Hazards*, *66*(2), 995–1008. DOI: https://doi.org/10.1007/s11069-012-0527-4

Nandintsetseg, B., Shinoda, M., Du, C., & Munkhjargal, E. (2018a). Cold-season disasters on the Eurasian steppes: Climate-driven or man-made. *Scientific Reports*, *8*(1). DOI: https://doi.org/10.1038/s41598-018-33046-1

Nandintsetseg, B., Shinoda, M., & Erdenetsetseg, B. (2018b). Contributions of multiple climate hazards and overgrazing to the 2009/2010 winter disaster in Mongolia. *Natural Hazards*, *92*(1), 109–126. DOI: https://doi.org/10.1007/s11069-017-2954-8

Nanzad, L., Zhang, J., Tuvdendorj, B., Nabil, M., Zhang, S., & Bai, Y. (2019). NDVI anomaly for drought monitoring and its correlation with climate factors over Mongolia from 2000 to 2016. *Journal of Arid Environments*, *164*, 69–77. DOI: https://doi.org/10.1016/j.jaridenv.2019.01.019

National Agency Meteorology and the Environmental Monitoring of Mongolia

National Remote Sensing Center of Mongolia. Remote sensing product. http://www.icc.mn/

National Statistical Office of Mongolia : Annual reports. https://www.en.nso.mn/page/35

National Statistical Office of Mongolia. *National Statistical Office of Mongolia (1990)*

National Statistical Office of Mongolia. *Mongolian Statistical Yearbook (2009)*

National Statistical Office of Mongolia. *NSO (2015): Number of livestock, by type, by regions, soums, aimags and the Capital: Mongolian Statistical Information Service*

National Statistics Office of Mongolia (2021). http://www.en.nso.mn/stat_main

Natsagdorj, E., & Renchin, T. (2010). Determination of moisture in Mongolia using Remotely sensed data. *Proceedings of the Asian Conference on Remote Sensing, Hanoi, Vietnam*, 1–5.

NATSAGDORJ, & L. (2001). Some aspects of assessment of the dzud phenomena. *Papers in Meteorology and Hydrology*, *23*, 3–18

Natsagdorj L. Munkhbat B. and Gomboluudev P. (2019). Climate biocapacity of Mongolia and its change. *Proceedings of the Mongolian Academy of Sciences*, 54–70. DOI: https://doi.org/10.5564/pmas.v59i2.1219

Nepal, S., Pradhananga, S., Shrestha, N. K., Kralisch, S., Shrestha, J., & Fink, M. (2020). Space-time variability of soil moisture droughts in the Himalayan region. *Hydrology and Earth System Sciences Discussions*, 1-30. DOI: https://doi.org/10.5194/hess-2020-337

Ni, J. (2003). Plant functional types and climate along a precipitation gradient in temperate grasslands, north-east China, and south-east Mongolia. *Journal of Arid Environments*, *53*(4), 501–516. DOI: https://doi.org/10.1006/jare.2002.1063

Ni, J., & Zhang, X.-S. (2000). Climate variability, ecological gradient, and the Northeast China Transect (NECT). *Journal of Arid Environments*, *46*, 313–325. DOI: https://doi.org/10.1006/jare.2000.0667

NYAMTSEREN, M., JAMSRAN, T., & SODOV, K. (2015). UNCCD 3rd Scientific Conference. *THE ASSESSMENT AND MAPPING OF DESERTIFICATION IN MONGOLIA*

Oliver, J. E., & Fairbridge, R. W. (1987). *The Encyclopedia of climatology*

Oliver, T. H., Isaac, N. J. B., August, T. A., Woodcock, B. A., Roy, D. B., & Bullock, J. M. (2015). Declining resilience of ecosystem functions under biodiversity loss. *Nature Communications*, *6*(1), 1–8. DOI: https://doi.org/10.1038/ncomms10122

Ongoing climatic change in Northern Eurasia: justification for expedient research - IOPscience. DOI: https://iopscience.iop.org/article/10.1088/1748-9326/4/4/045002/meta

O'Neill, P. E., S. Chan, E. G. Njoku, T. Jackson, R. Bindlish, and J. Chaubell. (2019). *SMAP Enhanced L3 Radiometer Global Daily 9 km EASE-Grid Soil Moisture, Version 3*. Boulder, Colorado USA. NASA National Snow and Ice Data Center Distributed Active Archive Center. DOI: https://doi.org/10.5067/T90W6VRLCBHI

Palmer, W. (1965). Meteorological drought. *US Weather Bur Res Pap*, *45*, 58

Palmer, W. C. (1968). Keeping Track of Crop Moisture Conditions, Nationwide: The New Crop Moisture Index. *Weatherwise*, *21*(4), 156–161. DOI: https://doi.org/10.1080/00431672.1968.9932814

Pan, C. G., Kimball, J. S., Munkhjargal, M., Robinson, N. P., Tijdeman, E., Menzel, L., & Kirchner, P. B. (2019). Role of Surface Melt and Icing Events in Livestock Mortality across Mongolia's Semi-Arid Landscape. *Remote Sensing*, *11*(20), 2392. DOI: https://doi.org/10.3390/rs11202392

Peel, M. C., & Blöschl, G. (2011). Hydrological modeling in a changing world. *Progress in Physical Geography*, *35*(2), 249–261

Prigent, C., Aires, F., Rossow, W. B., & Robock, A. (2005). The sensitivity of satellite microwave and infrared observations to soil moisture at a global scale: Relationship of satellite observations to in situ soil moisture measurements. *Journal of Geophysical Research*, *110*(D7), D07110. DOI: https://doi.org/10.1029/2004JD005087

Purevsuren, T., Hoshino, B., Ganzorig, S., & Sawamukai, M. (2012). *Spatial and Temporal Patterns of NDVI Response to Precipitation and Temperature in Mongolian Steppe*

Puth, M. T., Neuhäuser, M., & Ruxton, G. D. (2014). Effective use of Pearson's product-moment correlation coefficient. In *Animal Behaviour* (Vol. 93, pp. 183–189). DOI: https://doi.org/10.1016/j.anbehav.2014.05.003

Rafiei Emam, A., Kappas, M., Linh, N., Renchin, T., Rafiei Emam, A., Kappas, M., Linh, N. H. K., & Renchin, T. (2017). Hydrological Modeling and Runoff Mitigation in an Ungauged Basin of Central Vietnam Using SWAT Model. *Hydrology*, *4*(1), 16. DOI: https://doi.org/10.3390/hydrology4010016

Rahimzadeh-Bajgiran, P., & Berg, A. (2016). Soil Moisture Retrievals Using Optical/TIR Methods. In *Satellite Soil Moisture Retrieval: Techniques and Applications* (pp. 47–72). DOI: https://doi.org/10.1016/B978-0-12-803388-3.00003-6

Rasmussen, D., & Annor-Frempong, C. (2015). *Mongolia Agricultural Productivity and Marketing*

Ravi, S., Breshears, D. D., Huxman, T. E., & D'Odorico, P. (2010). Land degradation in drylands: Interactions among hydrologic–aeolian erosion and vegetation dynamics. *Geomorphology*, *116*(3–4), 236–245. DOI: https://doi.org/10.1016/J.GEOMORPH.2009.11.023

Recommended Citation Berhan, G., Hill, S., Tadesse, T., & Atnafu, S. (2011). Using Satellite Images for Drought Monitoring: A Knowledge Discovery Approach. In *Journal of Strategic Innovation and Sustainability* (Vol. 7, Issue 1)

Regional workshop on understanding the operational aspects of the drought observation system in Mongolia | United Nations ESCAP

Renza, D., Martinez, E., Arquero, A., & Sanchez, J. (2010). Drought Estimation Maps by Means of Multidate Landsat Fused Images. http://earthexplorer.usgs.gov

Ribeiro, A. F. S., Russo, A., Gouveia, C. M., & Páscoa, P. (2019). Modelling drought-related yield losses in Iberia using remote sensing and multiscalar indices. *Theoretical and Applied Climatology*, *136*(1–2), 203–220. DOI: https://doi.org/10.1007/s00704-018-2478-5

Rind, D., Goldberg, R., Hansen, J., Rosenzweig, C., & Ruedy, R. (1990). Potential evapotranspiration and the likelihood of future drought. *Journal of Geophysical Research*, *95*(D7), 9983–10004. DOI: https://doi.org/10.1029/jd095id07p09983

Robinson, D. A., Campbell, C. S., Hopmans, J. W., Hornbuckle, B. K., Jones, S. B., Knight, R., Ogden, F., Selker, J., & Wendroth, O. (2008). Soil Moisture Measurement for Ecological and Hydrological Watershed-Scale Observatories: A Review. *Vadose Zone Journal*, *7*(1), 358–389. DOI: https://doi.org/10.2136/vzj2007.0143

Rodriguez-Iturbe, I. (2000). Ecohydrology: A hydrologic perspective of climate-soil-vegetation dynamics. *Water Resources Research*, *36*(1), 3–9

Rüdiger, C., Walker, J. P., Kerr, Y. H., Mialon, A., Merlin, O., & Kim, E. J. (2011). *Validation of the Level 1 c and Level 2 SMOS Products with Airborne and Ground-based Observations*

Sala, O. E., Parton, W. J., Joyce, L. A., & Lauenroth, W. K. (1988). Primary production of the central grassland region of the United States. *Ecology*, *69*(1), 40–45

Sanchez, N., Martinez-Fernandez, J., Scaini, A., & Perez-Gutierrez, C. (2012a). Validation of the SMOS L2 Soil Moisture Data in the REMEDHUS Network (Spain). *IEEE Transactions on Geoscience and Remote Sensing*, *50*(5), 1602–1611. DOI: https://doi.org/10.1109/TGRS.2012.2186971

Sanchez, N. et al. (2012b) Spatial patterns of SMOS downscaled soil moisture maps over the remedhus network (Spain). A: IEEE International Geoscience and Remote Sensing Symposium. "IGARSS 2012: International Geoscience and Remote Sensing Symposium: remote science for a dynamic earth: proceedings, Munich: Institute of Electrical and Electronics Engineers (IEEE), 2012, p. 714-717

Sánchez, Nilda, González-Zamora, Á., Piles, M., & Martínez-Fernández, J. (2016). A New Soil Moisture Agricultural Drought Index (SMADI) Integrating MODIS and SMOS Products: A Case of Study over the Iberian Peninsula. *Remote Sensing*, *8*(4), 287. DOI: https://doi.org/10.3390/rs8040287

Satellite-based system to monitor droughts/dzuds handed over to Mongolia - Mongolia | ReliefWeb. from https://reliefweb.int/report/mongolia/satellite-based-system-monitor-droughtsdzuds-handed-over-mongolia

Sathaye, J., Shukla, P. R., & Ravindranath, N. H. (2006). Climate change, sustainable development, and India: Global and national concerns. *Current Science*, 314–325

Saxton, K. E., & Rawls, W. J. (2006). Soil Water Characteristic Estimates by Texture and Organic Matter for Hydrologic Solutions. *Soil Science Society of America Journal*, *70*(5), 1569. DOI: https://doi.org/10.2136/sssaj2005.0117

Scaini, A., Sánchez, N., Vicente-Serrano, S. M., & Martínez-Fernández, J. (2015). SMOS-derived soil moisture anomalies and drought indices: a comparative analysis using *in situ* measurements. *Hydrological Processes*, *29*(3), 373–383. DOI: https://doi.org/10.1002/hyp.10150

Scheff, J., & Frierson, D. M. W. (2014). Scaling potential evapotranspiration with greenhouse warming. *Journal of Climate*, *27*(4), 1539–1558

Schlaepfer, D. R., Bradford, J. B., Lauenroth, W. K., Munson, S. M., Tietjen, B., Hall, S. A., Wilson, S. D., Duniway, M. C., Jia, G., & Pyke, D. A. (2017). *Climate change reduces the extent of temperate drylands and intensifies drought in deep soils. Nat Commun 8: 14196*

Schlenz, F., dall'Amico, J. T., Loew, A., & Mauser, W. (2012). Uncertainty Assessment of the SMOS Validation in the Upper Danube Catchment. *IEEE Transactions on Geoscience and Remote Sensing*, *50*(5), 1517–1529. DOI: https://doi.org/10.1109/TGRS.2011.2171694

Sedgwick, P. (2012). Pearson's correlation coefficient. In *BMJ (Online)* (Vol. 345, Issue 7864). British Medical Journal Publishing Group. DOI: https://doi.org/10.1136/bmj.e4483

Sekiyama, A., Takeuchi, W., & Shimada, S. (2014) *Detection of Grassland Degradation Using MODIS Data in Mongolia*. *Journal of Arid Land Studies*. 24-1, 175-178

Seneviratne, S. I., Corti, T., Davin, E. L., Hirschi, M., Jaeger, E. B., Lehner, I., Orlowsky, B., & Teuling, A. J. (2010). Investigating soil moisture-climate interactions in a changing climate: A review. In *Earth-Science Reviews* (Vol. 99, Issues 3–4, pp. 125–161). DOI: https://doi.org/10.1016/j.earscirev.2010.02.004

Shah, D., & Mishra, V. (2020). Integrated Drought Index (IDI) for Drought Monitoring and Assessment in India. *Water Resources Research*, *56*(2). DOI: https://doi.org/10.1029/2019WR026284

Sheffield, J., & Wood, E. F. (2008). Global trends and variability in soil moisture and drought characteristics, 1950–2000, from observation-driven simulations of the terrestrial hydrologic cycle. *Journal of Climate*, *21*(3), 432–458

Shen, Z., Zhang, Q., Singh, V. P., Sun, P., Song, C., & Yu, H. (2019). Agricultural drought monitoring across Inner Mongolia, China: Model development, spatiotemporal patterns, and impacts. *Journal of Hydrology*, *571*, 793–804. DOI: https://doi.org/10.1016/j.jhydrol.2019.02.028

Shestakovich, N. (2010). *Exploratory analysis of spatial and temporal dynamics of Dzud development in Mongolia, 1993-2004.* School of Natural Resources & Environment of the University of Michigan

Shinoda, M., Nachinshonhor, G. U., & Nemoto, M. (2010). Impact of drought on vegetation dynamics of the Mongolian steppe: A field experiment. *Journal of Arid Environments*, *74*(1), 63–69. DOI: https://doi.org/10.1016/j.jaridenv.2009.07.004

Shinoda, M. (2015). High-impact weather in a changing climate over arid Eurasia and proactive disaster management. *Procedia IUTAM*, *17*, 47–52. DOI: https://doi.org/10.1016/j.piutam.2015.06.008

Shinoda, M., & Morinaga, Y. (2005). Developing a combined drought-dzud early warning system in Mongolia. *Geographical Review of Japan*, *78*(13), 928–950

Shinoda, M., & Nandintsetseg, B. (2011). Soil moisture and vegetation memories in a cold, arid climate. *Global and Planetary Change*, *79*(1–2), 110–117. DOI: https://doi.org/10.1016/j.gloplacha.2011.08.005

Shuttle Radar Topography Mission. https://www2.jpl.nasa.gov/srtm/

Souza, A. G. S. S., Neto, A. R., Rossato, L., Alvalá, R. C. S., & Souza, L. L. (2018). Use of SMOS L3 soil moisture data: Validation and drought assessment for Pernambuco State, Northeast Brazil *Remote Sensing*, *10*(8). DOI: https://doi.org/10.3390/RS10081314

Sternberg, T. (2010). Unraveling Mongolia's extreme winter disaster of 2010. *Nomadic Peoples*, *14*(1), 72–86. DOI: https://doi.org/10.3167/np.2010.140105

Sternberg, T. (2011). Regional drought has a global impact. In *Nature* (Vol. 472, Issue 7342, p. 169). Nature Publishing Group. DOI: https://doi.org/10.1038/472169d

Sternberg, T. (2018). Investigating the presumed causal links between drought and dzud in Mongolia. *Natural Hazards*, *92*(1), 27–43. DOI: https://doi.org/10.1007/s11069-017-2848-9

Sternberg, T., Middleton, N., & Thomas, D. (2009). Pressurized pastoralism in South Gobi, Mongolia: What is the role of drought? *Transactions of the Institute of British Geographers*, *34*(3), 364–377. DOI: https://doi.org/10.1111/j.1475-5661.2009.00348.x

Sternberg, T., Rueff, H., & Middleton, N. (2015). Contraction of the Gobi desert, 2000-2012. *Remote Sensing*, *7*(2), 1346–1358. DOI: https://doi.org/10.3390/rs70201346

Sternberg, T., Thomas, D., & Middleton, N. (2011). Drought dynamics on the Mongolian steppe, 1970-2006. *International Journal of Climatology*, *31*(12), 1823–1830. DOI: https://doi.org/10.1002/joc.2195

Su, C. H., Ryu, D., Young, R. I., Western, A. W., & Wagner, W. (2013). Inter-comparison of microwave satellite soil moisture retrievals over the Murrumbidgee Basin, southeast Australia. *Remote Sensing of Environment*, *134*, 1–11. DOI: https://doi.org/10.1016/j.rse.2013.02.016

Sustainable Adapted Use The Crop (2020). *On sustainable and climate change adapted land use in the Mongolian crop sector*

Svoboda, M., LeComte, D., Hayes, M., Heim, R., Gleason, K., Angel, J., Rippey, B., Tinker, R., Palecki, M., Stooksbury, D., Miskus, D., & Stephens, S. (2002). THE DROUGHT MONITOR. *Bulletin of the American Meteorological Society*, *83*(8), 1181–1190. DOI: https://doi.org/10.1175/1520-0477-83.8.1181

Svoboda, M., Svoboda, M., Hayes, M., Wood, D. A., & (WMO), W. M. O. (2012). *Standardized Precipitation Index User Guide*

Szép, I. J., Mika, J., & Dunkel, Z. (2005). Palmer drought severity index as soil moisture indicator: Physical interpretation, statistical behaviour, and relation to global climate. *Physics and Chemistry of the Earth*, 231–243. DOI: https://doi.org/10.1016/j.pce.2004.08.039

Szlazak, R., Rojek, E., Lukowski, M., Marczewski, W., Slominski, J., Sagan, J., Gluba, L., Usowicz, J., & Usowicz, B. (2017). Comparison of remote sensing and in-situ soil moisture measurements: 6 years survey of SMOS data and agrometeorological stations in Eastern Poland. *19th EGU General Assembly, EGU2017, Proceedings from the Conference Held 23-28 April 2017 in Vienna, Austria., p.13809*, *19*, 13809

Tachiiri, K., Shinoda, M., Klinkenberg, B., & Morinaga, Y. (2008). Assessing Mongolian snow disaster risk using livestock and satellite data. *Journal of Arid Environments*, *72*(12), 2251–2263. DOI: https://doi.org/10.1016/j.jaridenv.2008.06.015

Takagi, K., & Lin, H. S. (2011). Temporal dynamics of soil moisture spatial variability in the Shale Hills Critical Zone Observatory. *Vadose Zone Journal*, *10*(3), 832–842

Taking the Temperature of the Earth. (2019). In *Taking the Temperature of the Earth*. Elsevier. DOI: https://doi.org/10.1016/c2017-0-01600-2

Tao, S., Fang, J., Zhao, X., Zhao, S., Shen, H., Hu, H., Tang, Z., Wang, Z., & Guo, Q. (2015). Rapid loss of lakes on the Mongolian Plateau. *Proceedings of the National Academy of Sciences of the United States of America*, *112*(7), 2281–2286. DOI: https://doi.org/10.1073/pnas.1411748112

Templer, G., Swift, J., & Payne, P. (1993). The changing significance of risk in the Mongolian pastoral economy. *Nomadic Peoples*, 105–122

The impact of disasters and crises on agriculture and food security 2017: FAO in Emergencies. http://www.fao.org/emergencies/resources/documents/resources-detail/en/c/1106859/

The ripple effect: A Fresh Approach to Reducing Drought Impacts and Building Resilience | UNCCD. https://www.unccd.int/publications/ripple-effect-fresh-approach-reducing-drought-impacts-and-building-resilience

THIRD NATIONAL COMMUNICATION OF MONGOLIA Under the United Nations Framework Convention on Climate Change

Tilman, D., & El Haddi, A. (1992). Drought and biodiversity in grasslands. *Oecologia*, *89*(2), 257–264

Tranmer M. and M. Elliot (2008) "Multiple Linear Regression," The Cathie Marsh Centre for Census and Survey Research (CCSR)

Trenberth, K. E., Dai, A., Van Der Schrier, G., Jones, P. D., Barichivich, J., Briffa, K. R., & Sheffield, J. (2014). Global warming and changes in drought. *Nature Climate Change*, *4*(1), 17–22

Tucker, C. J. (1979). Red and photographic infrared linear combinations for monitoring vegetation. *Remote Sensing of Environment*, *8*(2), 127–150

Tucker, C. J., & Choudhury, B. J. (1987). Satellite remote sensing of drought conditions. *Remote Sensing of Environment*, *23*(2), 243–251. DOI: https://doi.org/10.1016/0034-4257(87)90040-X

TUCKER, C. J., NEWCOMB, W. W., LOS, S. O., & PRINCE, S. D. (1991). Mean and inter-year variation of growing-season normalized difference vegetation index for the Sahel 1981-1989. *International Journal of Remote Sensing*, *12*(6), 1133–1135. DOI: https://doi.org/10.1080/01431169108929717

Tumenjargal, S., Fassnacht, S. R., Venable, N. B. H., Kingston, A. P., Fernández-Giménez, M. E., Batbuyan, B., Laituri, M. J., Kappas, M., & Adyabadam, G. (2020). Variability and change of climate extremes from indigenous herder knowledge and at meteorological stations across central Mongolia. *Frontiers of Earth Science*, *14*(2), 286–297. DOI: https://doi.org/10.1007/s11707-019-0812-6

Tuvdendorj, B., Wu, B., Zeng, H., Batdelger, G., & Nanzad, L. (2019). Determination of Appropriate Remote Sensing Indices for Spring Wheat Yield Estimation in Mongolia. *Remote Sensing*, *11*(21), 2568. DOI: https://doi.org/10.3390/rs11212568

Ulaanbaatar, T. S.-A. P. H., & 1998, *Biological Diversity in Mongolia, First National Report, Ministry for Nature and the Environment*

Um, M. J., Kim, Y., Park, D., Jung, K., Wang, Z., Kim, M. M., & Shin, H. (2020). Impacts of potential evapotranspiration on drought phenomena in different regions and climate zones. *Science of the Total Environment*, *703*, 135590. DOI: https://doi.org/10.1016/j.scitotenv.2019.135590

UNDP/NEMA. (2010). *How Mongolian herders affected by Dzud, natural phenomena, 2009-2010: government and pastoralist's disaster management. Dzud National Report 2009-2010*.

Unganai, L. S., & Kogan, F. N. (1998). Drought monitoring and corn yield estimation in southern Africa from AVHRR data. *Remote Sensing of Environment*, *63*(3), 219–232. DOI: https://doi.org/10.1016/S0034-4257(97)00132-6

United Nations General Assembly. (2011). *High-level meeting on addressing desertification, land degradation, and drought in the context of sustainable development and poverty eradication* (Issue 6)

USGS EROS Archive - Digital Elevation - SRTM Mission Summary. https://www.usgs.gov/centers/eros/science/usgs-eros-archive-digital-elevation-srtm-mission-summary?qt-science_center_objects=0#qt-science_center_objects

Usowicz, B., Lipiec, J., Lukowski, M., Usowicz, B., Lipiec, J., & Lukowski, M. (2019). Evaluation of Soil Moisture Variability in Poland from SMOS Satellite Observations. *Remote Sensing*, *11*(11), 1280. DOI: https://doi.org/10.3390/rs11111280

Uyanık, G. K., & Güler, N. (2013). A Study on Multiple Linear Regression Analysis. *Procedia - Social and Behavioral Sciences*, *106*, 234–240. DOI: https://doi.org/https://doi.org/10.1016/j.sbspro.2013.12.027

Van Lanen, H. A. J., Wanders, N., Tallaksen, L. M., & Van Loon, A. F. (2013). Hydrological drought across the world: impact of climate and physical catchment structure. *Hydrology and Earth System Sciences*, *17*(5), 1715–1732. DOI: https://doi.org/10.5194/hess-17-1715-2013

Van Loon, A. F., Tijdeman, E., Wanders, N., Van Lanen, H. A. J., Teuling, A. J., & Uijlenhoet, R. (2014). How climate seasonality modifies drought duration and deficit. *Journal of Geophysical Research*, *119*(8), 4640–4656. DOI: https://doi.org/10.1002/2013JD020383

Vegetation Dynamics of Mongolia. (1999). In *Vegetation Dynamics of Mongolia*. Springer Netherlands. DOI: https://doi.org/10.1007/978-94-015-9143-0

Vermote, E. F., El Saleous, N. Z., & Justice, C. O. (2002). Atmospheric correction of MODIS data in the visible to middle infrared: First results. *Remote Sensing of Environment*, *83*(1–2), 97–111. DOI: https://doi.org/10.1016/S0034-4257(02)00089-5

Vicente-Serrano, S. M., Beguería, S., & López-Moreno, J. I. (2010). A multiscalar drought index sensitive to global warming: The standardized precipitation evapotranspiration index. *Journal of Climate*, *23*(7), 1696–1718. DOI: https://doi.org/10.1175/2009JCLI2909.1

Vicente-Serrano, S. M., Beguería, S., Lorenzo-Lacruz, J., Camarero, J. J., López-Moreno, J. I., Azorin-Molina, C., Revuelto, J., Morán-Tejeda, E., & Sanchez-Lorenzo, A. (2012). Performance of drought indices for ecological, agricultural, and hydrological applications. *Earth Interactions*, *16*(10). DOI: https://doi.org/10.1175/2012EI000434.1

Vicente-Serrano, S. M., Gouveia, C., Camarero, J. J., Beguería, S., Trigo, R., López-Moreno, J. I., Azorín-Molina, C., Pasho, E., Lorenzo-Lacruz, J., Revuelto, J., Morán-Tejeda, E., & Sanchez-Lorenzo, A. (2013). Response of vegetation to drought time-scales across global land biomes. *Proceedings of the National Academy of Sciences of the United States of America*, *110*(1), 52–57. DOI: https://doi.org/10.1073/pnas.1207068110

Vogel, M. M., Orth, R., Cheruy, F., Hagemann, S., Lorenz, R., van den Hurk, B. J. J. M., & Seneviratne, S. I. (2017). Regional amplification of projected changes in extreme temperatures strongly controlled by soil moisture-temperature feedbacks. *Geophysical Research Letters*, *44*(3), 1511–1519. DOI: https://doi.org/10.1002/2016GL071235

Vova, O., Kappas, M., & Emmam, A. R. (2019). Comparison of Satellite soil Moisture products in Mongolia and their relation to Grassland condition. *Land*, *8*(9). DOI: https://doi.org/10.3390/land8090142

Vova, Oyudari, Kappas, M., Renchin, T., & Fassnacht, S. (2020). Extreme Climate Event and Its Impact on Landscape Resilience in Gobi Region of Mongolia. *Remote Sensing*, *12*(18), 2881. DOI: https://doi.org/10.3390/rs12182881

Vyas, S. S., Bhattacharya, B. K., Nigam, R., Guhathakurta, P., Ghosh, K., Chattopadhyay, N., & Gairola, R. M. (2015). A combined deficit index for regional agricultural drought assessment over a semi-arid tract of India using geostationary meteorological satellite data. *International Journal of Applied Earth Observation and Geoinformation*, *39*, 28–39. DOI: https://doi.org/10.1016/j.jag.2015.02.009

Walker, J. P., & Houser, P. R. (2001). A methodology for initializing soil moisture in a global climate model: Assimilation of near-surface soil moisture observations. *Journal of Geophysical Research: Atmospheres*, *106*(D11), 11761–11774

Wan, Z., Wang, P., & Li, X. (2004). Using MODIS Land Surface Temperature and Normalized Difference Vegetation Index products for monitoring drought in the southern Great Plains, USA. *International Journal of Remote Sensing*, *25*(1), 61–72. DOI: https://doi.org/10.1080/0143116031000115328

(WMO), W. M. O., Commission (2006). (IOC) Intergovernmental Oceanographic, Programme, (UNEP) United Nations Environment, & Science, (ICSU) International Council for *Systematic Observation Requirements for Satellite-based Products for Climate: Supplemental details to the satellite-based component of the Implementation Plan for the Global Observing System for Climate in Support of the UNFCCC*

Wan, Zhengming. (2006). *MODIS Land Surface Temperature Products Users' Guide*

Wanders, N., Bierkens, M. F. P., de Jong, S. M., de Roo, A., & Karssenberg, D. (2014). The benefits of using remotely sensed soil moisture in parameter identification of large-scale hydrological models. *Water Resources Research*, *50*(8), 6874–6891. DOI: https://doi.org/10.1002/2013WR014639

Wanders, Niko, Karssenberg, D., Roo, A. de, De Jong, S. M., & Bierkens, M. F. P. (2014). The suitability of remotely sensed soil moisture for improving operational flood forecasting. *Hydrology and Earth System Sciences*, *18*(6), 2343–2357

Wang, G. (2005). Agricultural drought in a future climate: results from 15 global climate models participating in the IPCC 4th assessment. *Climate Dynamics*, *25*(7–8), 739–753

Wang, L., & Qu, J. J. (2007). NMDI: A normalized multi-band drought index for monitoring soil and vegetation moisture with satellite remote sensing. *Geophysical Research Letters*, *34*(20). DOI: https://doi.org/10.1029/2007GL031021

Wang, X., Wu, C., Wang, H., Gonsamo, A., & Liu, Z. (2017). No evidence of widespread decline of snow cover on the Tibetan Plateau over 2000-2015. *Scientific Reports*, *7*(1), 1–10. DOI: https://doi.org/10.1038/s41598-017-15208-9

Wardlow, B. D., Tadesse, T., Brown, J. F., Callahan, K., & Swain, S. (2012). *Vegetation DroughtResponse IndexAn Integration of Satellite,Climate, and Biophysical Data*

Wen, W., Maurits ., Ertsen., Mark D., Svoboda., & Hafeez, M. (2016). *Propagation of Drought: From Meteorological Drought to Agricultural and Hydrological Drought*. DOI: http://dx.doi.org/10.1155/2016/6547209

Wen, G., & Fu, C. B. (2000). Defination of climate and ecological transitional zones with satellite data sets. *Chinese Journal of Atmospheric Sciences*, *24*, 324–332

Wessels, K. J., Prince, S. D., Carroll, M., & Malherbe, J. (2007). RELEVANCE OF RANGELAND DEGRADATION IN SEMIARID NORTHEASTERN SOUTH AFRICA TO THE NONEQUILIBRIUM THEORY. *Ecological Applications*, *17*(3), 815–827. DOI: https://doi.org/10.1890/06-1109

West, H., Quinn, N., & Horswell, M. (2019). Remote sensing for drought monitoring & impact assessment: Progress, past challenges and future opportunities. *Remote Sensing of Environment*, *232*, 111291. DOI: https://doi.org/10.1016/j.rse.2019.111291

Wigneron, J.-P., Kerr, Y., Waldteufel, P., Saleh, K., Escorihuela, M.-J., Richaume, P., Ferrazzoli, P., De Rosnay, P., Gurney, R., & Calvet, J.-C. (2007). L-band Microwave Emission of the Biosphere (L-MEB) Model: Description and calibration against experimental data sets over crop fields. *Remote Sensing of Environment*, *107*(4), 639–655

Wilhite, D. A. (2000a). *Chapter 1, Drought as a Natural Hazard: Concepts and Definitions*

Wilhite, D. A. (2000b). Drought Preparedness and Response in the Context of Sub-Saharan Africa. *Journal of Contingencies and Crisis Management*, *8*(2), 81–92. DOI: https://doi.org/10.1111/1468-5973.00127

Wilhite, D. A., & Glantz, M. H. (1985a). Understanding: The drought phenomenon: The role of definitions. *Water International*, *10*(3), 111–120. DOI: https://doi.org/10.1080/02508068508686328

Wilhite, D. A., & Rhodes, S. L. (1993). Drought Mitigation in the United States: Progress by State Government. In *Drought Assessment, Management, and Planning: Theory and Case Studies* (pp. 237–251). Springer US. DOI: https://doi.org/10.1007/978-1-4615-3224-8_13

Wu, J., Zhou, L., Liu, M., Zhang, J., Leng, S., & Diao, C. (2013). Establishing and assessing the Integrated Surface Drought Index (ISDI) for agricultural drought monitoring in mid-eastern China. *International Journal of Applied Earth Observation and Geoinformation*, *23*(1), 397–410. DOI: https://doi.org/10.1016/j.jag.2012.11.003

Xu, X., Piao, S., Wang, X., Chen, A., Ciais, P., & Myneni, R. B. (2012). Spatio-temporal patterns of the area experiencing negative vegetation growth anomalies in China over the last three decades. *Environ. Res. Lett*, *7*, 9. DOI: https://doi.org/10.1088/1748-9326/7/3/035701

Yang, Y., Wang, Z., Li, J., Gang, C., Zhang, Y., Zhang, Y., Odeh, I., & Qi, J. (2016). Comparative assessment of grassland degradation dynamics in response to climate variation and human activities in China, Mongolia, Pakistan and Uzbekistan from 2000 to 2013. *Journal of Arid Environments*, *135*, 164–172. DOI: https://doi.org/10.1016/J.JARIDENV.2016.09.004

Yengoh, G. T., Dent, D., Olsson, L., Tengberg, A. E., & Tucker III, C. J. (2016). *Use of the Normalized Difference Vegetation Index (NDVI) to Assess Land Degradation at Multiple Scales*. Springer International Publishing. DOI: https://doi.org/10.1007/978-3-319-24112-8

Yihdego, Y., Vaheddoost, B., & Al-Weshah, R. A. (2019). Drought indices and indicators revisited. In *Arabian Journal of Geosciences* (Vol. 12, Issue 3, pp. 1–12). Springer Verlag. DOI: https://doi.org/10.1007/s12517-019-4237-z

Yu, F., Price, K. P., Ellis, J., & Shi, P. (2003). Response of seasonal vegetation development to climatic variations in eastern central Asia. *Remote Sensing of Environment*, *87*(1), 42–54. https://doi.org/10.1016/S0034-4257(03)00144-5

Zargar, A., Sadiq, R., Naser, B., & Khan, F. I. (2011). A review of drought indices. In *Environmental Reviews* (Vol. 19, Issue 1, pp. 333–349). National Research Council of Canada. DOI: https://doi.org/10.1139/a11-013

Zeng, J., Li, Z., Chen, Q., Bi, H., Qiu, J., & Zou, P. (2015). Evaluation of remotely sensed and reanalysis soil moisture products over the Tibetan Plateau using in-situ observations. *Remote Sensing of Environment*, *163*, 91–110. DOI: https://doi.org/10.1016/J.RSE.2015.03.008

Zhang, D., Li, Z. L., Tang, R., Tang, B. H., Wu, H., Lu, J., & Shao, K. (2015). Validation of a practical normalized soil moisture model with in situ measurements in humid and semi-arid regions. *International Journal of Remote Sensing*, *36*(19–20), 5015–5030. DOI: https://doi.org/10.1080/01431161.2015.1055610

Zhang, D., & Zhou, G. (2016). Estimation of soil moisture from optical and thermal remote sensing: A review. In *Sensors (Switzerland)* (Vol. 16, Issue 8). DOI: https://doi.org/10.3390/s16081308

Zhang, N., Hong, Y., Qin, Q., & Liu, L. (2013). VSDI: A visible and shortwave infrared drought index for monitoring soil and vegetation moisture based on optical remote sensing. *International Journal of Remote Sensing*, *34*(13), 4585–4609. DOI: https://doi.org/10.1080/01431161.2013.779046

Zhang, Y.-C., & Zhang, L.-J. (2005). Precipitation and temperature probability characteristics in climatic and ecological transition zone of Northeast China in recent 50 years. *Scientia Geographica Sinica/Dili Kexue*, *25*(5), 561–566

Zhao, H. L., Zhao, X. Y., Zhou, R. L., Zhang, T. H., & Drake, S. (2005). Desertification processes due to heavy grazing in sandy rangeland, Inner Mongolia. *Journal of Arid Environments*, *62*(2), 309–319. DOI: https://doi.org/10.1016/j.jaridenv.2004.11.009

Zhao, M., & Running, S. W. (2010). Drought-induced reduction in global terrestrial net primary production from 2000 through 2009. *Science*, *329*(5994), 940–943. DOI: https://doi.org/10.1126/science.1192666

Zhao, T., & Dai, A. (2015). The magnitude and causes of global drought changes in the twenty-first century under a low-moderate emissions scenario. *Journal of Climate*, *28*(11), 4490–4512. DOI: https://doi.org/10.1175/JCLI-D-14-00363.1

Zhao, Y., Yu, Z., & Chen, F. (2009). Spatial and temporal patterns of Holocene vegetation and climate changes in arid and semi-arid China. *Quaternary International*, *194*(1–2), 6–18

Zhou, H., Zhao, X., Tang, Y., Gu, S., & Zhou, L. (2005). Alpine grassland degradation and its control in the source region of the Yangtze and Yellow Rivers, China. *Grassland Science*, *51*(3), 191–203. DOI: https://doi.org/10.1111/j.1744-697X.2005.00028.x

Zhou, W., Gang, C., Zhou, F., Li, J., Dong, X., & Zhao, C. (2015). Quantitative assessment of the individual contribution of climate and human factors to desertification in northwest China using net primary productivity as an indicator. *Ecological Indicators*, *48*, 560–569. DOI: https://doi.org/10.1016/J.ECOLIND.2014.08.043

Zink, M., Samaniego, L., Kumar, R., Thober, S., Mai, J., Schäfer, D., & Marx, A. (2016). The German drought monitor. *Environmental Research Letters*, *11*(7), 74002

Zolotokrylin, A. N., Gunin, P. D., Titkova, T. B., Bazha, S. N., Danzhalova, E. V., & Kazantseva, T. I. (2016). Diagnosis of the desertification dynamics of arid pastures in Mongolia from observation in key areas and MODIS data. *Arid Ecosystems*, *6*(3), 149–157. DOI: https://doi.org/10.1134/S2079096116030100

Zucca, C., Wu, W., Dessena, L., & Mulas, M. (2015). Assessing the Effectiveness of Land Restoration Interventions in Dry Lands by Multitemporal Remote Sensing - A Case Study in Ouled DLIM (Marrakech, Morocco). *Land Degradation & Development*, *26*(1), 80–91. DOI: https://doi.org/10.1002/ldr.2307